SEQUENTIAL ACTIONS OF VCP/p97 AND THE PROTEASOME 19S REGULATORY PARTICLE IN STEROL-ACCELERATED, ER-ASSOCIATED DEGRADATION OF HMG COA REDUCTASE

APPROVED BY SUPERVISORY COMMITTEE

Russell DeBose-Boyd, Ph.D.

Joel Goodman, Ph.D.

George DeMartino, Ph.D.

Mark Lehrman, Ph.D.

DEDICATION

To Josh Morris, my husband and best friend. Thank you for the loving support over the last six years.

To Kline and Tina Addington, my parents and my foundation. Thank you for the never ceasing encouragement you have given me throughout my life.

To Clint Addington, my little brother and lifelong friend.

Words cannot express how much I appreciate and love all of you.

ACKNOWLEDGEMENT

I would like to acknowledge all of the current and past members of the DeBose-Boyd lab for their assistance over the last several years. I would like to express my deep appreciation and gratitude to my advisor, Dr. Russell DeBose-Boyd, for the patient guidance and mentorship he provided to me through to the completion of this degree. Dr. DeBose-Boyd's intellectual capacity is matched only by his genuinely good nature and down-to-earth humility. I am very fortunate to have had the opportunity to work with him. Isamu Hartman, for all of the time you spent working with me in the lab and teaching me all of the techniques I know and use today. Tammy Dinh and Kristi Brasher, for all of the technical assistance you provide to the DeBose-Boyd lab. Tammy, I appreciate all of the great advice you have given me during my early morning experiments. Youngah Jo, for all of the guidance you gave me for my molecular cloning projects. Rebecca Faulkner, who as a good friend was always willing to help and give her best suggestions whenever needed, I am so glad you joined our lab.

Thank you to my thesis committee members, Drs. Joel Goodman, Mark Lehrman, and George DeMartino for the guidance and suggestions. Thank you to Joachim Seemann for the help with my Immunostaining experiments. I really appreciate the collaboration between our labs and especially for the help you provided me in setting up an assay that became incredibly important to my dissertation work. I would also like to thank my fellow doctoral students. I appreciate the support, feedback, and most of all the friendship.

SEQUENTIAL ACTIONS OF VCP/p97 AND THE PROTEASOME 19S REGULATORY PARTICLE IN STEROL-ACCELERATED, ER-ASSOCIATED DEGRADATION OF HMG COA REDUCTASE

by

LINDSEY LACHELLE MORRIS

DISSERTATION

Presented to the Faculty of the Graduate School of Biomedical Sciences

The University of Texas Southwestern Medical Center at Dallas

In Partial Fulfillment of the Requirements

For the Degree of

DOCTOR OF PHILOSOPHY

The University of Texas Southwestern Medical Center

Dallas, Texas

August, 2014

SEQUENTIAL ACTIONS OF VCP/p97 AND THE PROTEASOME 19S REGULATORY PARTICLE IN STEROL-ACCELERATED, ER-ASSOCIATED DEGRADATION OF HMG COA REDUCTASE

LINDSEY LACHELLE MORRIS, Ph.D.

The University of Texas Southwestern Medical Center at Dallas, 2014

RUSSELL DEBOSE-BOYD, Ph.D.

Accelerated endoplasmic reticulum (ER)-associated degradation (ERAD) of the cholesterol biosynthetic enzyme HMG CoA reductase results from its sterol-induced binding to ER membrane proteins called Insig-1 and Insig-2. This binding allows for subsequent ubiquitination of reductase by Insig-associated ubiquitin ligases. Once ubiquitinated, reductase becomes dislocated from ER membranes into the cytosol for degradation by 26S proteasomes through poorly defined reactions mediated by the AAA-ATPase VCP/p97 and augmented by the nonsterol isoprenoid geranylgeraniol. Here, we report that the oxysterol 25-hydroxycholesterol and geranylgeraniol combine to trigger extraction of reductase across ER membranes prior to

its cytosolic release. This conclusion was drawn from studies utilizing a novel assay that measures membrane extraction of reductase by determining susceptibility of a lumenal epitope in the enzyme to *in vitro* protease digestion. Susceptibility of the lumenal epitope to protease digestion, and thus membrane extraction of reductase, was tightly regulated by 25-hydroxycholesterol and geranylgeraniol. The reaction was inhibited by RNA interference-mediated knockdown of either Insigs or VCP/p97. In contrast, reductase continued to become membrane extracted, but not cytosolically dislocated, in cells deficient for AAA-ATPases of the proteasome 19S regulatory particle. These findings establish sequential roles for VCP/p97 and the 19S regulatory particle in the sterol-accelerated ERAD of reductase that may be applicable to the ERAD of other substrates.

TABLE OF CONTENTS

CONTRIBUTIONS TO DISSERTATION

Chapter 1, Chapter 3, and Chapter 4 were written by Lindsey Morris. Chapter 2 was written by co-authors Lindsey Morris, Russell DeBose-Boyd, and Isamu Hartman of an accepted manuscript. Lindsey Morris conducted all experiments shown, except for Supplemental Figure 6 performed by Isamu Hartman.

PRIOR PUBLICATIONS

Fernandes NV, Yeganehjoo H, Katuru R, DeBose-Boyd RA, **Morris LL**, Michon R, Yu ZL, and Mo H. 2013. Geranylgeraniol suppresses the viability of human DU145 prostate carcinoma cells and the level of HMG CoA reductase. Exp Biol Med. 238: 1265-74. PMID: 24006306

LIST OF FIGURES

LIST OF TABLES

LIST OF ABBREVIATIONS

19S RP, 19S regulatory particle

20S CP, 20S core particle

25-HC, 25-hydroxycholesterol

AAA, ATPases Associated with diverse cellular activities

DHFR, dihydrofolate reductase

ER, endoplasmic reticulum

ERAD, ER-associated degradation

FCS, fetal calf serum

GGOH, geranylgeraniol

HMG CoA, 3-hydroxy-3-methylglutaryl coenzyme A

LPDS, lipoprotein deficient serum

MTX, methotrexate

RNAi, RNA interference

SCAP, SREBP Cleavage Activating Protein

siRNA, small interfering RNA

SREBP, sterol regulatory element binding protein

TEV, tobacco etch virus

VCP, Vasolin Containing Protein

CHAPTER ONE:

Introduction

1.1 Endoplasmic Reticulum Associated Degradation

Roughly 30% of newly synthesized proteins are translocated into the lumen of the endoplasmic reticulum (ER) prior to being directed into the secretory pathway [1]. While in the lumen, nascent polypeptides interact with a network of chaperones that assist in proper folding of proteins. In addition, enzymes involved in disulfide bond formation and glycosylation, essential modifications that facilitate proper folding, are located within the lumen of the ER. If a protein fails to achieve the correct confirmation due to genetic mutations, cellular stress, or unsuccessful assimilation into an oligomeric complex, it is targeted for ER-associated degradation (ERAD) [2-6]. The ERAD pathway is a process through which soluble and membrane bound proteins of the ER are targeted for ubiquitination and subsequent degradation by the 26S proteasome in the cytosol. The ERAD pathway plays an important role in the regulation of many substrates linked to human diseases and aids in the removal of aberrant proteins that might compete with their functional counterparts within the cell [7]. Lack of balance between protein synthesis, degradation, and transport into the secretory pathway results in ER stress that if left unchecked can influence cell survival and pathologies such as cancer, diabetes, and neurodegenerative diseases [8].

Maintenance of ER homeostasis is managed by the unfolded protein response (UPR), which regulates expression levels of genes involved in processes such as protein folding, transport, and degradation. There are three branches of the UPR mediated by: inositol-requiring enzyme-1 (IRE1), activating transcription factor-6 (ATF6), and protein kinase RNA (PKR)-like ER kinase (PERK). In the absence of ER stress, immunoglobulin binding protein (BiP) binds to

Ire1 keeping it in an inactive state. During ER stress, Ire1 forms oligomeric complexes through association with the ER lumenal domains of other Ire1 enzymes [9, 10]. Oligomerization is required for activation of Ire1's cytosolic RNase domain, which acts to relieve ER stress through: (1) cleavage of x-box binding protein 1 (XBP-1) mRNA resulting in modulation of ER-stress responsive genes and (2) degradation of a subset of mRNAs which may lead to decreased protein influx into the ER [11-13]. Under ER stress, ATF6 traffics to the Golgi where it is proteolytically processed to release the transcription factor portion of ATF6 [14, 15]. This ATF6 fragment translocates to the nucleus and modulates expression of target genes. While Ire1 and ATF6 influence the cell response to ER stress through modulating gene expression, PERK inhibits protein translation via phosphorylation of the α-subunit of the eukaryotic translation initiation factor-2 (eIF2a) [16]. If the UPR system is unable to restore ER homeostasis then cell death pathways are initiated. One of the important mechanisms used by the UPR to alleviate ER stress is to increase degradation of proteins from the ER through upregulation of ERAD components [17].

As depicted in Figure 1, the process of ERAD can be roughly divided into five steps: substrate recognition, substrate targeting, ubiquitination and dislocation of substrate into the cytosol, and finally, substrate degradation by proteasomes. Misfolded substrates can be either completely soluble within the ER lumen or integrated in the ER membrane through one or more transmembrane domains. Misfolded domains can thus be present either in the ER lumen, the cytosol, or within the membrane. Studies in the yeast *Saccharomyces cerevisiae* have revealed that distinct ERAD pathways are engaged depending upon the location of the misfolded domain in a given substrate [18, 19]. Misfolded domains within the ER lumen are recognized by lumenal chaperones and engage what is called the ERAD-L pathway. Cytosolic chaperones recognize misfolded regions presented in the cytosol and direct substrates through the ERAD-C pathway.

Misfolded domains embedded within the membrane engage the ERAD-M pathway; however, the molecular chaperones that recognize these types of misfolded domains have not been described in detail. The ERAD pathway in mammalian cells is more complex than in yeast and cannot be simply divided into three separate pathways. For example, the number of ubiquitin ligases that mediate the mammalian ERAD pathway far exceeds that which mediates ERAD in yeast [20]. In addition, the mammalian genome encodes for more potential substrates of ERAD and factors that mediate each step of the reaction. The ERAD of a given mammalian substrate, particularly those with membrane-spanning domains, may utilize various aspects of the described ERAD-M, ERAD-L, and ERAD-C pathways in yeast.

1.1.1 Mechanisms of ERAD of Soluble Substrates

Much of what is known about the ERAD pathway has been provided through the study of model substrates, most of which are soluble proteins such as mutant forms of the yeast proteins carboxypeptidase Y and alpha-factor precursor as well as the mammalian protein alpha-1 antitrypsin [21-23]. These types of proteins are separated from proteasomes by the ER membrane. Thus, it is generally accepted that following selection by ER lumenal chaperones (e.g., Bip/Kar2p, calnexin/calreticulin, and protein disulfide isomerase [24]), soluble ERAD substrates are targeted for transport across the membrane into the cytosol through a protein-conducting channel formed by Sec61, a component of the translocation channel that imports polypeptides into the ER or by the polytopic protein Derlin-1 [2, 25-28]. The energy to drive dislocation of lumenal ERAD substrates into the cytosol is thought to be provided by the AAA-ATPase VCP/p97 (cdc48 in yeast) [29, 30]. During or soon after cytosolic dislocation, lumenal ERAD substrates become ubiquitinated by the combined actions of ubiquitin-conjugating enzymes (E2s) and ubiquitin ligases (E3s), which transfer activated ubiquitin from ubiquitin-activating enzyme (E1) to particular lysines residues in the substrate [31]. It should be noted

that the yeast ERAD ubiquitin ligases, Doa10 and Hrd1, are anchored to ER membranes through a membrane domain with multiple membrane-spanning segments [18]. It has been postulated that Hrd1 and Doa10 serve dual roles as both ubiquitin ligases and retrotranslocation channels [32, 33]. Recent studies have suggested the need for two rounds of ubiquitination including a round of deubiquitination for efficient ERAD to take place. One model proposes that the first round of ubiquitination is required to promote binding with VCP/p97, but polyubiquitin chains must then be removed by an associated deubiquitylating enzyme to allow the ERAD substrate to be dislocated [34, 35]. The second round of ubiquitination is required to facilitate recognition and targeting of the substrate to the proteasome for degradation.

In the final steps of ERAD, ubiquitinated substrates are delivered to proteasomes for degradation through reactions mediated in part by VCP/p97 [29]. VCP/p97 associates with ubiquitinated proteins through substrate recruitment factors Npl4 and Ufd1, which bind to polyubiquitin chains; the ATPase also associates with ubiquitin regulatory X (UBX), ubiquitin-associated (UBA), and ubiquitin-like (UBL) domain-containing proteins [36]. These proteins include Ufd2, an E4 enzyme that extends polyubiquitin chains [37], and the deubiquitinating enzymes Otu1, Rad23 and Dsk2, which can associate with both polyubiquitin chains and proteasomes simultaneously [38]. Extraction and proteasomal delivery of non-ubiquitinated ERAD substrates may be mediated by the 19S regulatory particle of the proteasome, which also contains AAA-ATPase activity [39].

1.1.2 ERAD of Integral Membrane Substrates

In contrast to lumenal ERAD substrates, a detailed understanding of mechanisms for ERAD of integral membrane proteins with one or more membrane-spanning segments is lacking. Following selection by chaperones that recognize the misfolded region, integral membrane ERAD substrates are targeted to ubiquitin ligases for subsequent ubiquitination. Following

ubiquitination, integral membrane substrates are recognized by VCP/p97 and its associated co-factors Npl4 and Ufd1 for extraction from the membrane and dislocation into the cytosol for proteasomal degradation.

This phase of ERAD, cytosolic dislocation, has been observed for several integral membrane ERAD substrates including: major histocompatibility complex class I heavy chains (MHCI), cystic fibrosis transmembrane conductance regulator (CFTR), connexins, and Ste6p* [40-43]. For example, treatment of cells with proteasome inhibitors blocks degradation of polytopic CFTR and increases the amount of the ubiquitinated protein. Interestingly, CFTR appeared in the supernatant fraction following 100,000 x g centrifugation of post nuclear supernatants [44]. Similarly cytosolic dislocation of MHCI heavy chains from microsomal fractions to the 100,000 g supernatant (cytosol) has been observed. This dislocation required treatment of cells with the protease inhibitor, LLnL, and the expression of US11, a viral protein shown to target MHCI heavy chains for ERAD [40]. These and other studies indicate that cytosolic dislocation is an intermediate step in the ERAD of not only soluble ERAD substrates, but also of those containing one or more transmembrane helices.

Although cytosolic dislocation of membrane bound ERAD substrates is well established in the literature, the mechanism through which these ERAD substrates are dislodged from ER membranes into the cytosol is unclear. It is also unclear whether cytosolic dislocation of membrane bound substrates would require a retrotranslocon channel formed by a protein such as Sec61 or Derlins. The AAA-ATPase VCP/p97 plays a key role in ERAD of integral membrane substrates by driving their retrotranslocation across the ER membrane into the cytosol. However, it is unclear whether VCP/p97 actively pulls the integral membrane substrate through a retrotranslocon, the lipid bilayer, or whether the ATPase dislodges extracted substrates from the ER membrane into the cytosol. Additionally, it has been suggested that proteasomes work

together with VCP/p97 to play a direct role in the extraction of polytopic ERAD substrates from the ER membrane [45].

An outstanding question in the ERAD field pertains to whether degradation and membrane extraction are a tightly coupled process or if cytosolic dislocation must occur prior to the commencement of degradation. As mentioned previously, if integral membrane substrates become dislocated to the cytosol prior to degradation then what mechanism and factors are required to mediate this reaction and how is the solubility of the transmembrane domains maintained in the cytosol? The coordination of extraction and degradation of integral membrane proteins could be envisioned in three primary ways: (1) degradation might commence after retrotranslocation of the substrate through a membrane channel, (2) the substrate could be directly extracted out of the membrane bilayer, (3) or degradation could begin from an internal site of the substrate that is exposed to the cytosol. In these models it is assumed that retrotranslocation and degradation are tightly coupled to one another and occur in close proximity to the ER membrane. Contrary to those models, substrates such as MHCI and CFTR accumulate in the cytosol when proteasomes are compromised [40, 46]. This would suggest that membrane-spanning segments of these substrates must be solubilized in the cytosol prior to degradation and implies that retrotranslocation and degradation are not tightly coupled for all integral membrane ERAD substrates. Detailed answers to these outstanding questions require the examination of ERAD in a model integral membrane substrate such as HMG CoA reductase.

1.2 Cholesterol Regulation

Cholesterol is a lipid, essential to the structural integrity of cell membranes. Cholesterol also serves as a precursor for the synthesis of steroid hormones, bile acids, and vitamin D [47, 48]. For these reasons cholesterol is essential to animal life, however, aberrant accumulation of

cholesterol can be toxic and is strongly associated with the progression of atherosclerosis [47, 49]. Thus, cholesterol levels must be tightly regulated in cells through coordinated regulation of *de novo* cholesterol synthesis and low-density lipoprotein (LDL) receptor-mediated endocytosis of cholesterol-containing LDL particles. When excess cholesterol accumulates in cells, expression of biosynthetic enzymes and the LDL receptor are suppressed. As depicted in Figure 2, *de novo* synthesis of cholesterol is mediated by the mevalonate pathway that produces both cholesterol and essential nonsterol isoprenoids such as heme A, ubiquinone, farnesyl, and geranylgeranyl groups that are attached to many proteins [50]. The rate-limiting step in this pathway is the reduction of 3-hydroxy-3-methylglutaryl coenzyme A (HMG CoA) to mevalonate, which is mediated by the enzyme HMG CoA reductase. Cells must avoid the potentially toxic overproduction of cholesterol and its sterol precursors while maintaining constant production of essential nonsterol isoprenoids. Thus, sterol and nonsterol isoprenoid end products of mevalonate metabolism exert stringent feedback control on reductase through negative feedback mechanisms: 1) sterol-dependent transcriptional regulation of reductase along with the LDL receptor and other cholesterol biosynthetic enzymes, 2) translational regulation of reductase mRNA, and 3) post-transcriptional regulation of reductase degradation.

Translational control of HMG CoA reductase is regulated by nonsterol end products of the mevalonate pathway acting through an unknown mechanism that may be mediated by the complex 5' untranslated region of reductase [51]. Transcriptional regulation of reductase depends upon sterol regulatory element binding protein-2 (SREBP-2). SREBP2 belongs to the family of basic helix-loop-helix leucine zipper (bHLH-Zip) transcription factors and is synthesized as a membrane bound inactive precursor that is known to constitutively bind SREBP cleavage activating protein (SCAP). SCAP is a polytopic ER membrane protein that is composed of a NH_2-terminal domain containing eight membrane-spanning segments that anchors the protein

into the membrane [52]. SCAP is also composed of a large COOH-terminal domain that extends into the cytosol and is important for complex formation with the SREBP family of transcription factors [53]. During sterol deprivation, SCAP facilitates the movement of SREBPs from the ER to the Golgi where SREBPs are processed through two sequential cleavages to release the transcription factor. Processed SREBP migrates to the nucleus and enhances transcription of reductase as well as other cholesterol biosynthetic enzymes. When sterols are abundant, the ER-to-Golgi transport of SCAP and SREBP is blocked due to binding between SCAP and Insigs [54, 55]. Insigs bind to a region within the membrane domain of Scap that comprises transmembrane helices 2-6; this region is known as the sterol-sensing domain [56].

There are two Insigs, Insig-1 and Insig-2, in the mammalian genome; these ER-localized proteins contain six transmembrane domains and are 85% identical within this region [57, 58]. Insigs serve an important role in feedback control of cholesterol synthesis through both their sterol-regulated binding to SCAP and to HMG CoA reductase (see below). When cholesterol levels are high cells acts to reduce subsequent cholesterol synthesis by Insig mediated ER retention of SREBP and SCAP and by Insig dependent ubiquitination of reductase. Thereby, slowing the rate of cholesterol synthesis at two levels.

1.2.1 HMG CoA Reductase as a Model ERAD Substrate

In addition to its role in regulating protein quality in the cell, the ERAD pathway is utilized for the physiological regulation of sterol-accelerated degradation of 3-hydroxy-3-methylglutaryl coenzyme (HMG CoA) reductase [59]. Reductase is anchored in the ER membrane through eight membrane-spanning helices at the N-terminus and contains a single N-linked glycosylation site located in the lumenal loop between transmembrane helices seven and eight [60, 61]. The N-terminal membrane-spanning region of reductase is necessary and sufficient for

conferring sterol-dependent degradation upon reductase. The C-terminal domain of reductase extends into the cytosol and exerts all catalytic activity of the enzyme [60, 62].

Reductase degradation is rigorously regulated through a feedback system dependent upon sterol and nonsterol end products of the mevalonate pathway. As depicted in Figure 3, the intracellular accumulation of hydroxylated forms of cholesterol called oxysterols or the cholesterol synthesis intermediate 24,25-dihydrolanosterol [63, 64] triggers binding of the membrane domain of reductase to Insigs [65-67]. A tetrapeptide sequence YIYF in the second membrane-spanning helix of reductase, and similarly found in the sterol-sensing domain of SCAP, is required for binding to Insig [65, 66]. This binding with Insigs results in ubiquitination of reductase on two cytosolically exposed lysine residues (K89 and K248) in the membrane domain of reductase; ubiquitination of reductase is mediated by Insig-associated E3 ubiquitin ligases Trc8 and gp78 [68, 69]. Insig-1 is solely responsible for the recruitment of the RING-finger ubiquitin ligase gp78, while both Insig-1 and Insig-2 bind the other membrane-bound RING-finger ubiquitin ligase Trc8. Gp78, but not Trc8, also serves as an E3 ubiquitin ligase for Insig-1. Once ubiquitinated, reductase becomes extracted from ER membranes and delivered to cytosolic proteasomes for degradation [70]. The 20-carbon nonsterol isoprenoid geranylgeraniol, but not the 15-carbon farnesol, augments sterol-accelerated degradation of reductase [66]. Geranylgeraniol does not appear to modulate reductase ubiquitination or sterol-dependent binding to Insigs. Thus, it has been postulated that geranylgeraniol enhances reductase degradation by modulating post-ubiquitination steps in the reaction such as extraction and/or cytosolic dislocation.

Several lines of evidence point to the physiologic relevance of reductase dislocation from ER membranes into the cytosol including its tight regulation by sterols and geranylgeraniol and its requirement for the actions of Insig-1/2 and VCP/p97 [70]. In recent studies, our laboratory

has reconstituted dislocation of reductase from ER membrane *in vitro* [71]. This dislocation required *in vitro* additions of sterols, an energy source in the form of ATP, and exogenous cytosol. Moreover, the in vitro reaction was augmented by geranylgeraniol, but not by farnesol. Finally, our laboratory has found deglycosylated forms of reductase in the cytosol of sterol and proteasome inhibitor treated cells, further verifying the physiological relevance of a cytosolic intermediate in reductase degradation. However, the precise mechanism through which ubiquitinated reductase is extracted from membranes and dislocated to the cytosol is poorly understood. Ubiquitination appears to be a requirement for cytosolic dislocation; forms of reductase that cannot become ubiquitinated fail to become dislocated into the cytosol [70]. Moreover, VCP/p97 plays a key role in cytosolic dislocation, as indicated by the observation that its knockdown prevents reductase dislocation.

Many questions still remain pertaining to the degradation of reductase. Although reductase cytosolic dislocation is stringently regulated it appears to be very inefficient as only approximately 10% of reductase is found in the cytosol. While this hinders further efforts to study the mechanism of cytosolic dislocation of reductase, it also suggests that there might be an intermediate step in reductase degradation before cytosolic dislocation and after ubiquitination that would serve as a more substantial intermediate to study. Another outstanding problem is to identify the role geranylgeraniol and VCP/p97 play in reductase degradation. Studies show that geranylgeraniol augments reductase degradation and cytosolic dislocation without enhancing ubiquitination [66, 71, 72]. Similarly VCP/p97 is required for degradation and cytosolic dislocation of reductase but not ubiquitination, indicating that both factors play an important role in late stages of reductase degradation. Lastly, does the proteasome play any role in reductase degradation beyond mediating the proteolytic degradation of the enzyme?

Figure 1:

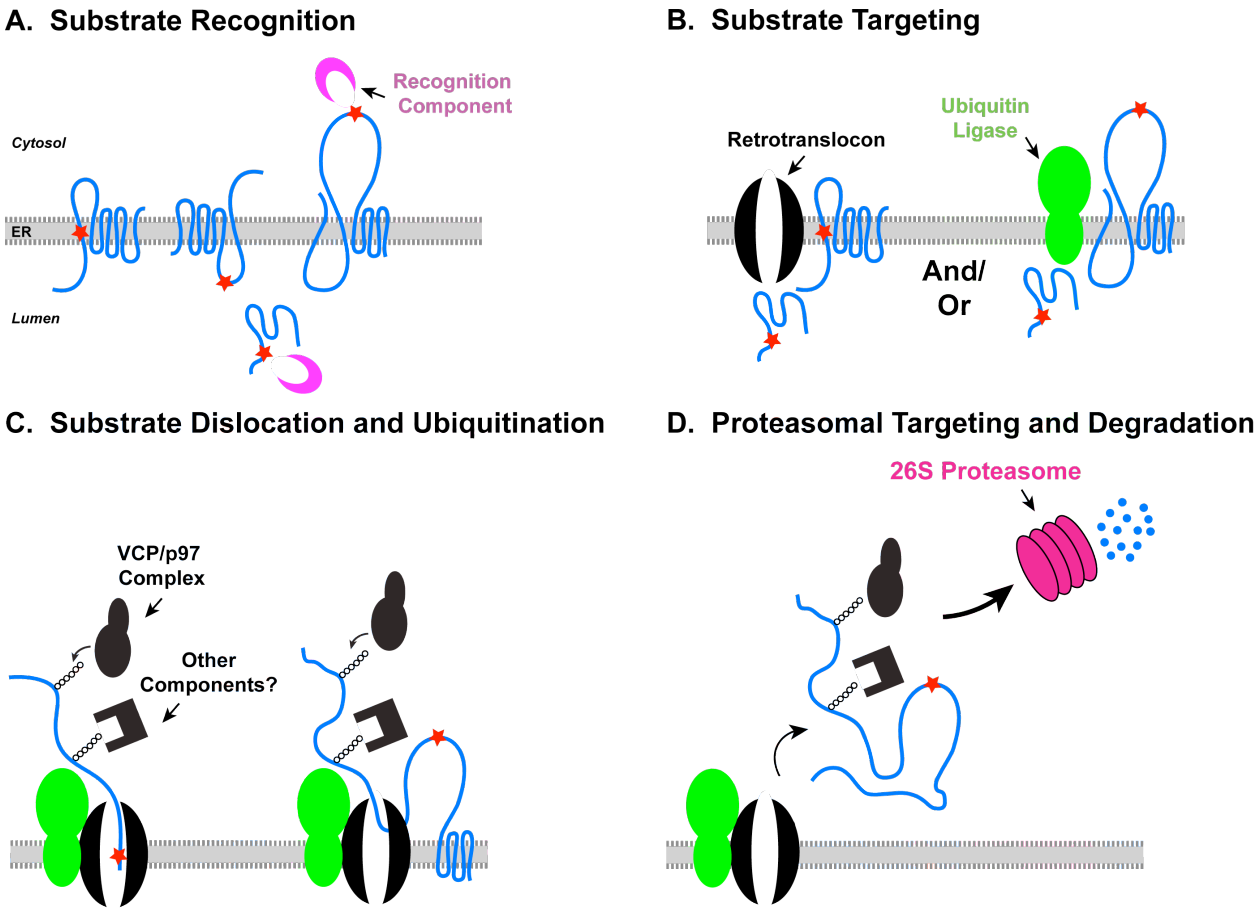

Figure 1. Illustration of ER-associated degradation. (A) Substrate Recognition: Misfolded regions of substrate are recognized by cytoplasmic and lumenal chaperones. (B) Substrate Targeting: Substrates are targeted to the retrotranslocon and/or to an E3 ubiquitin ligase. (C) Substrate Dislocation and Ubiquitination: Retrotranslocation is initiated. As substrates exit the retrotranslocon they are ubiquitinated, which promotes further retrotranslocation of the substrate. (D) Proteasomal Targeting and Degradation: After substrates are dislocated into the cytosol they are recognized by and targeted to the proteasome for degradation.

Figure 2:

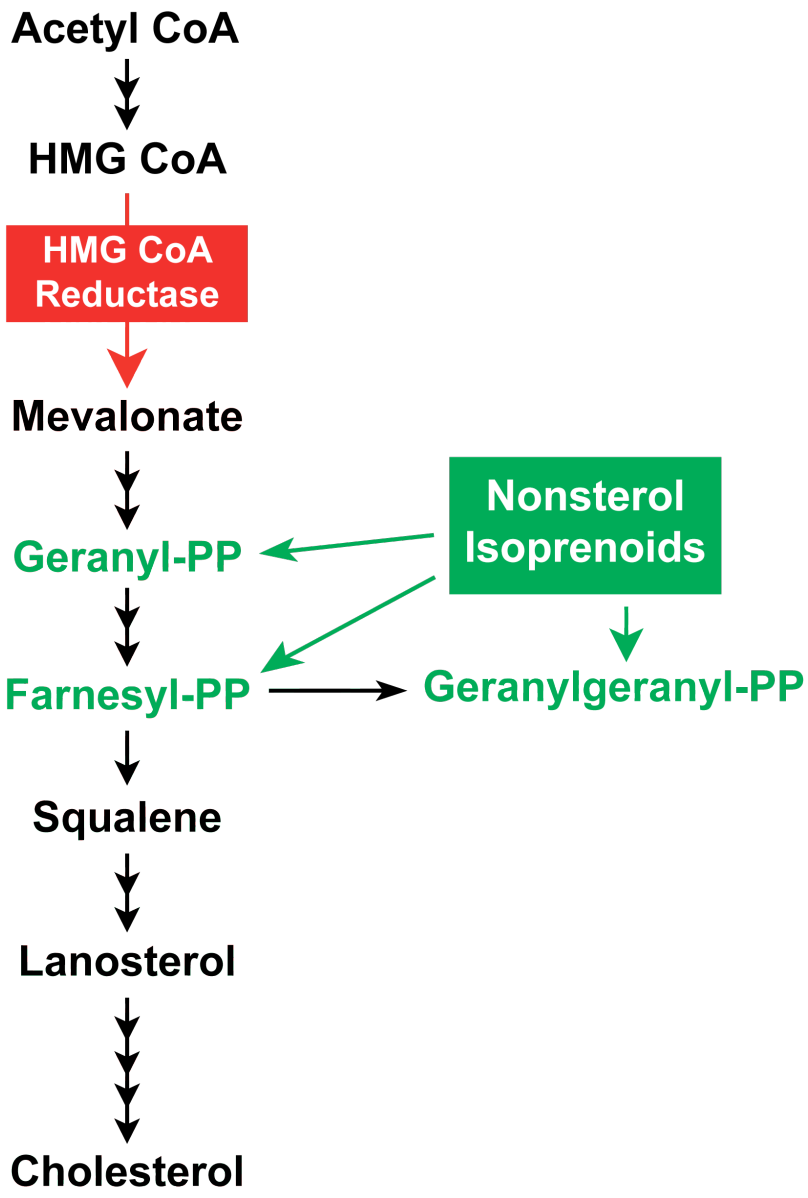

Figure 2. Mevalonate Pathway. HMG CoA Reductase catalyzes the conversion of HMG CoA into mevalonate. Reductase is the major rate-limiting enzyme in the production of sterol and nonsterol isoprenoids. Reductase is subject to feedback control by both end products of the mevalonate metabolism.

Figure 3:

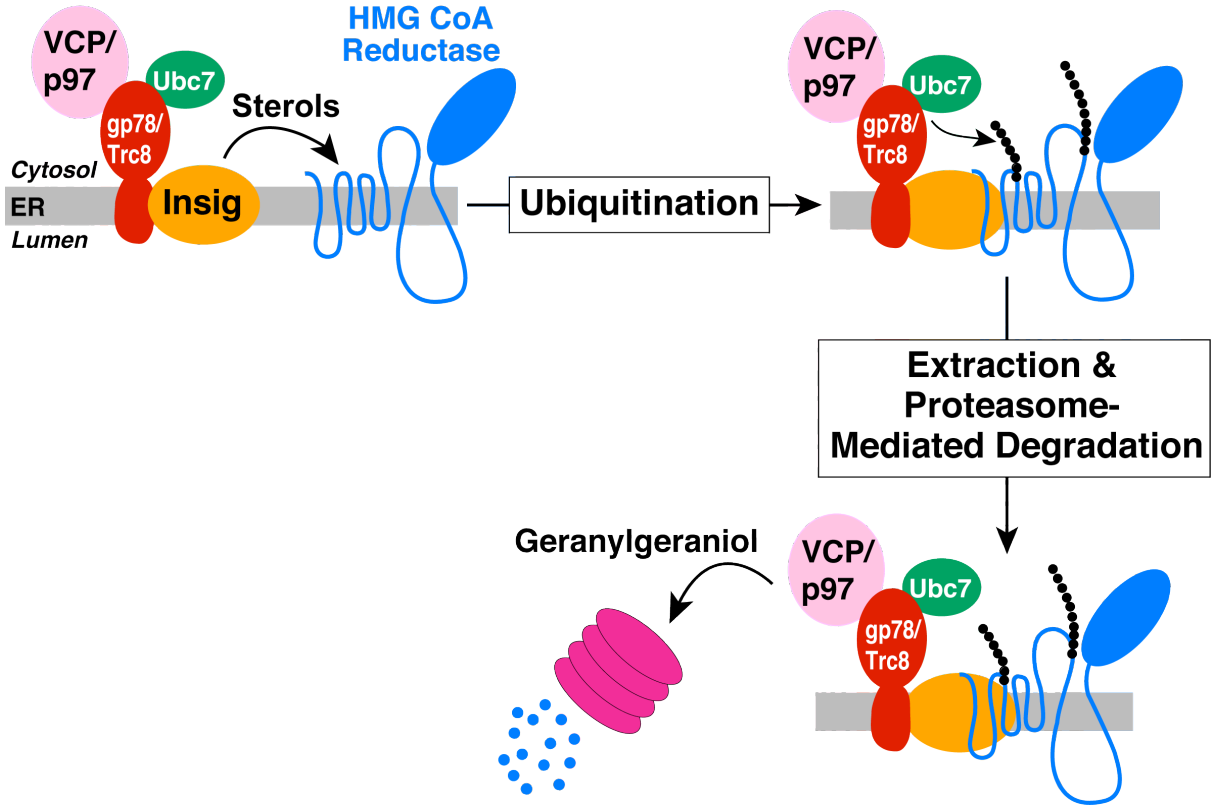

Figure 3. Model for Insig-mediated sterol-accelerated degradation of HMG CoA Reductase. In the presence of sterols, Insig binds to the membrane domain of HMGCR, thereby leading to ubiquitination on two lysine residues by the E3 ligases gp78 and Trc8. HMGCR is then extracted from the membrane through an unknown process, possibly facilitated by the ATPase VCP/p97 and the nonsterol isoprenoid geranylgeraniol.

CHAPTER TWO:

Sequential Actions of the AAA-ATPase VCP/p97 and the Proteasome 19S Regulatory Particle in Sterol-Accelerated, ER-Associated Degradation of 3-Hydroxy-3-methylglutaryl Coenzyme A Reductase

2.1 Abstract

Accelerated endoplasmic reticulum (ER)-associated degradation (ERAD) of the cholesterol biosynthetic enzyme HMG CoA reductase results from its sterol-induced binding to ER membrane proteins called Insig-1 and Insig-2. This binding allows for subsequent ubiquitination of reductase by Insig-associated ubiquitin ligases. Once ubiquitinated, reductase becomes dislocated from ER membranes into the cytosol for degradation by 26S proteasomes through poorly defined reactions mediated by the AAA-ATPase VCP/p97 and augmented by the nonsterol isoprenoid geranylgeraniol. Here, we report that the oxysterol 25-hydroxycholesterol and geranylgeraniol combine to trigger extraction of reductase across ER membranes prior to its cytosolic release. This conclusion was drawn from studies utilizing a novel assay that measures membrane extraction of reductase by determining susceptibility of a lumenal epitope in the enzyme to *in vitro* protease digestion. Susceptibility of the lumenal epitope to protease digestion, and thus membrane extraction of reductase, was tightly regulated by 25-hydroxycholesterol and geranylgeraniol. The reaction was inhibited by RNA interference-mediated knockdown of either Insigs or VCP/p97. In contrast, reductase continued to become membrane extracted, but not cytosolically dislocated, in cells deficient for AAA-ATPases of the proteasome 19S regulatory particle. These findings establish sequential roles for VCP/p97 and the 19S regulatory particle in the sterol-accelerated ERAD of reductase that may be applicable to the ERAD of other substrates.

2.2 Introduction

In the current study, we develop an assay that measures the sterol-induced extraction of

reductase across ER membranes. Intact membranes isolated from cells expressing a form of reductase containing T7 epitopes in the N-glycosylated lumenal loop between transmembrane domains 7 and 8 were subjected to *in vitro* digestion with the protease trypsin. Trypsinolysis produced protected fragments of reductase that were observed in anti-T7 immunoblots. A substantial fraction of the lumenal T7 epitopes in reductase became susceptible to trypsin digestion when cells were treated with the oxysterol 25-hydroxycholesterol (25-HC) and geranylgeraniol prior to harvest and subcellular fractionation. This result indicates that sterols together with geranylgeraniol trigger extraction of reductase across the ER membrane, resulting in exposure of the lumenal loop between transmembrane domains 7 and 8 to the cytosol. The sterol-induced membrane extraction of reductase, as determined by susceptibility of the lumenal T7 epitope to trypsinolysis, was inhibited by RNA interference (RNAi)-mediated knockdown of Insigs or VCP/p97. In contrast, the extraction of reductase across membranes continued in cells subjected to RNAi-mediated knockdown of AAA-ATPases of the proteasome 19S regulatory particle (19S RP) [73, 74]. Knockdown of the 19S RP inhibited the cytosolic dislocation as well as the proteasome-mediated ERAD of reductase. These observations, considered together with our previous studies [70], indicate that VCP/p97 mediates the sterol-induced extraction of ubiquitinated reductase across ER membranes whereas the 19S RP mediates release of membrane-extracted reductase into the cytosol for proteasomal degradation.

2.3 Materials and Methods

Materials

We obtained MG-132 from Boston Biochem (Cambridge, MA); trypsin and trypsin inhibitor from Sigma (St. Louis, MO); horseradish peroxidase-conjugated donkey anti-mouse, anti-rabbit, and anti-biotin IgGs (affinity-purified) as well as biotin-conjugated anti-mouse IgGs (affinity-purified) from Jackson ImmunoResearch Laboratories (West Grove, PA); geranylgeraniol from

Santa Cruz Biotechnology (Dallas, TX); and 25-hydroxycholesterol from Steraloids (Newport, RI). Other reagents, including lipoprotein-deficient serum (LPDS, d > 1.215 g/ml), sodium compactin, and sodium mevalonate was prepared or obtained from previously described sources [75, 76].

Cell Culture

Monolayers of CHO-K1 cells were maintained in tissue culture at 37 °C in 8-9% CO_2. Stock cultures were maintained in medium A (1:1 mixture of Ham's F-12 medium and Dulbecco's modified Eagle's medium containing 100 units/ml penicillin and 100 µg/ml streptomycin sulfate) supplemented with 5% FCS. UT-2 cells, a clone of reductase-deficient CHO-K1 cells [77], were maintained in medium A supplemented with 5% FCS and 0.2 mM mevalonate. UT-2/pHMG-Red-T7 cells were generated as follows. On day 0, UT-2 cells were set up at a density of 4 X 10^5 cells per 100-mm dish in medium B containing 5% FCS and 0.2 mM mevalonate. On day 1, the cells were transfected with 2 µg/dish pCMV-HMG-Red-T7, which encodes full length hamster reductase with two copies of the T7 epitope inserted in the lumenal loop between transmembrane helices seven and eight of reductase [65], using FuGENE 6 transfection reagent (Roche Applied Science, Indianapolis, IN) as described previously [78]. Following incubation for 16 h at 37 ºC, the cells were switched to medium A supplemented with 5% FCS, 0.2 mM mevalonate, and 700 µg/ml G418. Fresh medium was added every 2-3 days until colonies formed after about 2 weeks. Individual colonies were isolated using cloning cylinders and expression of T7-tagged reductase was determined by immunoblot analysis. Cells from a single colony of cells expressing a moderate level of transfected reductase (as determined by immunoblot analysis with monoclonal anti-T7 IgG) were selected, cloned by limiting dilution, and maintained in medium B (medium A supplemented with 5% FCS, 0.2 mM mevalonate, and 500 µg/ml G418).

Isolation of Cell Membranes

(Protocol 1) **–** Triplicate (100-mm or 60-mm) dishes of cells were harvested by scraping into culture medium and washed with PBS. The cell pellets were resuspended in 500 µl of Buffer A (10 mM HEPES-KOH [pH 7.4], 10 mM KCL, 1.5 mM $MgCl_2$, 5 mM sodium EDTA, 5 mM sodium EGTA, 250 mM sucrose, 5 mM dithiothreitol, and 0.1 mM leupeptin), passed through a 22.5-gauge needle 30 times, and centrifuged at 1000 X g for 7 min at 4 °C. The resulting post-nuclear supernatants were then subjected to an additional round of centrifugation at 16,000 X g for 15 min at 4 °C. The resulting pellets were designated as the membrane fraction. (Protocol 2) – Triplicate (100-mm or 60-mm) dishes of cells were harvested by scraping into culture medium, washed with PBS, resuspended in Buffer A, and lysed for preparation of post-nuclear supernatants as described above. The post-nuclear supernatants were then subjected to centrifugation at 100,000 X g for 45 min at 4 °C. The resulting pellet and supernatant fractions were designated membrane and cytosol, respectively. Protocol 2 was used in all experiments where a cytosolic fraction was needed for subsequent immunoblot analysis.

Trypsin Proteolysis

Cells were harvested and the membrane fractions were prepared using Protocol 1 or 2 as indicated in the figure legends. The membrane pellets were resuspended in 100 µl Buffer B (Buffer A without dithiothreitol and leupeptin supplemented with 100 mM NaCl). The resuspended membranes were pooled together when appropriate and protein concentration was determined using the Coomassie Bradford Protein Assay (Thermo Scientific, Rockford, IL). Pooled samples were then divided into 56 µl aliquots (approximately 100 µg for experiments utilizing 100-mm dishes and 30 µg for those utilizing 60-mm dishes) for trypsin digestion. Some of the aliquots of membranes were treated with 1% NP-40 (v/v) (final concentration) prior to

trypsin digestion as indicated in the figure legends. Varying amounts of trypsin were added to the resuspended membranes in a volume of 2 µl and samples were incubated at 30 °C for the times indicated in the figure legends. Trypsin proteolysis was terminated by the addition of Buffer C (62.5 mM Tris-HCl [pH 6.8], 15% (w/v) SDS, 8 M urea, 10% (v/v) glycerol, and 100 mM dithiothreitol) containing 40 µg of soybean trypsin inhibitor, and 4X SDS loading buffer (1X final concentration). Samples were then heated at 37 °C for 20 min and subjected to SDS-PAGE, followed by immunoblot analysis as described below.

Immunoblot Analysis

The protein concentration of membrane and cytosol fractions was determined using the Coomassie Bradford and the BCA protein assay kits, respectively (Thermo Scientific, Rockford, IL). Aliquots of the fractions were mixed with an equal volume of Buffer C and 4X SDS loading buffer added to a final concentration of 1X. For anti-Scap immunoblots, fractions were directly mixed with 4X SDS loading buffer to a final concentration of 1X. Samples were fractionated on SDS-PAGE gels calibrated with prestained molecular mass markers (Bio-Rad, Hercules, CA), after which the proteins were transferred to nitrocellulose membranes and subjected to immunoblot analysis. Primary antibodies used for immunoblotting were as follows: IgG-A9, a mouse monoclonal antibody against hamster HMG CoA reductase [79]; IgG-838c, a rabbit polyclonal antibody raised against the catalytic domain of human reductase; monoclonal anti-T7 Tag IgG (EMD Biosciences, Darmstadt, Germany); IgG-9D5, a mouse monoclonal antibody against hamster Scap [80]; IgG-18, a mouse monoclonal antibody against VCP/p97 (BD Transduction Laboratories, San Jose, CA); rabbit polyclonal anti-calnexin IgG (Novus Biologicals, Littleton, CO); MLO7, rabbit polyclonal antiserum against rat GM130 [81]; IgG-TBP1-19, mouse monoclonal antibody against human Rpt5 (Enzo Life Sciences, Farmingdale, NY); IgG-p42-23, a mouse monoclonal antibody against human Rpt4 (Biomol International/Enzo

Life Sciences, Ann Arbor, MI), rabbit polyclonal anti-Rpt2 IgG (Enzo Life Sciences, Farmingdale, NY), and IgG-P4D1, mouse monoclonal antibody against bovine ubiquitin (Santa Cruz Biotechnology, Dallas, TX). Bound antibodies were visualized with peroxidase-conjugated donkey anti-mouse or anti-rabbit IgG using the SuperSignal West Pico Chemiluminescent Substrate (Thermo Scientific, Rockford, IL) according to the manufacturer's instructions. Filters were exposed to film at room temperature.

RNA Interference (RNAi)

RNAi was carried out as previously described with minor modifications [70]. Duplexes of small interfering RNA (siRNA) were designed and synthesized by Dharmacon/Thermo Fisher Scientific. The siRNA sequence targeting Insig-1 corresponds to nucleotides 708-726 of Chinese hamster Insig-1 (GenBank accession number NM_001244079.1) relative to the first nucleotide of its start codon. The siRNA sequence targeting Insig-2 corresponds to nucleotides 519-537 of Chinese hamster Insig-2 (GenBank accession number NM_001244078.1) relative to the first nucleotide of its start codon. The siRNA sequence targeting VCP/p97 corresponds to nucleotides 252-270 of mouse VCP/p97 (GenBank accession number NM_009503.4) relative to the first nucleotide of its start codon. This sequence is conserved in human, rat, cow, and wolf. The siRNA targeting Rpt4 corresponds to nucleotides 832-850 of mouse Rpt4. The siRNA targeting Rpt5 corresponds to nucleotides 508 to 526 of mouse Rpt5 (GenBank accession number NM_008948.2) relative to the first nucleotide of the start codon. A previously described siRNA duplex against the control gene, green fluorescent protein (GFP) was used as a negative control [82].

UT-2/pHMG-Red-T7 and CHO-K1 cells were set up for experiments in 60- or 100-mm dishes as described in the figure legends. Unless indicated otherwise, the cells were transfected

on days 1 and 2 with duplexes of siRNA using a ratio of 2 µl of Lipofectamine™ RNAiMAX (Invitrogen) to 40-50 pmol of siRNA duplexes per dish. Cells were washed with 2 ml of medium B (without antibiotics) and refed 1.6 ml of medium B (without antibiotics) per dish. Duplexes of siRNAs were diluted in Opti-MEM I reduced serum medium (Invitrogen) to a final volume of 370 µl per dish. Lipofectamine RNAiMAX was diluted with Opti-MEM I to a final volume of 30 µl per dish and incubated at room temperature for 5 min. The siRNA and Lipofectamine RNAiMAX mixtures were combined and further incubated for 10-20 min at room temperature. The combined siRNA and Lipofectamine RNAiMAX mixtures (400 µl) were then added to each dish. Incubation conditions are described in the figure legends. Following incubations, triplicate dishes of cells were harvested and pooled for analysis. When 100-mm dishes were used, cells were transfected on day 1 with duplexes of siRNA using a ratio of 6 µl of Lipofectamine RNAiMAX to 120 pmol of siRNA duplexes per dish. Cells were washed with 5 ml of medium B (without antibiotics) and refed 4.8 ml of medium B (without antibiotics) per dish. Duplexes of siRNAs were diluted in Opti-MEM I reduced serum medium (Invitrogen) to a final volume of 1110 µl per dish. Lipofecctamine RNAi MAX was diluted with Opti-MEM I to a final volume of 90 µl per dish and incubated at room temperature for 5 min. The siRNA and Lipofectamine RNAiMAX mixtures were combined and further incubated for 10-20 min at room temp. The combined siRNA and Lipofectamine RNAiMAX mixtures (1.2 ml) were then added to each dish. Incubation conditions are described in the figure legends. Following incubations, triplicate dishes of cells were harvested (70-80% confluence) and pooled for analysis.

Whole Cell Lysis

Triplicate dishes of cells were harvested into culture medium and washed with PBS. The cell pellets were resuspended in 200 µl of Buffer D (50 mM Tris-HCl, pH 8.0, 150 mM NaCl, 0.1% SDS, 1.5% NP-40, 0.5% deoxycholate, 2mM $MgCl_2$ with protease inhibitor cocktail),

passed through a 22.5-gauge needle 15 times, rotated for 30 min at 4 °C, and centrifuged at 16,000 X g for 15 min at 4 °C.

2.4 Results

A plausible explanation for the inefficiency of reductase dislocation from ER membranes of intact or permeabilized cells is the existence of additional post-ubiquitination steps that occur prior to cytosolic release. For example, ubiquitinated reductase may become extracted across the ER membrane and subsequently dislocated into the cytosol for degradation. To measure this putative extraction step, we examined the membrane association of reductase in sterol-treated cells. Reductase-deficient UT-2 cells [77] were transfected with an expression plasmid encoding a previously described version of full-length reductase, designated HMG-Red-T7, which contains two copies of the T7 epitope in the lumenal loop between transmembrane helices 7 and 8 [65]. A stable line expressing HMG-Red-T7 was isolated and designated UT-2/pHMG-Red-T7. In the experiment of Fig. 4*A*, UT-2/pHMG-Red-T7 cells were depleted of sterols and subsequently treated with the proteasome inhibitor MG-132 (to block reductase ERAD) in the absence or presence of 25-HC plus mevalonate (to provide nonsterol isoprenoids). Following treatments, cells were harvested for subcellular fractionation. Resulting membranes were then washed in control TBS, 100 mM Na_2CO_3, 1 M KCl, or 1% NP-40 buffers and subsequently separated into pellet and supernatant fractions by centrifugation. Immunoblot analysis of these fractions revealed that reductase remained associated with the pellet when membranes were washed with the control TBS buffer (Fig. 4*A*, top and bottom panels, lanes 1 and 2). However, 25-HC plus mevalonate caused a small fraction of reductase to become released from membranes that were treated with the high pH buffer containing 100 mM Na_2CO_3 (bottom panel, lane 4). Treatment of the membranes with the nonionic detergent NP-40 released reductase into the supernatant regardless of the absence or presence of 25-HC plus

mevalonate (lanes 7 and 8). The samples were also immunoblotted for two control proteins, GM130 and calnexin. The Golgi-localized GM130 lacks transmembrane helices and is associated with membranes via hydrophobic interactions [81]. Consistent with this, the protein was fully released from membranes by high pH (bottom panel, lanes 11 and 12). Calnexin, a molecular chaperone that is integrated in ER membranes by a single membrane-spanning segment [83], was only released into the supernatant when membranes were dissolved in NP-40 (bottom panel, lanes 23 and 24).

The experiment shown in Fig. 4*B* examines the individual and combined effects of sterol and nonsterol isoprenoids on the membrane association of reductase. The results show that, when added to cells alone, mevalonate or 25-HC had only a slight effect on the amount of reductase released from membranes by the high pH wash (Fig. 4*B*, second panel). The combination of 10 mM mevalonate and 25-HC enhanced the high pH-mediated release of reductase from isolated membranes (lane 10). GM130 was only released by high pH wash (fourth panel, lanes 3-10), whereas NP-40 treatment of membranes caused the complete release of calnexin from membranes (sixth panel, lanes 11 and 12). To more clearly demonstrate the effect of nonsterol isoprenoids on the membrane association of reductase, we conducted an experiment using geranylgeraniol, which, unlike mevalonate, cannot become incorporated into sterols. The results show that reductase remained associated with the membrane pellet when cells were treated with geranylgeraniol alone (Fig. 4*C*, second panel, lanes 4-6), but the nonsterol isoprenoid combined with 25-HC to cause release of reductase from membranes (Fig. 4*C*, second panel, lanes 8-10).

Results of Fig. 4 show that sterol and nonsterol isoprenoids combine to trigger the extraction of reductase across ER membranes. However, the reaction appeared visibly to be inefficient as determined by membrane association of reductase compared to reductase

solubilized by NP-40 (Fig. 4C, second panel, lanes 10-12). Thus, we next sought to develop a more robust assay for sterol-induced membrane extraction of reductase that exploits the lumenal orientation of the T7 epitope in HMG-Red-T7 (Fig. 5*A* and 6*A*). This orientation was confirmed by subjecting intact membranes from sterol-deprived UT-2/pHMG-Red-T7 cells to *in vitro* digestion with trypsin, which produced protected fragments of reductase that were detected by anti-T7 immunoblot analysis (Fig. 5*B*). Sequence analysis suggests that trypsinolysis should produce a 6.4 kD protected fragment of reductase. In my studies, ~30 kD protected fragments of reductase that likely result from alternative sites of trypsin cleavage were observed. Although the membrane domain of reductase contains several lysines and arginines, these residues localize to short cytosolic loops that may be closely opposed to the ER membrane and inaccessible to trypsin. The protected fragments of reductase were susceptible to trypsinolysis when membranes were dissolved in NP-40 (Fig. 5*B*, *top panel*, *lanes 7-10*), indicating the T7 epitopes were sequestered within the ER lumen. To control for membrane integrity, samples were immunoblotted for the cholesterol-sensing escort protein Scap and calnexin. Scap is integrated in ER membranes with a topology similar to that of reductase: the N-terminal domain of Scap contains eight membrane-spanning helices and is followed by a large cytosolic domain that contains WD repeats (Fig. 5*A*) [52, 80]. The monoclonal antibody IgG-9D5 recognizes residues 540-707 of Scap, which corresponds to the large, N-glycosylated lumenal loop between transmembrane helices 7 and 8 of the protein; this antibody was previously used to define Scap's membrane orientation [52]. Trypsinolysis of membranes led to the appearance of a protected fragment of Scap that was detected in IgG-9D5 immunoblots (Fig. 5*B*). Calnexin is a type II ER membrane protein that consists of a large N-terminal lumenal domain, a single transmembrane helix, and a short cytoplasmic tail [83]. Immunoblot analysis with polyclonal antibodies against the lumenal domain of calnexin revealed the generation of a protected fragment of the protein in the presence of trypsin (Fig. 5*B*). The lumenal orientation of the T7

epitope in HMG-Red-T7 is further supported by the observation that the trypsin-protected fragments were sensitive to digestion by either PNGase F or EndoH, which removed the single N-glycan in reductase (Fig. 5*C*).

Having established the membrane orientation of the T7 epitope in HMG-Red-T7, we next set out to determine whether *in vitro* trypsin digestion could be used to monitor sterol- and geranylgeraniol-induced extraction of the protein across ER membranes. In the experiment of Fig. 6*B*, UT-2/pHMG-Red-T7 cells were subjected to treatment with MG-132 in the absence or presence of 25-HC plus mevalonate prior to harvest and subcellular fractionation. Aliquots of the resulting membrane fractions were then incubated with a fixed concentration of trypsin for various periods of time, and subsequently analyzed by anti-T7 immunoblot. In the absence of trypsin, equivalent amounts of full-length reductase were detected in membranes isolated from cells incubated with or without 25-HC plus mevalonate (Fig. 6*B*, top panel, lanes 1-6). Protected fragments of reductase were observed in immunoblots of membranes from sterol-deprived cells treated with trypsin for the shortest period of time, 15 min (lane 7); the amount of these fragments was reduced in membranes from 25-HC plus mevalonate-treated cells (lane 8). Longer incubations with trypsin led to a slight visible reduction of the protected fragments of reductase in membranes from sterol-deprived cells (lanes 9 and 11), a likely reflection of the basal membrane extraction and degradation of reductase. The susceptibility of these fragments to trypsin was visibly enhanced when cells were treated with 25-HC plus mevalonate prior to subcellular fractionation (lanes 10 and 12). Membrane integrity was confirmed by subjecting the proteolytic digests to immunoblot analysis with IgG-9D5 against Scap (Fig. 6*B*, bottom panel). The expected protease-protected fragment of Scap was observed in the IgG-9D5 immunoblot and importantly, the susceptibility of this fragment to trypsinolysis was not influenced by the absence or presence of 25-HC plus mevalonate (7-12). The experiment shown in Fig. 6*C* shows

that the sterol-dependent digestion of the protected fragments of reductase by trypsin was comparative to the amount of the protease in the assay.

The contribution of sterol and nonsterol isoprenoids to the membrane extraction of reductase, as determined by sensitivity to trypsin digestion, was examined by treating UT-2/pHMG-Red-T7 cells with 25-HC, mevalonate, and geranylgeraniol individually or in combination prior to harvest and subcellular fractionation. Immunoblot analysis shows that, in the absence of 25-HC, a high concentration (10 mM) of mevalonate caused a significant fraction of the protected fragment of reductase to become fully digested by trypsin *in vitro* (Fig. 7*A*, top panel, lanes 3-6). This is consistent with conversion of mevalonate to both sterol and nonsterol isoprenoids that maximally stimulate the degradation [65, 84] as well as the membrane extraction of reductase. Treatment of the cells with 25-HC alone did not render the protected fragment susceptible to trypsinolysis (lane 7); however, 25-HC together with low concentrations of mevalonate (1 and 3 mM) caused the fragment to disappear upon trypsin digestion (lanes 8 and 9). Levels of the protected fragment of Scap remained constant, regardless of whether or not cells were treated with 25-HC and/or mevalonate (bottom panel, lanes 3-10). Similar results were obtained when we measured the effect of geranylgeraniol on the membrane extraction of reductase (Fig. 7*B*). The trypsin-protected fragment of reductase persisted in membranes from cells treated individually with geranylgeraniol (Fig. 7*B*, top panel, lanes 4-6) or 25-HC (lane 7). However, geranylgeraniol combined with 25-HC to cause the protected fragments to become susceptible to trypsinolysis (lanes 8-10). These results obtained for membrane extraction of HMG-Red-T7 are consistent with those that demonstrate the requirement of sterol and nonsterol isoprenoids for accelerated ERAD of the protein (see Fig. 8*A* and 8*B*).

In cultured cells, the 1,1-bisphosphonate ester Apomine (Fig. 7*C*), and its structurally related analog SR-12813, mimic 25-HC in stimulating Insig-dependent ubiquitination and

subsequent ERAD of reductase [72, 85]. Thus, we next designed an experiment to evaluate Apomine in triggering the extraction of reductase across membranes. In membranes from UT-2/pHMG-Red-T7 cells treated with 25-HC plus mevalonate (3 mM), the protected fragments of reductase were digested by trypsin as expected (Fig. 7*C*, top panel, compare lanes 5 and 6). Treatment of the cells with Apomine and 3 mM mevalonate rendered the protected fragments susceptible to trypsinolysis (lanes 6-8), indicating that like 25-HC, Apomine induces extraction of reductase across ER membranes en route to degradation.

To further establish the physiologic relevance of the membrane extraction of reductase, we next examined a role for Insigs in the reaction using RNA interference (RNAi). UT-2/pHMG-Red-T7 cells were transfected with duplexes of small interfering RNAs (siRNAs) targeting a control mRNA encoding green fluorescent protein (GFP) or mRNAs encoding Insig-1 and Insig-2. Following siRNA transfection, cells were treated in the absence or presence of 25-HC plus mevalonate and MG-132 prior to harvest, subcellular fractionation, and treatment of membranes with or without trypsin. The results show that in the presence of 25-HC plus mevalonate and absence of MG-132, reductase was appropriately degraded from membranes of cells transfected with GFP siRNA (Fig. 9*A*, top panel, lanes 1 and 2). Trypsin digestion of sterol-deprived membranes led to the appearance of the expected protected fragments of reductase (lane 3). These protected fragments were absent in membranes from sterol-treated cells (lane 4). However, this absence was due to accelerated ERAD of reductase rather than from extraction of the protein across ER membranes. Treatment with NP-40 disrupted membrane integrity and rendered the protected fragments of reductase susceptible to trypsinolysis (lane 5). As expected, RNAi-mediated knockdown of Insig-1 and Insig-2 blocked sterol-accelerated degradation of reductase (Fig. 9*A*, top panel, compare lanes 1 and 2 with lanes 7 and 8). The 25-HC plus mevalonate-dependent susceptibility of the protected fragments to trypsinolysis was

blunted in Insig-1 and -2 knockdown cells (lanes 9 and 10). The fragments were fully digested by trypsin in the presence of NP-40 (lanes 11 and 12), indicating their sequestration in the ER lumen. Levels of trypsin-protected fragments of Scap and calnexin were not affected by the absence or presence of 25-HC plus mevalonate in control or Insig-1/-2 knockdown cells (middle and bottom panels, lanes 3, 4, 9, and 10).

In the experiment of Figure 9*B*, the membrane extraction assay was conducted with membranes from cells in which reductase degradation was blocked by either proteasome inhibition or by RNAi-mediated knockdown of Insigs. In control cells transfected with the GFP siRNA and treated with MG-132, sterol-accelerated degradation of reductase was blocked (Fig. 9*B*, top panel, lanes 1 and 2). Trypsin digestion led to the appearance of the protected fragment of reductase in membranes isolated from cells incubated in the absence (lane 3), but not in the presence of 25-HC plus mevalonate (lane 4). Knockdown of Insig-1 and Insig-2 resulted in visible resistance of the protected fragments of reductase to trypsinolysis (lanes 7 and 8), demonstrating their requirement in the membrane extraction of reductase.

Considering its role in cytosolic dislocation of reductase [70], we next conducted RNAi experiments to determine whether VCP/p97 is required for membrane extraction of the enzyme. As expected, knockdown of VCP/p97 blunted sterol-accelerated reductase ERAD (Fig. 9*C*, top panel, compare lanes 1 and 2 with lanes 5 and 6). In the absence of MG-132, the trypsin-protected fragments of reductase were observed in membranes from control-transfected cells deprived of sterols (lane 3), but not in membranes isolated from cells treated with 25-HC plus mevalonate (lane 4). The protected fragments of reductase in membranes from VCP/p97 knockdown cells resisted trypsin digestion (lanes 7 and 8), regardless of whether the cells had been treated with or without 25-HC plus mevalonate before harvest. In the presence of MG-132, 25-HC plus mevalonate rendered the protected fragments of reductase susceptible to

trypsinolysis in GFP knockdown cells (Fig. 9*D*, top panel, lanes 3 and 4). However, these fragments were again resistant to digestion in VCP/p97 knockdown cells (lanes 7 and 8), consistent with a key role for VCP/p97 in sterol-induced extraction of reductase to the cytosolic face of the ER. It should be noted that RNAi-mediated knockdown of VCP/p97 or Insig-1 and Insig-2 prevented membrane extraction of reductase in MG-132-treated cells (Fig. 10).

In previous studies, we reconstituted Insig-mediated, sterol-accelerated ERAD of mammalian reductase in *Drosophila* S2 cells [72]. Building on this observation, a postdoctoral fellow in the laboratory, Dr. Dong-Jae Jun, conducted a high throughput genome-wide RNAi screen in S2 cells. Several genes encoding components of the 26S proteasome were identified among those required for sterol-accelerated ERAD of reductase in S2 cells (Jun, D.-J. and DeBose-Boyd, R.A., unpublished observations). Some of these genes encode *Drosophila* homologs of the AAA-ATPase subunits of the proteasome 19S regulatory particle (RP) [73, 74]. The 19S RP uses energy from ATP hydrolysis to unfold substrates, trigger the activation of the 20S core particle (20S CP) of the proteasome, and translocate the substrate into the proteolytic chamber of the 20S CP. Although the requirement for the 19S RP in reductase degradation in *Drosophila* cells was not surprising, it led us to the realization that the regulatory particle has been implicated in cytosolic dislocation of several ERAD substrates [74]. To determine whether the 19S RP is required for cytosolic dislocation of reductase, we began by screening siRNAs that target the AAA-ATPases of the regulatory particle for the ability to block reductase degradation. The results show that knockdown of these ATPases blunted reductase degradation to various degrees (Fig. 11), which is likely due to the efficiency of their RNAi-mediated knockdown. Thus, we focused on three AAA-ATPases, Rpt2, Rpt5, and Rtp4, whose knockdown produced the most substantial and consistent inhibition of reductase degradation and for which specific antibodies are commercially available.

In the experiment of Figure 12*A*, CHO-K1 cells transfected with control GFP or Rpt5 siRNA duplexes were treated in the absence or presence of 25-HC plus mevalonate and MG-132. The cells were subsequently harvested and post nuclear supernatants were separated into membrane and cytosol fractions by 100,000 x g centrifugation. The results show that 25-HC plus mevalonate stimulated ERAD of reductase from membranes as expected (Fig. 12*A*, top panel, compare lanes 1 and 2). This degradation was blocked by treatment of the cells with MG-132 (lane 4) or by the RNAi-mediated knockdown of Rpt5 (compare lanes 5 and 6). In the presence of MG-132, full-length reductase appeared in the cytosol, but only when cells were also subjected to treatment with 25-HC plus mevalonate (second panel, lane 4). In contrast, reductase was not present in the cytosol of Rpt5 knockdown cells, regardless of the absence or presence of MG-132 (second panel, lanes 5-8). An experiment conducted by Dr. Isamu Hartman, a postdoctoral fellow in the laboratory showed in Figure 13 shows that Rpt5 co-precipitated with cytosolic reductase in 25-HC plus mevalonate treated cells, consistent with a role of the 19S RP in reductase dislocation. The sterol-accelerated ERAD (Fig. 12*B*, top panel, lanes 3 and 4) and the cytosolic dislocation of reductase (bottom panel, lanes 9 and 10) were blunted by RNAi-mediated knockdown of the Rpt4 AAA-ATPase subunit of the 19S RP. Knockdown of the other AAA-ATPases of the 19S RP similarly blunted the sterol-induced cytosolic dislocation of reductase (Figure 14). Ubiquitinated proteins accumulated in Rpt4 and Rpt5 knockdown cells to levels similar to those observed in MG-132-treated cells (Figure 15). Thus, the effect of Rpt4 and Rpt5 knockdown on cytosolic dislocation of reductase likely results from disruption of the entire 19S RP rather than a specific effect of the individual ATPase subunits.

We next examined whether ATPases of the 19S RP are required for sterol-induced membrane extraction of reductase using the trypsin protection assay. As shown in Figure 16*A*,

reductase was extracted across membranes of UT-2/pHMG-Red-T7 cells transfected with control GFP siRNA and treated with 25-HC plus mevalonate in the presence of MG-132 (top panel, compare lanes 3 and 4). The RNAi-mediated knockdown of VCP/p97 blunted sterol-induced membrane extraction of reductase as expected (lanes 7 and 8); however, the enzyme continued to become extracted in 25-HC plus mevalonate-treated Rpt5 knockdown cells (lanes 11 and 12). The replicate experiments shown in Supplemental 17 confirm the continued membrane extraction of reductase in Rpt5 knockdown cells. Similar results were obtained in cells lacking the Rpt2 AAA-ATPase subunit of the 19S RP. Knockdown of VCP/p97, but not of Rpt2, blunted sterol-induced extraction of reductase (Fig. 16*B,* top panel, compare lanes 3, 4, 7, 8, 11, and 12).

The results of Figure 16*A* and 16*B* indicate that VCP/p97 and the 19S RP mediate distinct steps (membrane extraction and cytosolic dislocation) in the reductase ERAD pathway. However, an alternative explanation for these results is that VCP/p97 solely mediates membrane extraction and cytosolic dislocation of reductase. The 19S RP has been shown to exhibit chaperone activity *in vitro* [86] and prevents aggregation of dislocated catalytic A chains of the toxin ricin [87]. In the absence of the 19S RP, membrane extracted and/or cytosolic reductase may become aggregated and pellet with membranes upon centrifugation. To rule out this possibility, membranes isolated from control and Rpt5 knockdown cells were resuspended in buffer containing a high concentration of sucrose; the samples were then overlaid with buffer of decreasing sucrose concentration. Following centrifugation overnight, aliquots taken from top to bottom of the gradient were analyzed by immunoblot. The results show that the majority of reductase as well as calnexin floated to the lower sucrose gradient in control knockdown cells (Fig. 16*C*, top two panels, lanes 2-4). A similar pattern was observed in Rpt5 knockdown cells (bottom two panels, lanes 2-4), indicating that reductase remained membrane-associated

regardless of the absence or presence of Rpt5. The cytosolic protein Bag6 has been identified in an ubiquitin ligase-associated multiprotein complex that chaperones dislocated ERAD substrates to proteasomes for degradation [88]. In Bag6 knockdown cells, degradation of these substrates is blocked, their solubility in the detergent NP-40 is reduced, and the proteins accumulate in detergent insoluble aggregates. The second line of evidence indicating that the 19S RP does not perform a chaperone function in reductase degradation is provided by the detergent solubility experiment shown in Figure 16*D*. The results of this experiment show that the solubility of reductase in NP-40 remained unchanged in control and Rpt5 knockdown cells (top panel, compare lanes 6 and 8).

2.5 Discussion

Figure 18 shows a model for the sterol-accelerated ERAD of reductase based on data presented in the current study. Similar to previously proposed models [69], the reaction is initiated by sterol-induced binding of reductase to Insigs, resulting in gp78/Trc8-mediated ubiquitination of the protein. The current results indicate that once ubiquitinated, reductase becomes extracted across the ER membrane through a reaction mediated by the AAA-ATPase VCP/p97. Membrane-associated, extracted reductase then becomes dislodged from membranes and dislocated into the cytosol where the protein is degraded by proteasomes. The novel aspect of this revised model is the proposed membrane extraction step that is distinct from, and precedes cytosolic dislocation of reductase. Initial evidence for this putative intermediate step is provided by experiments examining the membrane association of reductase (Fig. 4*A*). When proteasomes were inhibited by MG-132, the oxysterol 25-HC and the nonsterol isoprenoid geranylgeraniol caused a fraction of reductase to become peripherally associated with membranes as indicated by its release by high pH wash (Fig. 4*B* and 4*C*). These results indicate that sterol and nonsterol isoprenoids trigger reductase to become fully extracted across

the ER membrane prior to degradation. These results, taken together with our previous observation that geranylgeraniol also combines with 25-HC to maximally stimulate reductase ERAD but does not appreciably affect sterol-induced ubiquitination of the protein [66, 71], forms the basis for the conclusion that geranylgeraniol modulates post-ubiquitination steps in reductase ERAD (see Fig. 8).

Considering that reductase is embedded in ER membranes, it is logical to postulate that its extraction across ER membranes must precede cytosolic dislocation as depicted in Figure 18. However, it remained to be determined whether membrane extraction and cytosolic dislocation of reductase are distinct and separable or coupled reactions. In order to distinguish between these possibilities, we sought to develop an assay for membrane extraction of reductase that is more robust than measuring its association with membranes. For this purpose, we exploited a previously described version of reductase containing T7 epitopes in the lumenal loop between transmembrane domains 7 and 8 (Fig. 5*A*) (6). *In vitro* digestion of intact membranes isolated from sterol-deprived cells with trypsin-generated fragments of reductase detected in anti-T7 immunoblots that were protected from proteolysis (Fig. 5*B*). Trypsinolysis of membranes from sterol-treated cells led to a marked reduction in the amount of protected fragments in a manner that was proportional to the duration of incubation (Fig. 6*B*) and amount of trypsin in the assay (Fig. 6*C*). The extraction of reductase across the ER membrane, as determined by susceptibility of its lumenal T7 epitopes to trypsin digestion, required the additions of both 25-HC and geranylgeraniol to cells prior to harvest and subcellular fractionation (Fig. 7*A* and 7*B*). In addition, membrane extraction of reductase was triggered by the 1,1-bisphosphonate ester Apomine (Fig. 7*C*), which mimics sterols in accelerating reductase ERAD [85]. RNAi-mediated knockdown of Insig-1 and Insig-2 not only blunted sterol-accelerated ERAD of reductase but the treatment also blocked its membrane extraction (Fig. 9*A* and 9*B*). Knockdown of VCP/p97

similarly abolished both the sterol-induced membrane extraction and ERAD of reductase (Fig. 9*C* and 9*D*). These observations indicate that sterol- and geranylgeraniol-regulated susceptibility of the lumenal T7 epitopes in reductase to trypsinolysis results from its Insig-dependent, VCP/p97-mediated extraction across membranes, exposing the lumenal epitopes to the cytosolic face of the ER. It is important to note that a significant fraction of reductase was observed to be extracted in the trypsin protection assay, whereas only a small fraction of the protein was found to be extracted in membrane association studies. A plausible explanation for this difference is that membrane association studies using the high pH wash measures reductase that has become completely membrane extracted, while the trypsin protection assay measures both completely as well as partially extracted populations of reductase. Partially extracted reductase may result from a feedback mechanism that prevents accumulation of ERAD substrates in the cytosol when proteasomes are impaired or from the saturation of proteins required for extraction of reductase across membranes.

The 26S proteasome consists of two large subcomplexes designated the 20S core particle (CP) and the 19S regulatory particle (19S RP) [73, 74, 89]. The 20S CP is comprised of four stacked heptameric rings organized in a barrel structure with openings at each end. The two inner rings are composed of b-subunits that exhibit proteolytic activity whereas the two outer rings consist of structural a-subunits. Both ends of the 20S CP are associated with the 19S RP, which is composed of a base that contains six AAA-ATPases and a lid containing non-ATPase subunits. Factors within the lid of the 19S RP mediate recruitment of ubiquitinated substrates and their subsequent deubiquitination. Binding of the base to the 20S CP activates proteolysis and the AAA-ATPases of the base facilitate substrate unfolding and delivery into the proteolytic chamber for degradation. In addition, the 19S RP has been implicated in cytosolic dislocation of ERAD substrates [39, 74, 90, 91]; however, the majority of these studies focused on soluble

substrates sequestered within the ER lumen. In some cases, dislocation of these substrates was independent of ubiquitination and the action of VCP/p97. In the few studies in which a role for the 19S RP in the ERAD of membrane-bound substrates was examined, degradation appeared to be coupled to retrotranslocation and extraction; proteasome inhibition did not cause the appearance of these substrates in the cytosol [92, 93]. This contrasts with our previous and current findings that MG-132 uncoupled sterol-induced cytosolic dislocation of reductase from its sterol-accelerated proteasomal degradation. Treatment of cells with the inhibitor caused reductase to appear in the cytosol of sterol-treated cells [70]. This appearance, which required reductase ubiquitination as well as the presence of Insigs and VCP/p97, indicated that reductase might become dislocated from ER membranes before proteasomal degradation commences. Notably, AAA-ATPases of the 19S RP have been shown to be required for the ERAD of Hmg2p, a homolog of reductase in the yeast *Saccharomyces cerevisiae* [91]. However, a role for the 19S RP in the cytosolic dislocation of Hmg2p was not appraised in the study.

In the current study, we appraised a role for the 19S RP in post-ubiquitination steps of sterol-accelerated reductase degradation. Consistent with a role for proteasomes in sterol-accelerated reductase ERAD, the reaction was blunted by the proteasome inhibitor MG-132 or by the knockdown of AAA-ATPases of the 19S RP [73, 74] (Fig. 11). In surprising contrast to results obtained when proteolytic activity of proteasomes was inhibited, knockdown of the 19S RP ATPases prevented sterol-induced dislocation of reductase into the cytosol (Fig. 12*A*, 12*B,* and Fig. 14). Experiments utilizing the trypsin protection assay revealed that while VCP/p97 knockdown inhibited sterol-induced extraction of reductase across membranes, the reaction continued in cells deficient for the 19S RP (Fig. 16*A,* 16*B,* and Fig. 17). Knockdown of the 19S RP did not appear to cause membrane-extracted reductase to become aggregated as indicated

by its association with membranes in knockdown cells (Fig. 16*C*) and its detergent solubility (Fig. 16*D*). These findings not only demonstrate that the 19S RP and 20S CP mediate respectively, the cytosolic dislocation and proteolytic degradation of reductase, they also support our proposal that membrane extraction (mediated by VCP/p97 and enhanced by geranylgeraniol) and cytosolic dislocation (mediated by the 19S RP) are sequential, separable steps in the reductase ERAD pathway (see Fig. 18). It is noteworthy that dislocation of at least one lumenal ERAD substrate, the μs heavy chain of secretory IgM, involves consecutive membrane extraction and cytosolic dislocation steps mediated by VCP/p97 and proteasomes, respectively [94]. However, a major difference exists in the mechanism for membrane extraction and cytosolic dislocation of reductase and μs: proteolytic activity of proteasomes is required for dislocation of μs, whereas reductase dislocation can only be observed upon proteasome inhibition. Proteasome inhibition is known to cause several membrane-bound ERAD substrates in addition to reductase to accumulate in the cytosol of cells [40, 95-101]. It will thus be important to determine in future studies whether membrane extraction and release into the cytosol through sequential actions of VCP/p97 and the proteasome 19S RP is a general ERAD mechanism or a peculiarity in the sterol-accelerated ERAD of reductase. Finally, the current findings, together with our previous studies [66, 71], pinpoint the action of geranylgeraniol in reductase ERAD to reactions that underlie VCP/p97-mediated membrane extraction of ubiquitinated reductase. The establishment of a robust assay for membrane extraction of reductase provides a means to further characterize the mechanism through which geranylgeraniol augments reductase ERAD and to identify the target of the nonsterol isoprenoid.

FIGURE 4:

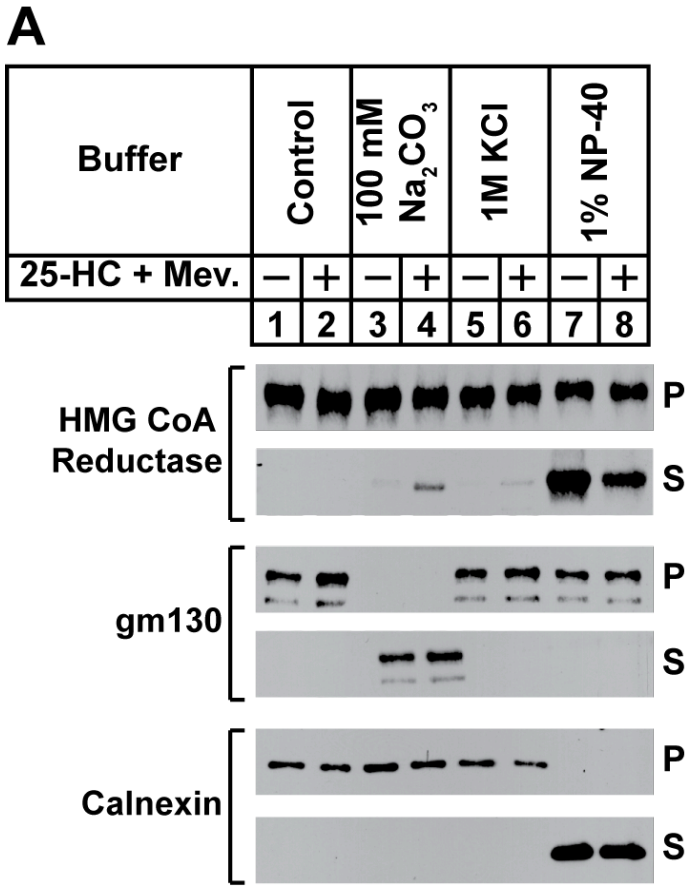
A
Buffer
Control
100 mM Na_2CO_3
1M KCl
1% NP-40
25-HC + Mev.
– + – + – + – +
1 2 3 4 5 6 7 8
HMG CoA Reductase
gm130
Calnexin
P
S

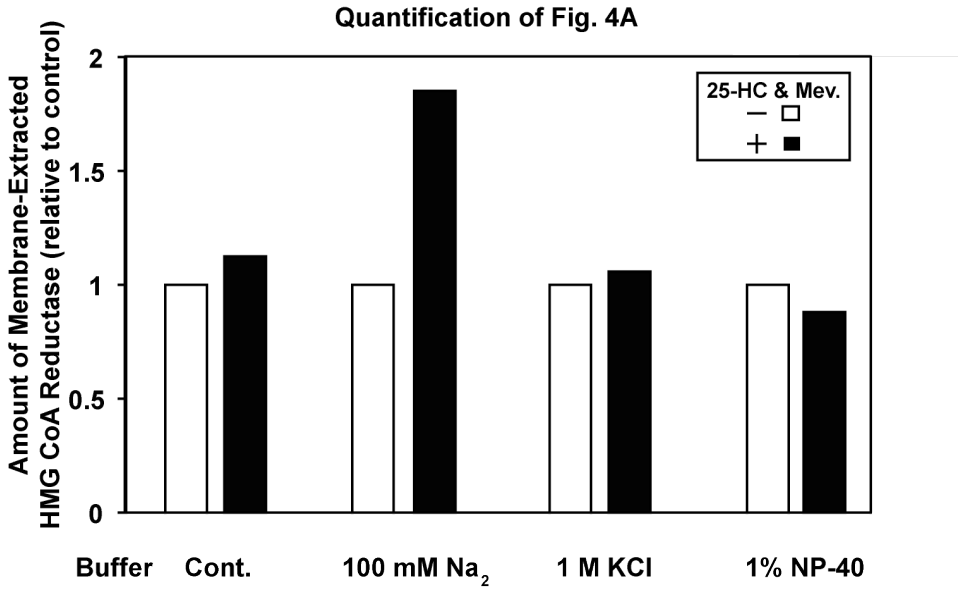
Quantification of Fig. 4A
Amount of Membrane-Extracted HMG CoA Reductase (relative to control)
2
1.5
1
0.5
0
25-HC & Mev.
– □
+ ■
Buffer
Cont.
100 mM Na_2
1 M KCl
1% NP-40

FIGURE 4 CONTINUED:

B

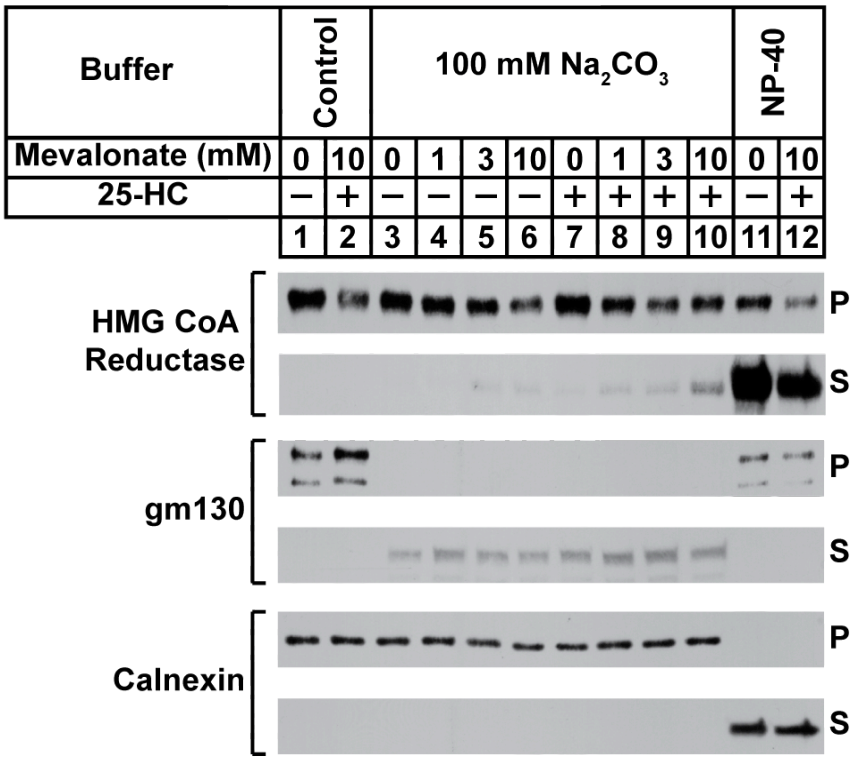

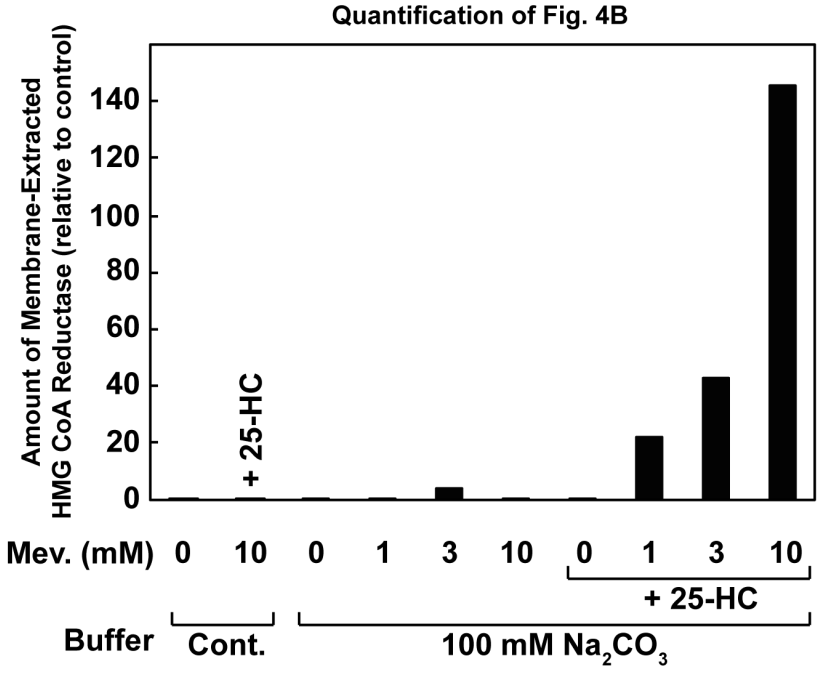

FIGURE 4 CONTINUED:

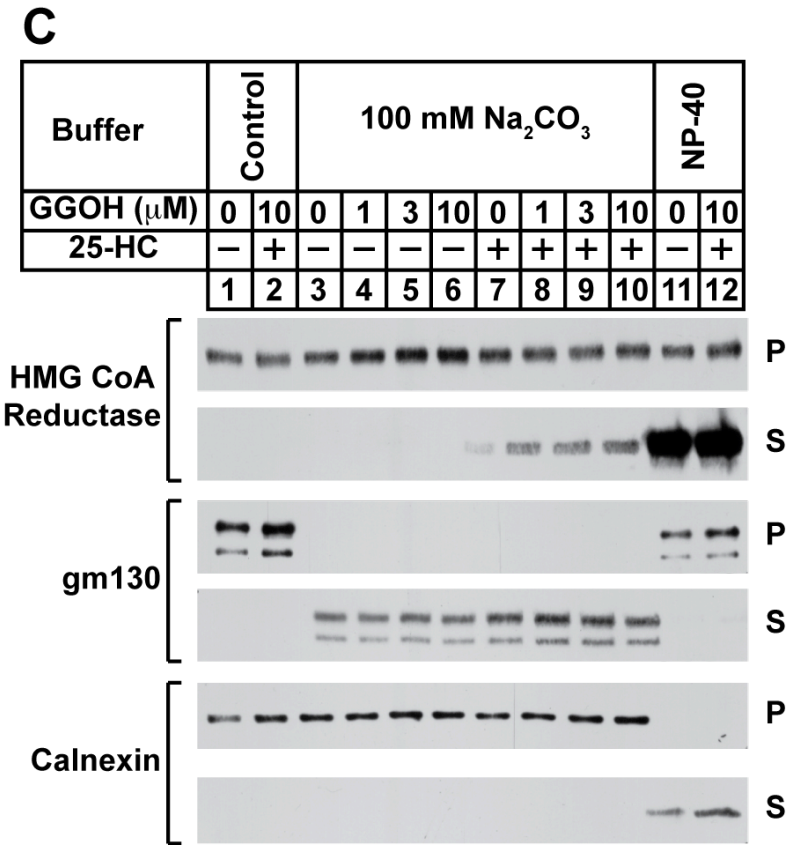

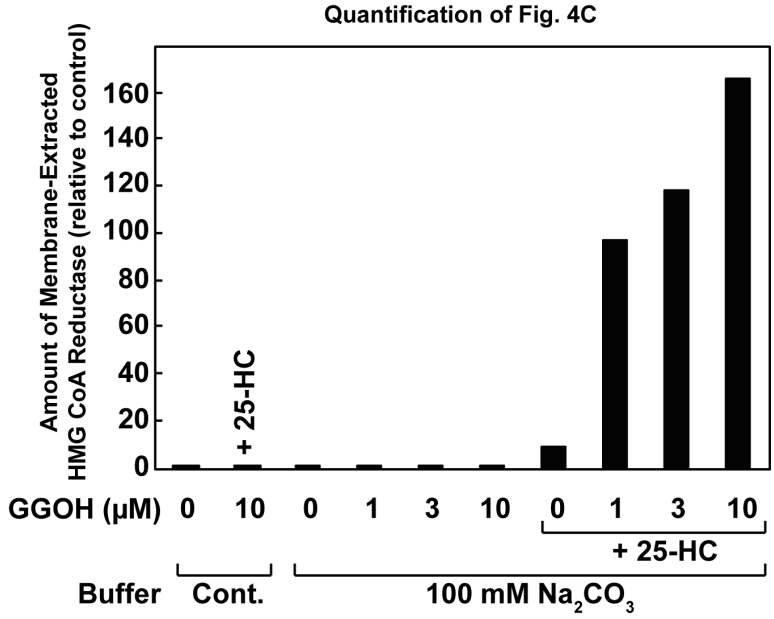

FIGURE 4 CONTINUED:

Figure 4. Peripheral association of HMG CoA reductase with membranes of sterol-treated cells. UT-2/pHMG-Red-T7 cells were set up for experiments on day 0 in medium B at a density of 2 X 10^5 (A) or 5 X 10^5 (B and C) cells per 100-mm dish. On day 3, the cells were switched to medium A supplemented with 5% LPDS, 10 μM compactin, 50 μM mevalonate, and 1 μM MG-132 in the absence or presence of 1 μg/ml 25-HC, 10 mM mevalonate (A), 1, 3, or 10 mM mevalonate (B) and 1, 3, or 10 μM geranylgeraniol (GGOH) (C) as indicated. Following incubation for 16 h at 37 °C, cells were harvested, resuspended in buffer containing 20 mM Tris-HCl, pH 7.4 and 250 mM sucrose, and lysed. Resulting lysates were then subjected to centrifugation at 1,000 X g to generate post nuclear supernatants that were subjected to an additional round of centrifugation at 20,000 X g. Membrane pellets were resuspended in an equal volume of one of the following buffers: 20 mM Tris-HCl, pH 7.4, 140 mM NaCl (Control); 20 mM Tris-HCl, pH 7.4, 1 M KCl; 100 mM Na_2CO_3; and 20 mM Tris-HCl, pH 7.4, 1% NP-40. Following rotation for 2 h at 4 °C, samples were layered on buffer containing 20 mM Tris-HCl, pH 7.4 and 500 mM sucrose and subjected to centrifugation for 30 min at 100,000 X g. Resulting supernatant fractions were concentrated through trichloroacetic acid (TCA) precipitation. Pellet (5% of total) and supernatant (37.5% of total) fractions were subjected to SDS-PAGE followed by immunoblot analysis with anti-T7 IgG (against reductase), MLO7 (against GM130), and anti-calnexin IgG. Bands corresponding to membrane-extracted reductase were quantified using ImageJ software. The intensities of these bands in the absence of 25-HC plus mevalonate or GGOH were arbitrarily set as 1.

FIGURE 5:

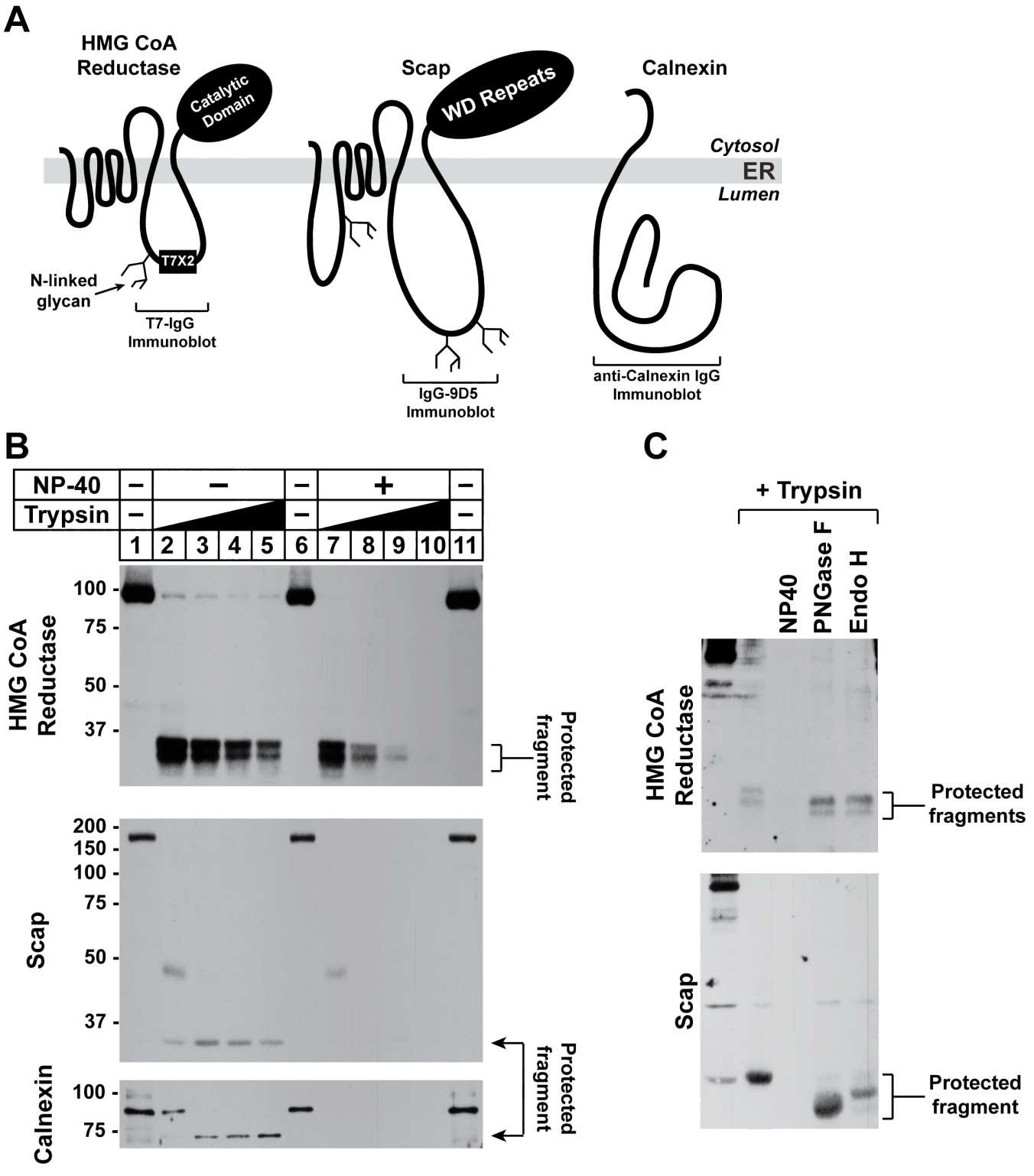
A
HMG CoA Reductase
Catalytic Domain
Scap
WD Repeats
Calnexin
Cytosol
ER
Lumen
T7X2
N-linked glycan
T7-IgG Immunoblot
IgG-9D5 Immunoblot
anti-Calnexin IgG Immunoblot
B
NP-40
Trypsin
1 2 3 4 5 6 7 8 9 10 11
HMG CoA Reductase
100
75
50
37
Protected fragment
Scap
200
150
100
75
50
37
Calnexin
100
75
C
+ Trypsin
NP40
PNGase F
Endo H
HMG CoA Reductase
Protected fragments
Scap
Protected fragment

Figure 5 continued:

Figure 5. Membrane orientation of T7 epitope in HMG CoA reductase encoded by pCMV-HMG-Red-T7. (*A*) Topology of HMG CoA reductase, Scap, and calnexin denoting the location of two T7 epitope tags in reductase encoded by pCMV-HMG-Red-T7, the epitope in SCAP recognized by monoclonal IgG-9D5, and the region in calnexin recognized by anti-calnexin IgG. Sites for N-linked glycosylation are indicated in each protein. (*B*) UT-2/pHMG-Red-T7 cells were set up on day 0 at a density of 5 X 10^5 cells per 100-mm dish in medium B. On day 2, the cells were switched to medium A supplemented with 5% LPDS, 10 μM compactin, 50 μM mevalonate, and 1 μM MG-132. Following incubation for 16 h at 37 °C, cells were harvested for subcellular fractionation using Protocol 1 as described in "Materials and Methods." Aliquots of resulting membrane fractions were resuspended in Buffer B and treated with various concentrations of trypsin (lanes 2 and 7: 2 μg, lanes 3 and 8: 6 μg, lanes 4 and 9: 10 μg, lanes 5 and 10: 14 μg) in the absence or presence of 1% NP-40 as indicated. Following incubation for 30 min at 30 °C, reactions were terminated and the samples were subjected to SDS-PAGE, followed by immunoblot analysis with anti-T7 IgG (against reductase), IgG-9D5 (against Scap), or anti-calnexin IgG. (*C*) UT-2/pHMG-Red-T7 cells were set up on day 0, treated on day 2, and harvested for subcellular fractionation using Protocol 1 as described in (*B*). Aliquots of resulting membrane fractions were then resuspended in Buffer B and subjected to trypsin proteolysis (20 μg) in the absence or presence of 1% NP-40 as indicated. Treatment of membrane fractions with PNGase F or EndoH_f (New England Biolabs, Ipswich, MA) following trypsin digestion was carried out according to the recommended manufacturer's procedure. Aliquots of the samples were then subjected to immunoblot analysis with anti-T7 IgG (against reductase) and IgG-9D5 (against Scap).

Figure 6

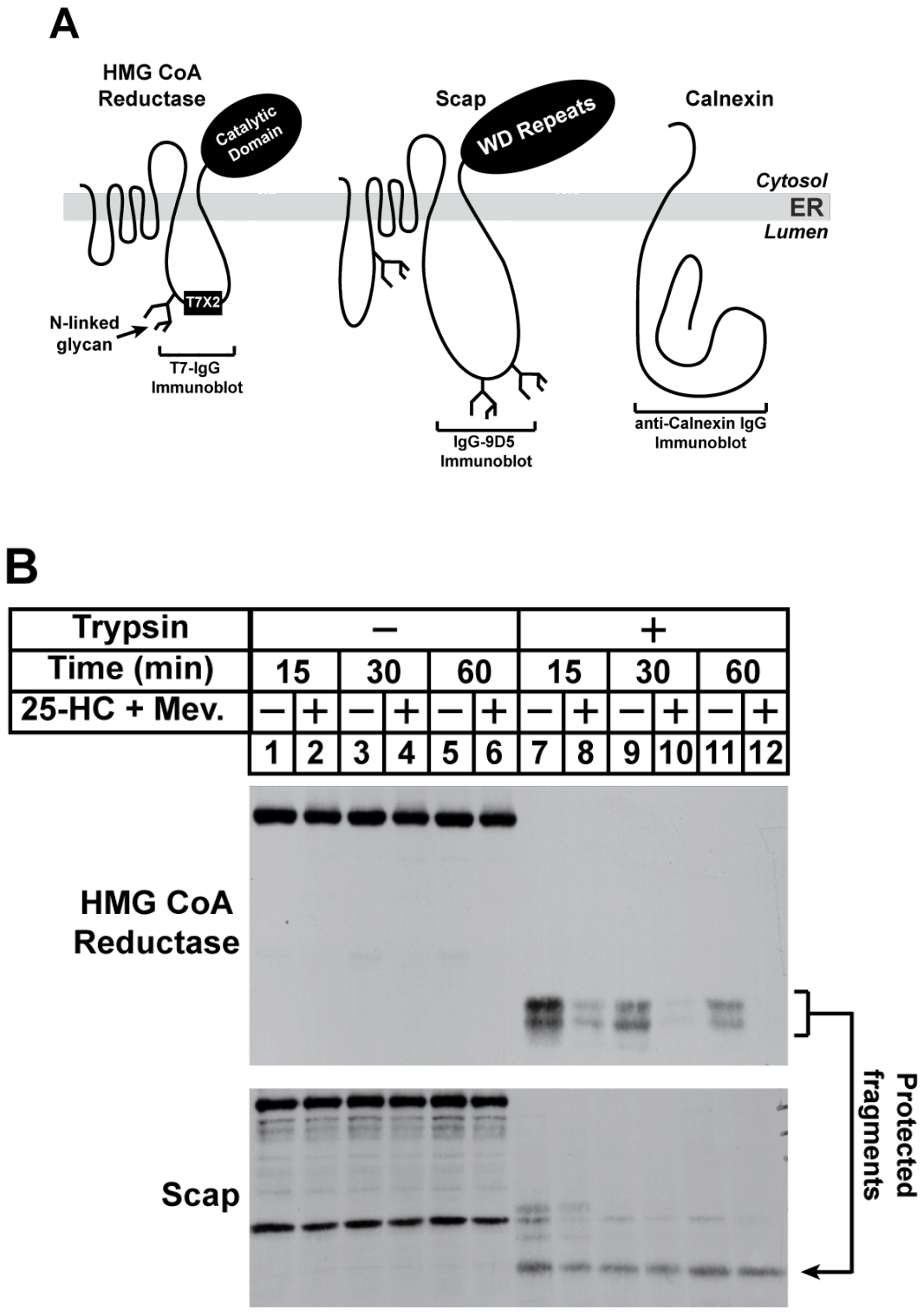
A
HMG CoA Reductase
Catalytic Domain
Scap
WD Repeats
Calnexin
Cytosol
ER
Lumen
T7X2
N-linked glycan
T7-IgG Immunoblot
IgG-9D5 Immunoblot
anti-Calnexin IgG Immunoblot
B
Trypsin
–
+
Time (min)
15
30
60
15
30
60
25-HC + Mev.
– + – + – + – + – + – +
1 2 3 4 5 6 7 8 9 10 11 12
HMG CoA Reductase
Scap
Protected fragments

FIGURE 6 CONTINUED:

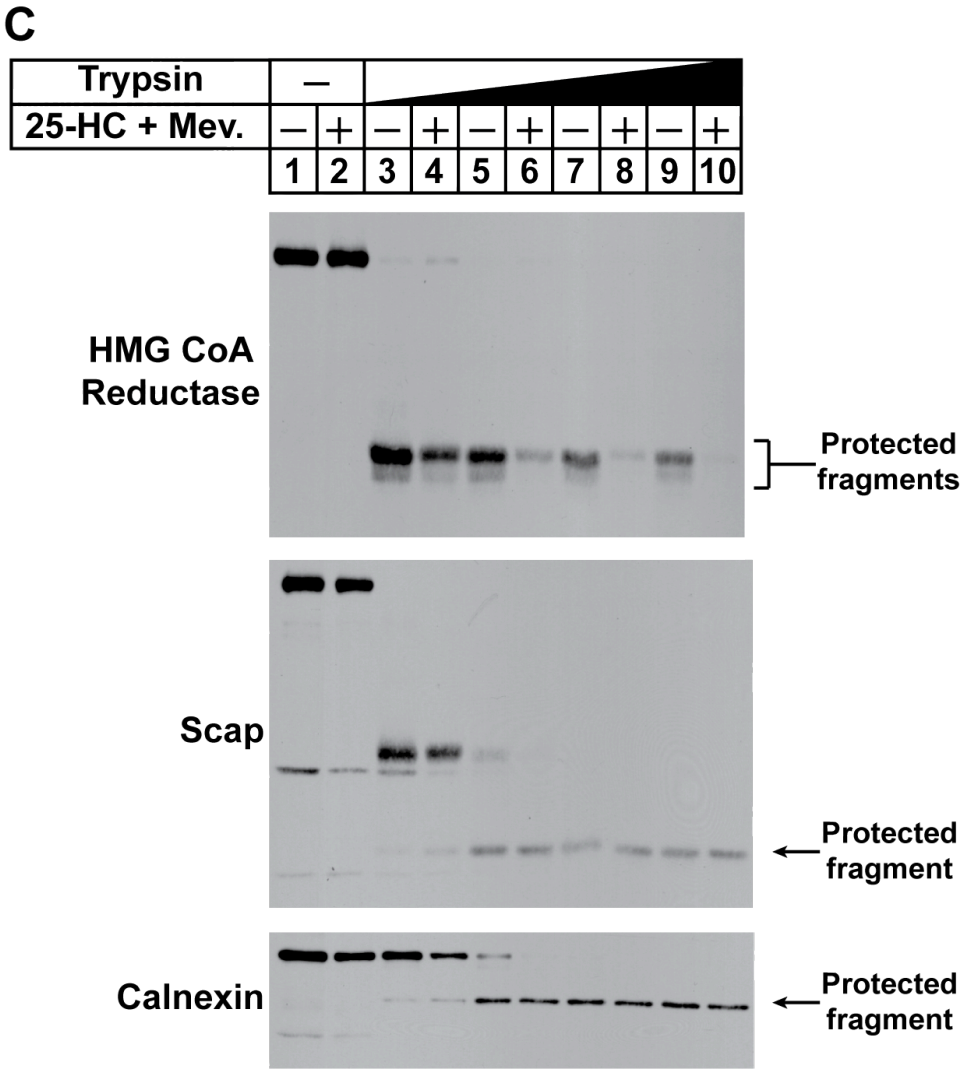

FIGURE 6 CONTINUED:

Figure 6. Sterols enhance susceptibility of lumenal T7 epitope in HMG CoA reductase to trypsin digestion. (*A*) Topology of HMG CoA reductase, Scap, and calnexin denoting the location of two T7 epitope tags in reductase encoded by pCMV-HMG-Red-T7, the epitope in Scap recognized by monoclonal IgG-9D5, and the region in calnexin recognized by anti-calnexin IgG. Sites for N-linked glycosylation are indicated in each protein. (*B* - *C*) UT-2/pHMG-Red-T7 cells were set up for experiments on day 0 at a density of 5 X 10^5 cells per 100-mm dish in medium B. On day 2, the cells were refed medium A supplemented with 5% LPDS, 10 μM compactin, 50 μM mevalonate, and 1 μM MG-132 in the absence or presence of 1 μg/ml 25-HC plus 10 mM mevalonate as indicated. Following incubation at 37 °C for 16 h, the cells were harvested for subcellular fractionation using Protocol 1; the resulting membrane fractions resuspended in Buffer B, pooled where appropriate, and membrane suspensions were digested with 20 μg trypsin (*B*) or 2-20 μg trypsin (*C*, lanes 3-4: 2 μg, lanes 5-6: 6 μg, lanes 7-8: 10 μg, lanes 9-10: 14 μg, lanes 11-12: 20 μg) for 30 min at 30 °C. Following treatments, reactions were terminated and samples were subjected to SDS-PAGE, followed by immunoblot analysis with anti-T7 IgG (against reductase), IgG-9D5 (against Scap), and anti-calnexin IgG. (*E*). Bands corresponding to trypsin-generated protected fragments of reductase were quantified using ImageJ software. The intensities of these bands in the absence of 25-HC plus mevalonate or GGOH were arbitrarily set as 1.

FIGURE 7:

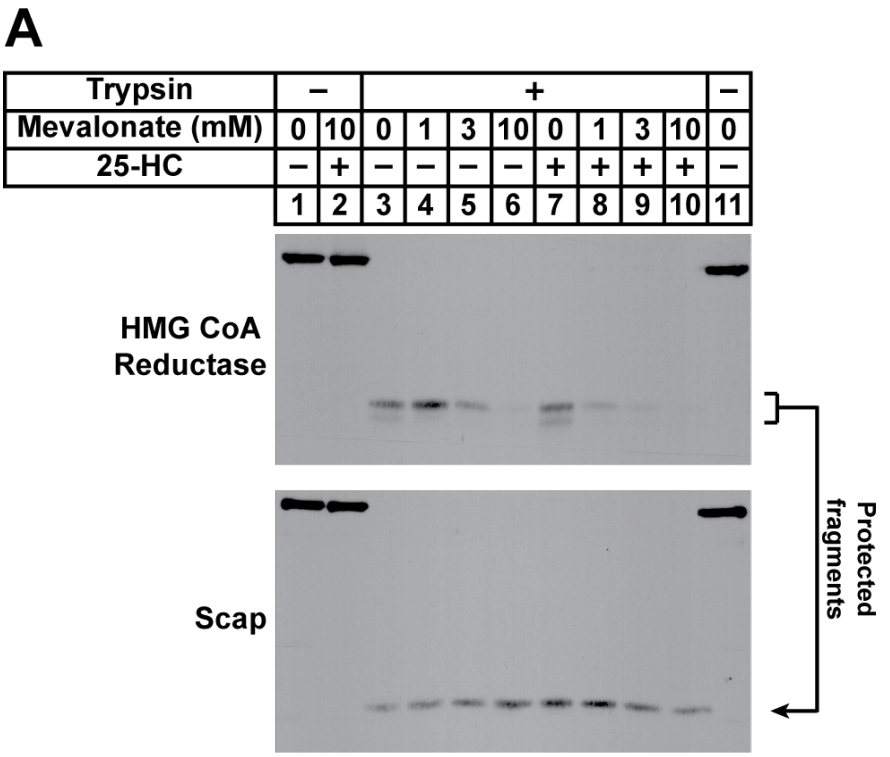
A
Trypsin
Mevalonate (mM)
25-HC
1 2 3 4 5 6 7 8 9 10 11
HMG CoA Reductase
Scap
Protected fragments

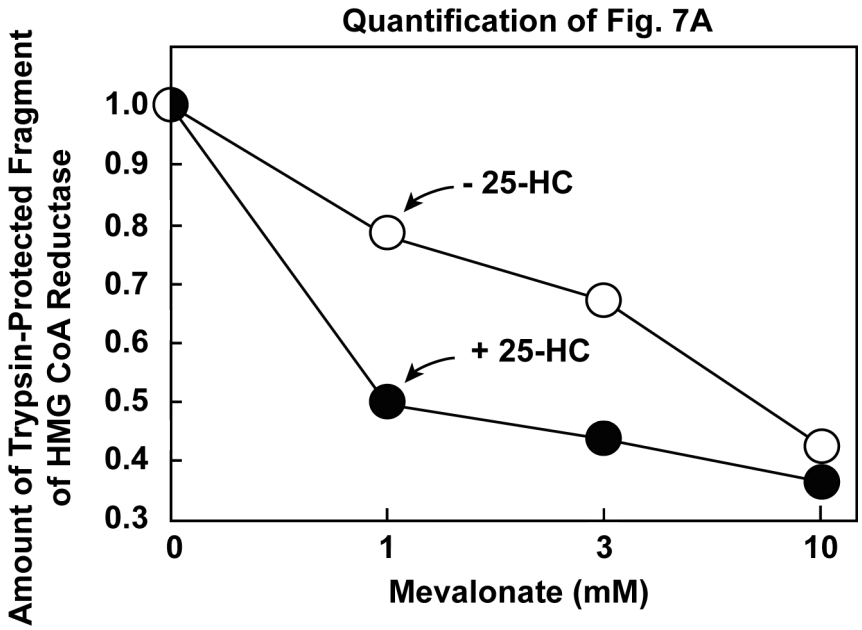
Quantification of Fig. 7A
Amount of Trypsin-Protected Fragment of HMG CoA Reductase
1.0
0.9
0.8
0.7
0.6
0.5
0.4
0.3
- 25-HC
+ 25-HC
0
1
3
10
Mevalonate (mM)

FIGURE 7 CONTINUED:

B

Trypsin	–		+								–
GGOH (μM)	0	10	0	1	3	10	0	1	3	10	0
25-HC	–	+	–	–	–	–	+	+	+	+	–
	1	2	3	4	5	6	7	8	9	10	11

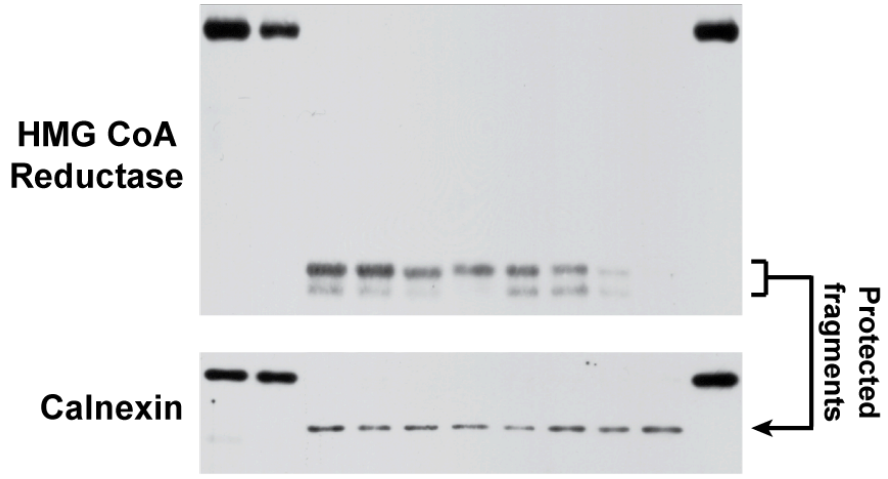

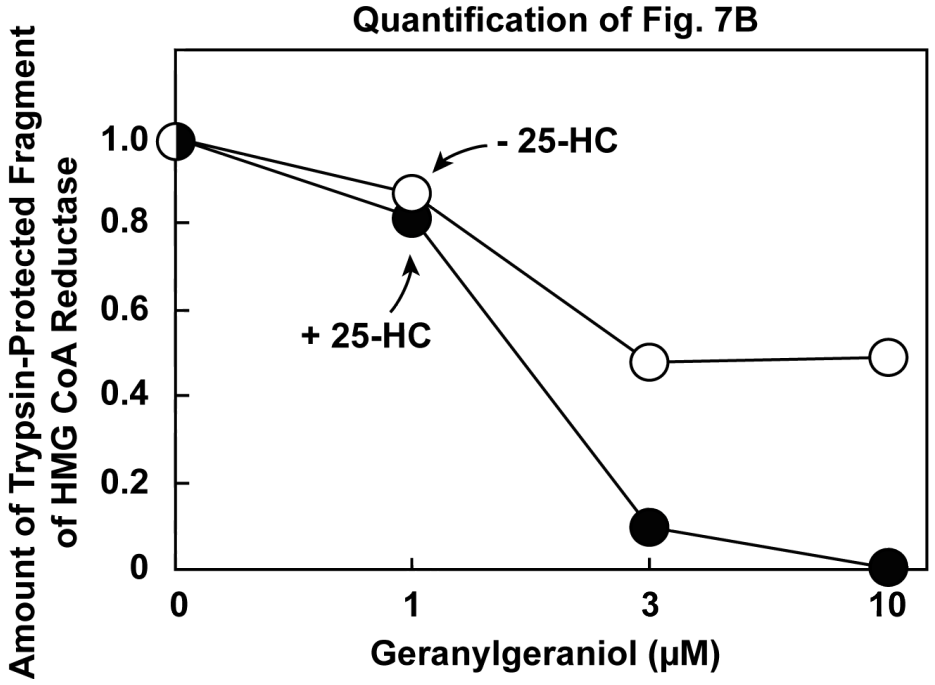

FIGURE 7 CONTINUED:

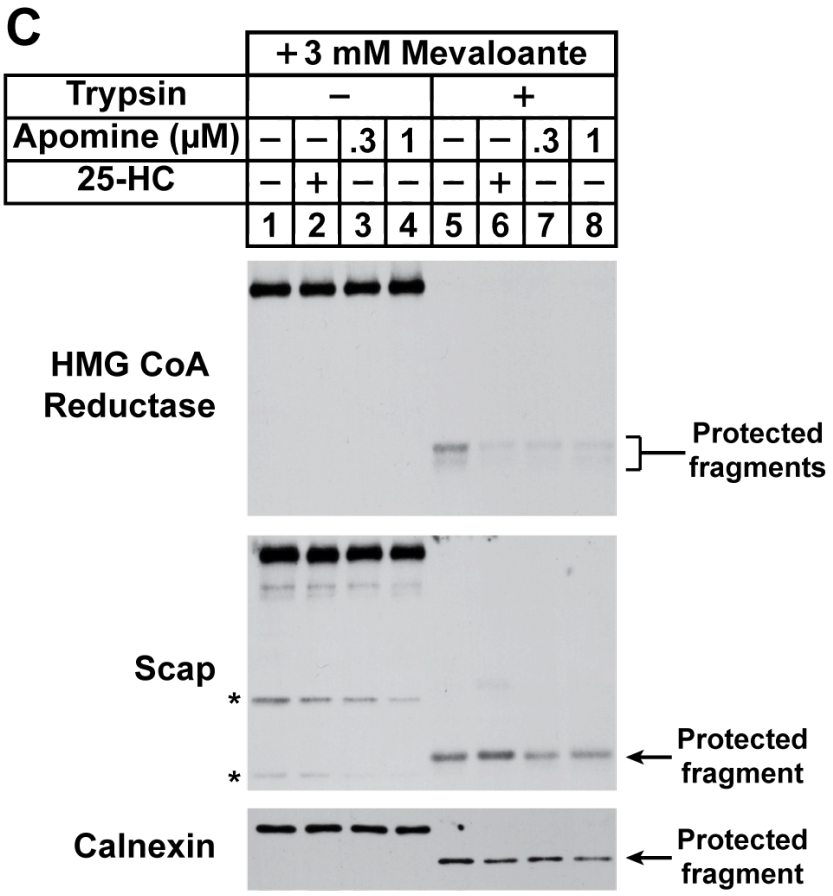

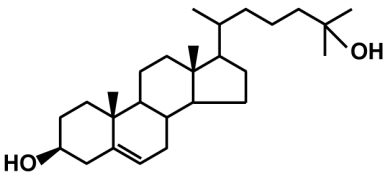

25-Hydroxycholesterol

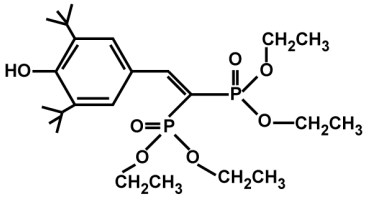

SR-12813

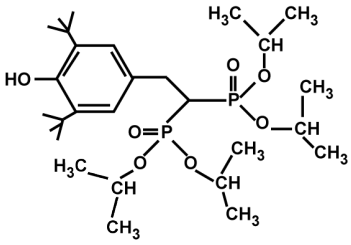

Apomine

FIGURE 7 CONTINUED:

Figure 7. Sterol and nonsterol isoprenoids trigger extraction of HMG CoA reductase across ER membranes as determined by protease protection. (*A* - *C*) UT-2/pHMG-Red-T7 cells were set up for experiments on day 0 at a density of 5 X 10^5 cells per 100-mm dish in medium B. On day 2, the cells were refed medium A supplemented with 5% LPDS, 10 μM compactin, 50 μM mevalonate, and 1 μM MG-132 in the absence or presence of 1 μg/ml 25-HC the indicated concentration of mevalonate (*A*), 0-10 μM geranylgeraniol (GGOH, *B*), or 3 mM mevalonate plus either 1μg/ml 25-HC or the indicated concentration of Apomine (*C*). Following incubation at 37 °C for 16 h, the cells were harvested for subcellular fractionation using Protocol 1; the resulting membrane fractions resuspended in Buffer B, pooled where appropriate, and equal amounts of membrane suspensions were digested with 10-20 μg trypsin for 30 min at 30 °C. Following treatments, reactions were terminated and samples were subjected to SDS-PAGE, followed by immunoblot analysis with anti-T7 IgG (against reductase), IgG-9D5 (against Scap), and anti-calnexin IgG. The chemical structures of 25-hydroxycholesterol, SR-12813, and Apomine are provided (*C*). Bands corresponding to trypsin-generated protected fragments of reductase were quantified using ImageJ software. The intensities of these bands in the absence of 25-HC plus mevalonate or GGOH were arbitrarily set as 1.

Figure 8:

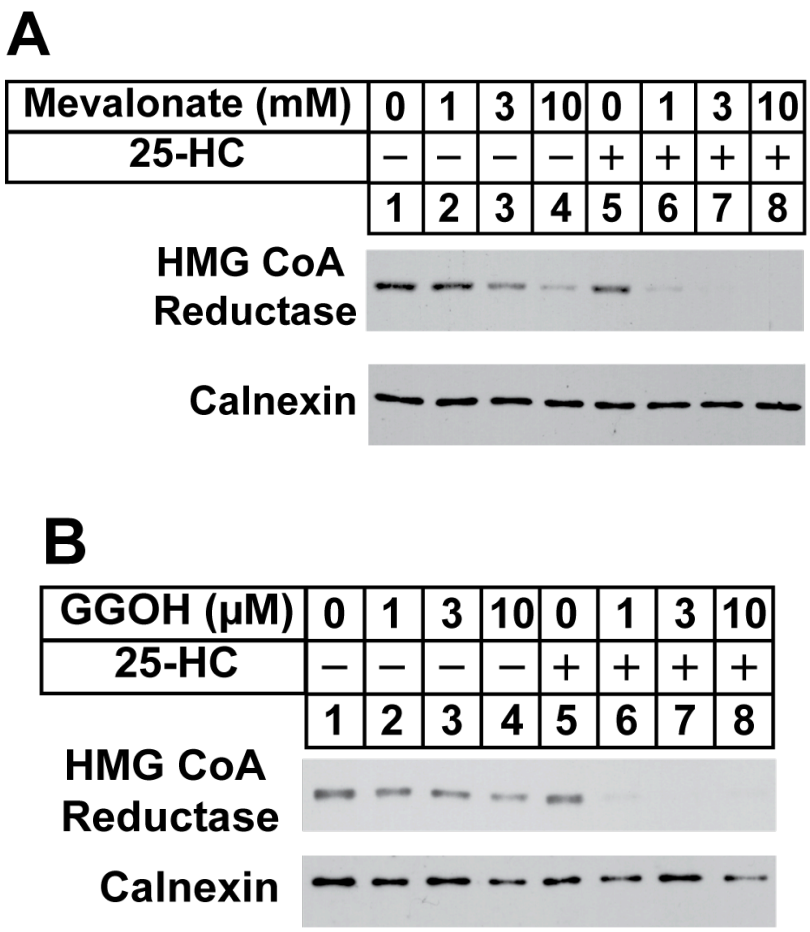
A
Mevalonate (mM) 0 1 3 10 0 1 3 10
25-HC – – – – + + + +
1 2 3 4 5 6 7 8
HMG CoA Reductase
Calnexin
B
GGOH (μM) 0 1 3 10 0 1 3 10
25-HC – – – – + + + +
1 2 3 4 5 6 7 8
HMG CoA Reductase
Calnexin

Figure 8 continued:

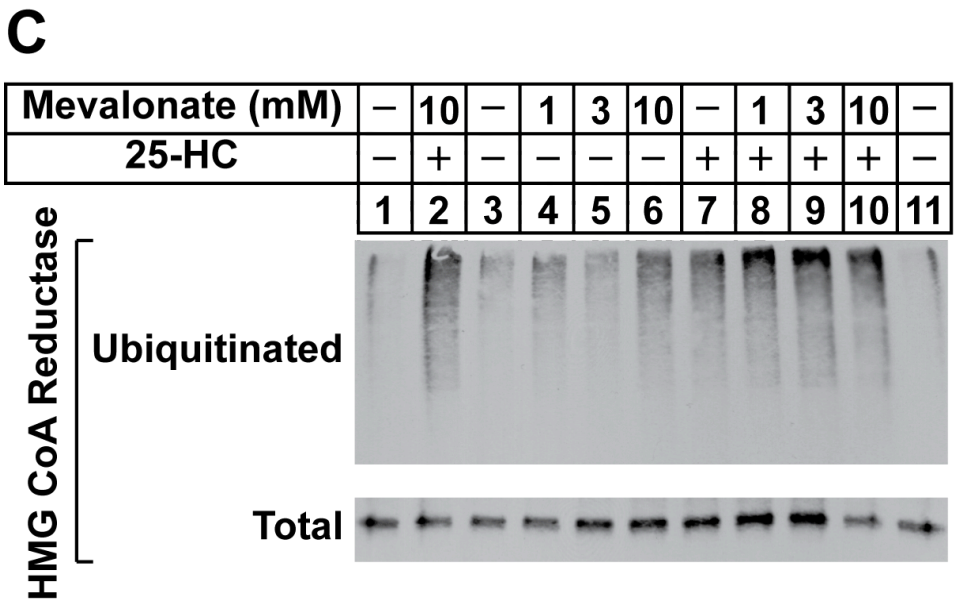

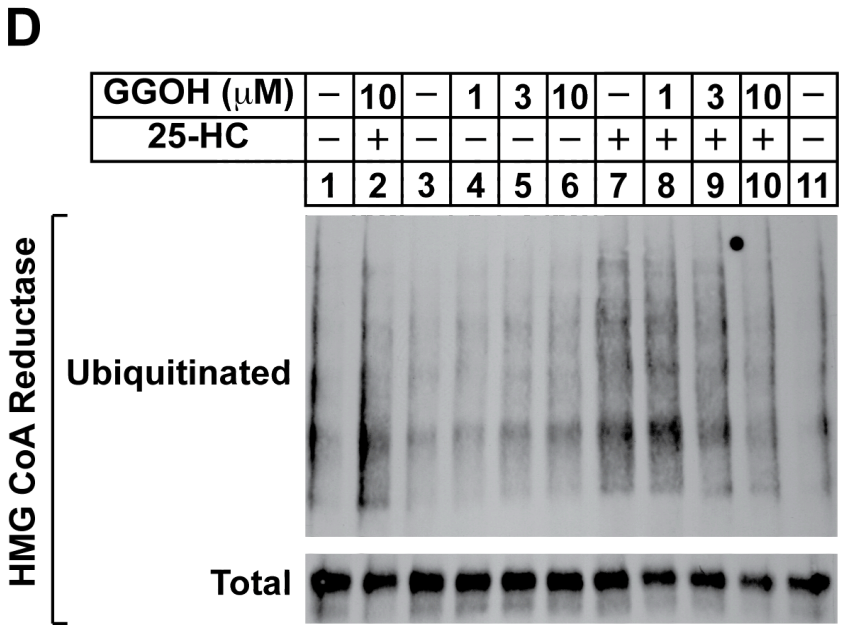

Figure 8 continued:

Figure 8. Sterol and nonsterol requirements for accelerated degradation (*A* and *B*) and ubiquitination (*C* and *D*) of HMG-Red-T7. UT-2/pHMG-Red-T7 cells were set up for experiments on day 0 in medium A at a density of 5 X 10^5 cells per 100-mm dish. (*A* and *B*) On day 2, cells were refed medium A supplemented with 5% LPDS, 10 μM compactin, and 50 μM mevalonate in the absence or presence of 1 μg/ml 25-HC plus the indicated concentration of mevalonate (*A*, 1-10 mM) or geranylgeraniol (*B*, 1-10 μM). Following incubation for 16 h at 37 °C, cells were harvested for subcellular fractionation using Protocol 1 as described in "Materials and Methods." Aliquots of the samples were subjected to SDS-PAGE, followed by immunoblot analysis with anti-T7 IgG (against reductase) and anti-calnexin IgG. (*C* and *D*) on day 2, cells were refed medium A supplemented with 5% LPDS, 10 μM compactin, and 50 μM mevalonate. Following incubation for 16 h at 37 °C, the cells were switched to medium A containing 5% LPDS, 10 μM compactin, 50 μM mevalonate, and 10 μM MG-132 in the absence or presence of 1 μg/ml 25-HC, 1-10 mM mevalonate (*C*), and 1-10 μM geranylgeraniol (*D*) as indicated. After 4-6 h, the cells were harvested, lysed, and immunoprecipitated with polyclonal antibodies against reductase (*C*) or anti-T7-coupled agarose beads (*D*). Aliquots of the immunoprecipitates were subjected to SDS-PAGE and immunoblot analysis with anti-T7 IgG (against reductase) and IgG-P4D1 (against ubiquitin).

FIGURE 9:

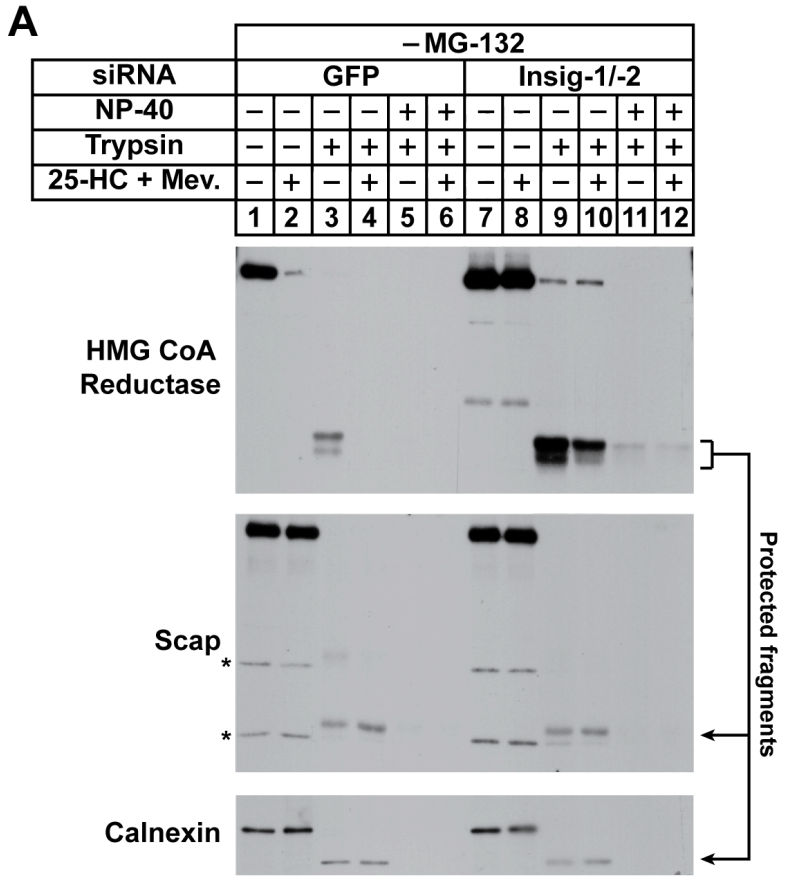
A
– MG-132
siRNA
GFP
Insig-1/-2
NP-40
Trypsin
25-HC + Mev.
1 2 3 4 5 6 7 8 9 10 11 12
HMG CoA Reductase
Scap
*
*
Calnexin
Protected fragments

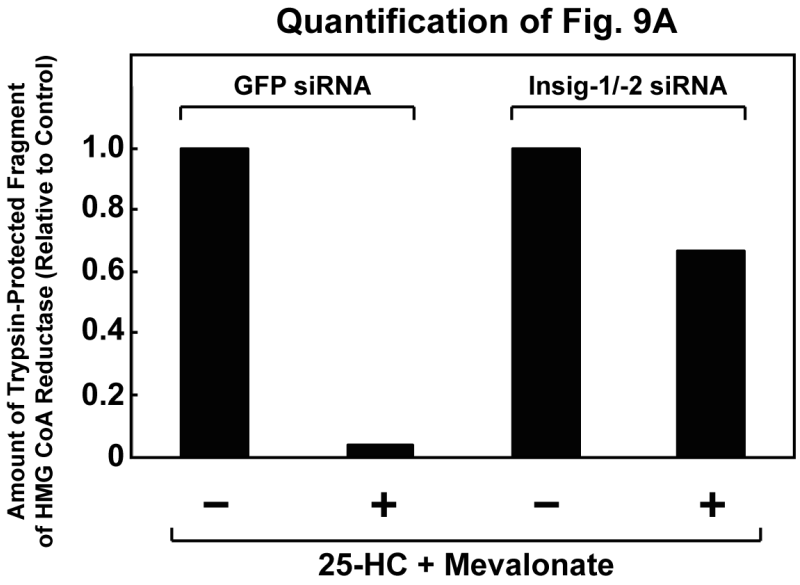
Quantification of Fig. 9A
Amount of Trypsin-Protected Fragment of HMG CoA Reductase (Relative to Control)
GFP siRNA
Insig-1/-2 siRNA
1.0
0.8
0.6
0.4
0.2
0
–
+
–
+
25-HC + Mevalonate

FIGURE 9 CONTINUED:

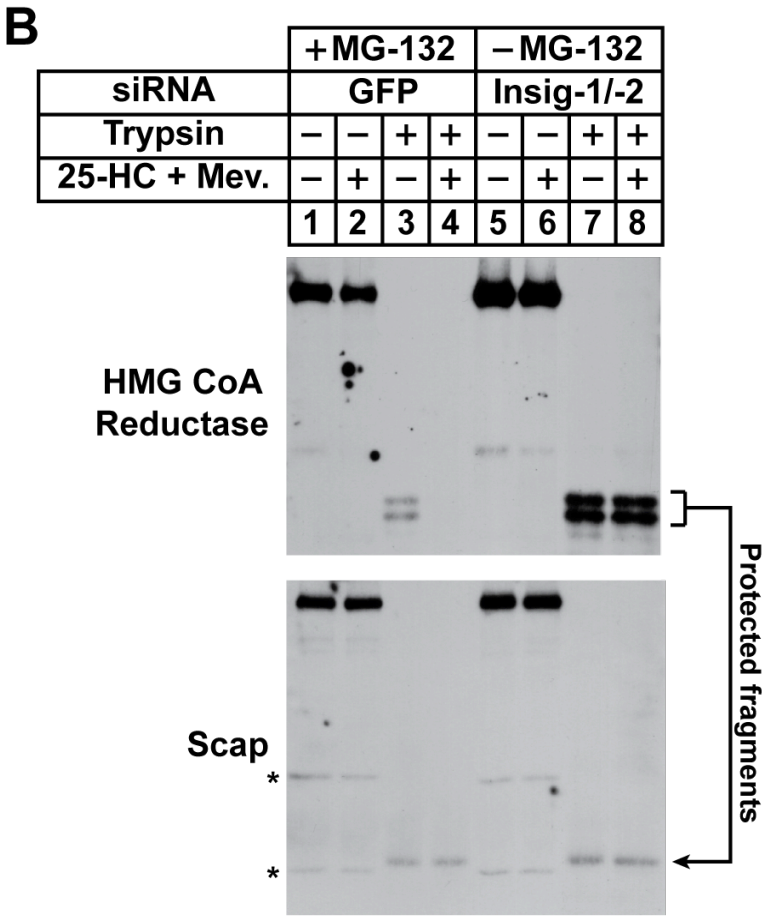

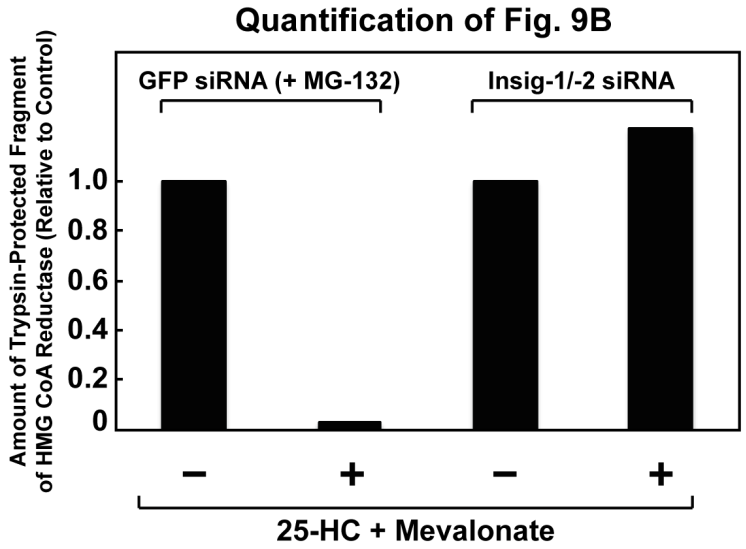

FIGURE 9 CONTINUED:

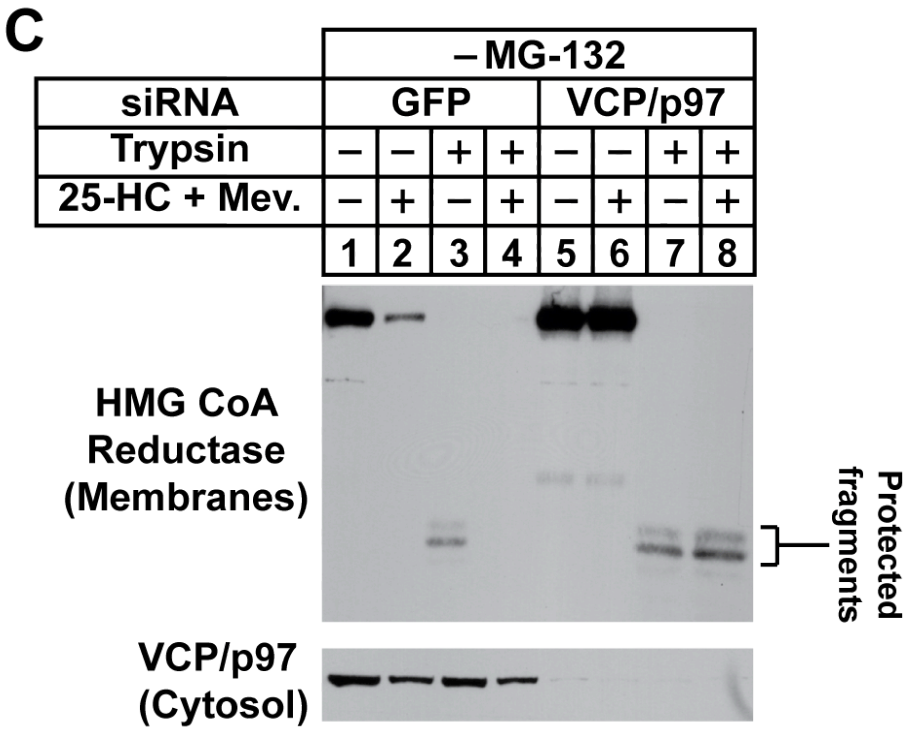

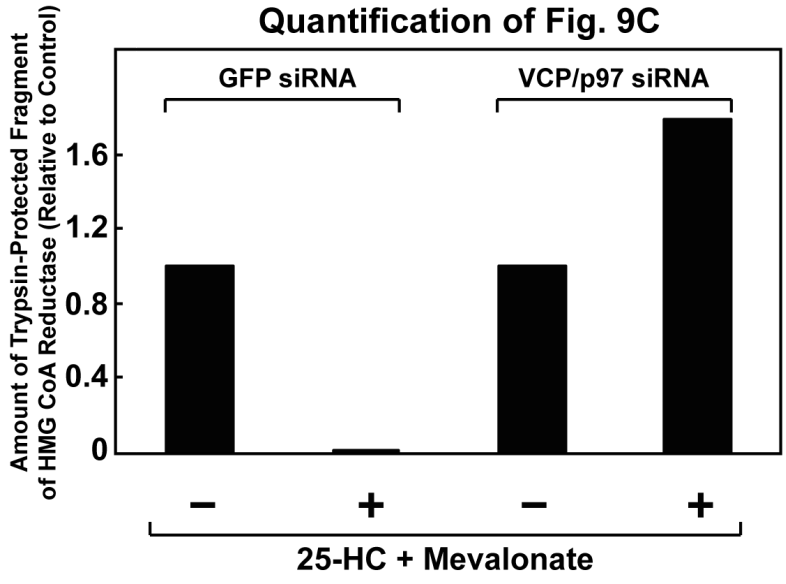

FIGURE 9 CONTINUED:

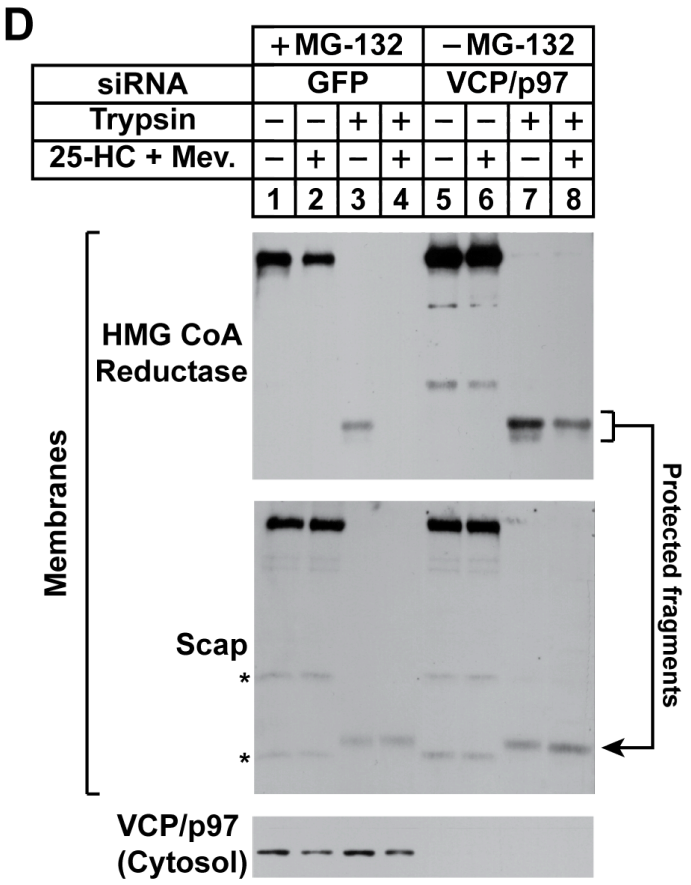

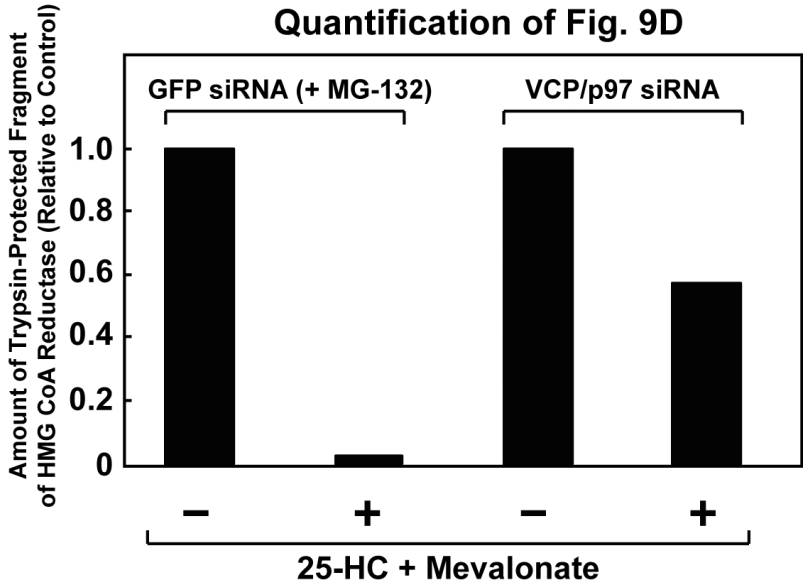

FIGURE 9 CONTINUED:

Figure 9. RNAi-mediated knockdown of Insigs or VCP/p97 blunts sterol-regulated extraction of HMG CoA reductase across ER membranes. UT-2/pHMG-Red-T7 cells were set up on day 0 at a density of 2 X 10^5 cells per 60-mm dish in medium B. On days 1 and 2, the cells were transfected with the indicated siRNA duplexes as described in "Materials and Methods." Following transfection on day 2, cells received a direct addition of medium A containing 5% LPDS, 10 μM compactin, 50 μM mevalonate in the absence or presence of 1 μg/ml 25-HC plus 10 mM mevalonate (final concentrations). In (*B* and *D*), some of the cells (lanes 1-4) were also treated with 1 μM MG-132. Following incubation at 37 °C for 16 h, cells were harvested for subcellular fractionation using Protocol 1. Aliquots of the resulting membrane fractions were resuspended in Buffer B, pooled where appropriate, and equal amounts of membrane suspensions were digested with 10 μg trypsin. Some of the samples (lanes 5, 6, 11, and 12 in *A*) were treated with 1% NP-40 prior to proteolysis. After 30 min at 30 °C, the reactions were terminated and samples were subjected to SDS-PAGE, followed by immunoblot analysis with anti-T7 IgG (against reductase), IgG-9D5 (against Scap), IgG-18 (against VCP/p97), and anti-calnexin IgG. Bands corresponding to trypsin-protected fragments of reductase were quantified using ImageJ software. The intensities of these bands in the absence of 25-HC plus mevalonate were arbitrarily set as 1 for each of the RNAi-mediated knockdowns.

Figure 10:

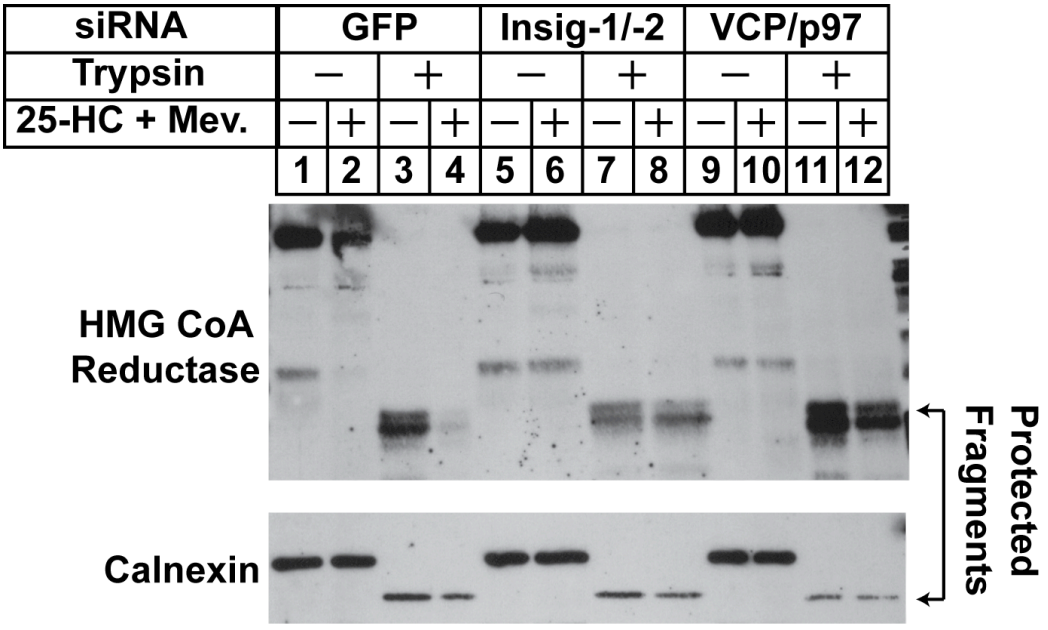
siRNA
GFP
Insig-1/-2
VCP/p97
Trypsin
25-HC + Mev.
1 2 3 4 5 6 7 8 9 10 11 12
HMG CoA Reductase
Calnexin
Protected Fragments

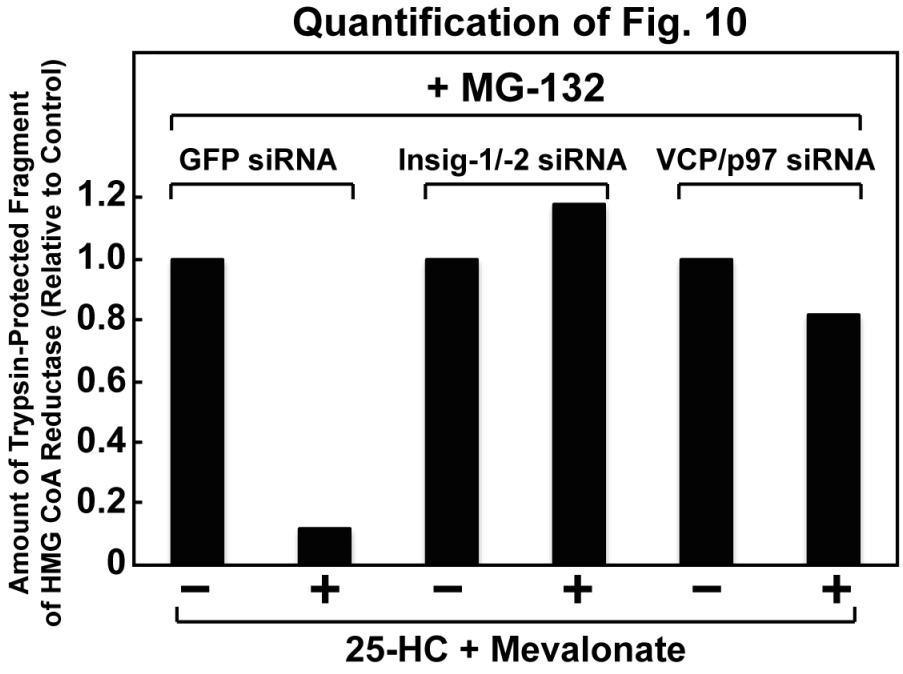
Quantification of Fig. 10
+ MG-132
GFP siRNA
Insig-1/-2 siRNA
VCP/p97 siRNA
Amount of Trypsin-Protected Fragment of HMG CoA Reductase (Relative to Control)
0
0.2
0.4
0.6
0.8
1.0
1.2
25-HC + Mevalonate

Figure 10 continued:

Figure 10. RNAi-mediated knockdown of Insigs or VCP/p97 inhibit membrane extraction of HMG CoA reductase in MG-132-treated cells. UT-2/pHMG-Red-T7 cells were set up for experiments on day 0 at a density of 1.5 X 10^5 cells per 60-mm dish in medium B. On days 1 and 2, the cells were transfected with the indicated siRNA duplexes as described in the legend to Figure 9. Four hours following transfection on day 2, cells received a direct addition of medium A supplemented with 5% LPDS, 10 μM compactin, 50 μM mevalonate, and 1 μM MG-132 in the absence or presence of 1 μg/ml 25-HC plus 10 mM mevalonate as indicated. Following incubation at 37 °C for 16 h, the cells were harvested for subcellular fractionation using Protocol 1. Resulting membrane fractions were resuspended in Buffer B and digested with 10 μg trypsin for 30 min at 30 °C. Following treatments, reactions were terminated and the samples were subjected to SDS-PAGE, followed by immunoblot analysis with anti-T7 IgG (against reductase) and anti-calnexin IgG. Bands corresponding to trypsin-protected fragments of reductase were quantified using ImageJ software. The intensities of these bands in the absence of 25-HC plus mevalonate were arbitrarily set as 1 for each of the RNAi-mediated knockdowns.

Figure 11:

A

siRNA	GFP		Rpt5						Rpt4			
			#1		#2		#3		#1		#2	
25-HC + Mev.	−	+	−	+	−	+	−	+	−	+	−	+
	1	2	3	4	5	6	7	8	9	10	11	12

HMG CoA Reductase

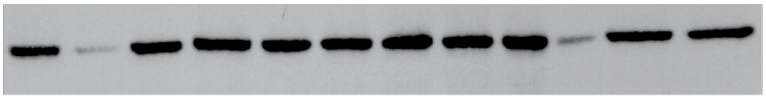

B

siRNA	GFP		Rpt5				Rpt6			
			#1		#2		#1		#2	
25-HC + Mev.	−	+	−	+	−	+	−	+	−	+
	1	2	3	4	5	6	7	8	9	10

HMG CoA Reductase

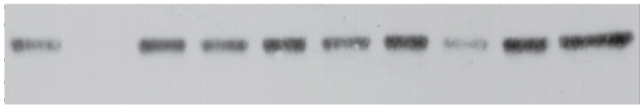

C

siRNA	GFP		Rpt1				Rpt2			
			#1		#2		#1		#2	
25-HC + Mev.	−	+	−	+	−	+	−	+	−	+
	1	2	3	4	5	6	7	8	9	10

HMG CoA Reductase

GFP		Rpt3				Rpt4			
		#1		#2		#2		#3	
−	+	−	+	−	+	−	+	−	+
11	12	13	14	15	16	17	18	19	20

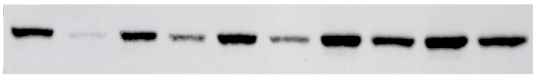

Figure 11 continued:

Figure 11. RNAi-mediated knockdown of AAA-ATPases of the proteasome 19S regulatory particle blunts sterol-accelerated degradation of HMG CoA reductase. CHO-K1 cells were set up for experiments on day 0 at a density of 2 X 10^5 cells per 60-mm dish (A) or 5 X 10^5 cells per 100-mm dish (B and C) in medium A containing 5% FCS. On day 1, cells were transfected with the indicated duplex of siRNA as described in the legend to Figure 9. Four hours following transfection, cells were depleted of sterols for 16 h by the direct addition of medium A containing 5% LPDS, 10 μM compactin, and 50 μM mevalonate (final concentrations). Sterol-depleted cells were switched to identical medium in the absence or presence of 1 μg/ml 25-HC plus 10 mM mevalonate as indicated. After 4-5 h, cells were harvested and subjected to cellular fractionation. Aliquots of resulting membrane fractions (15-20 μg protein/lane) were subjected to SDS-PAGE and immunoblot analysis with IgG-A9 (against reductase).

FIGURE 12:

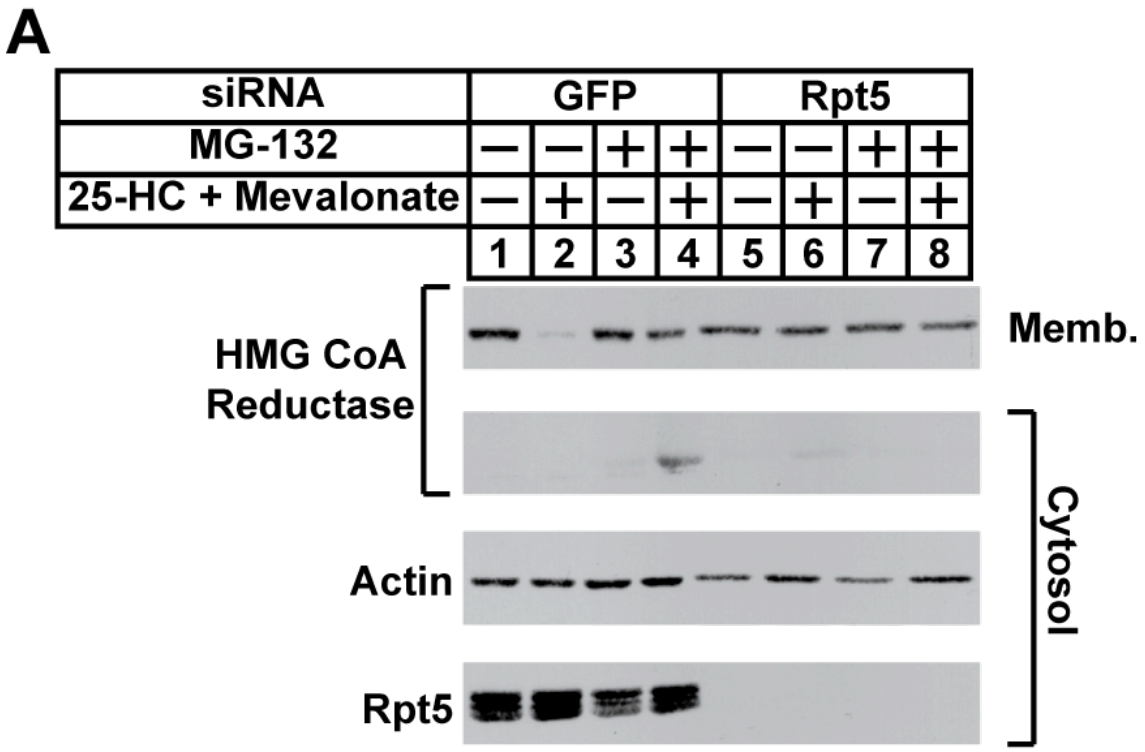
A
siRNA
GFP
Rpt5
MG-132
25-HC + Mevalonate
1 2 3 4 5 6 7 8
HMG CoA Reductase
Memb.
Cytosol
Actin
Rpt5

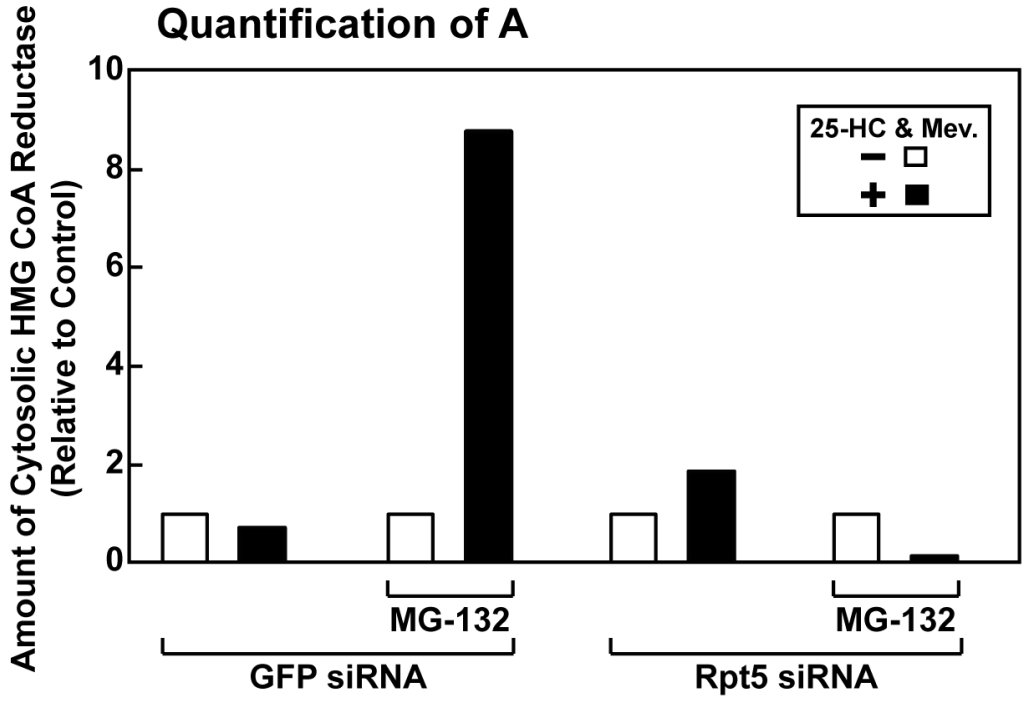
Quantification of A
Amount of Cytosolic HMG CoA Reductase (Relative to Control)
0
2
4
6
8
10
25-HC & Mev.
MG-132
MG-132
GFP siRNA
Rpt5 siRNA

FIGURE 12 CONTINUED:

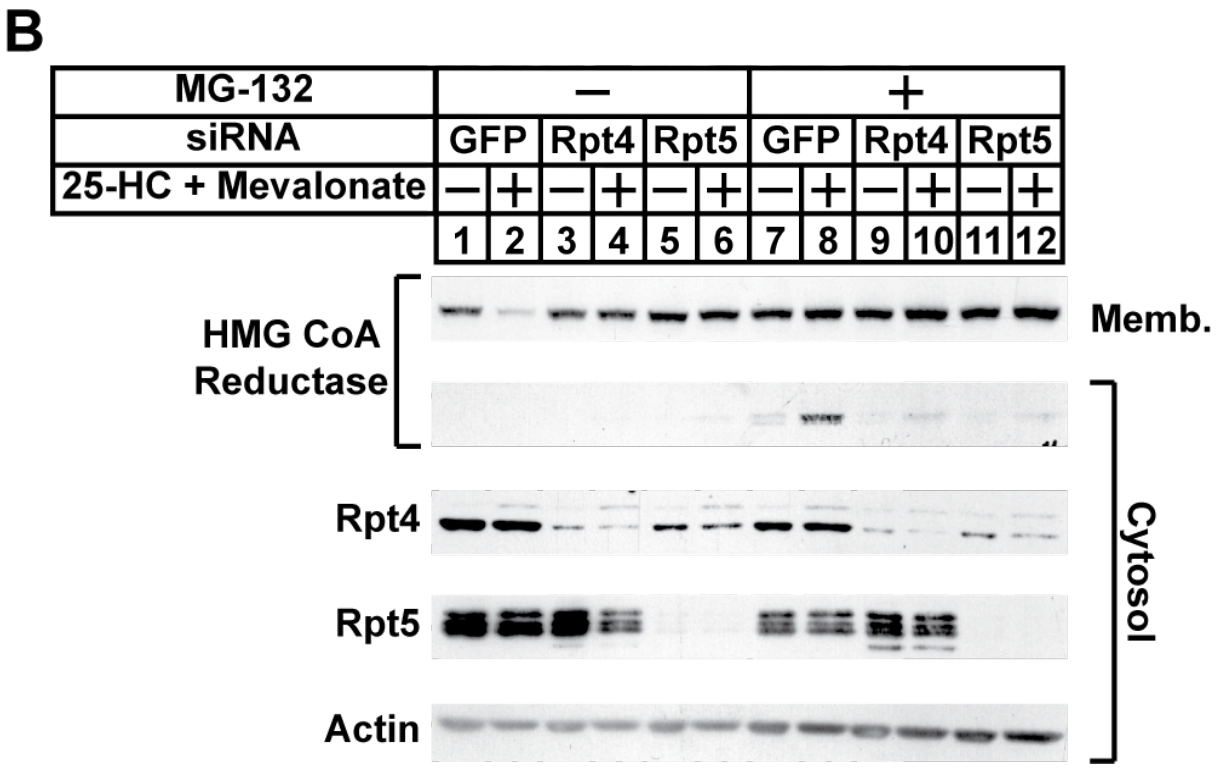

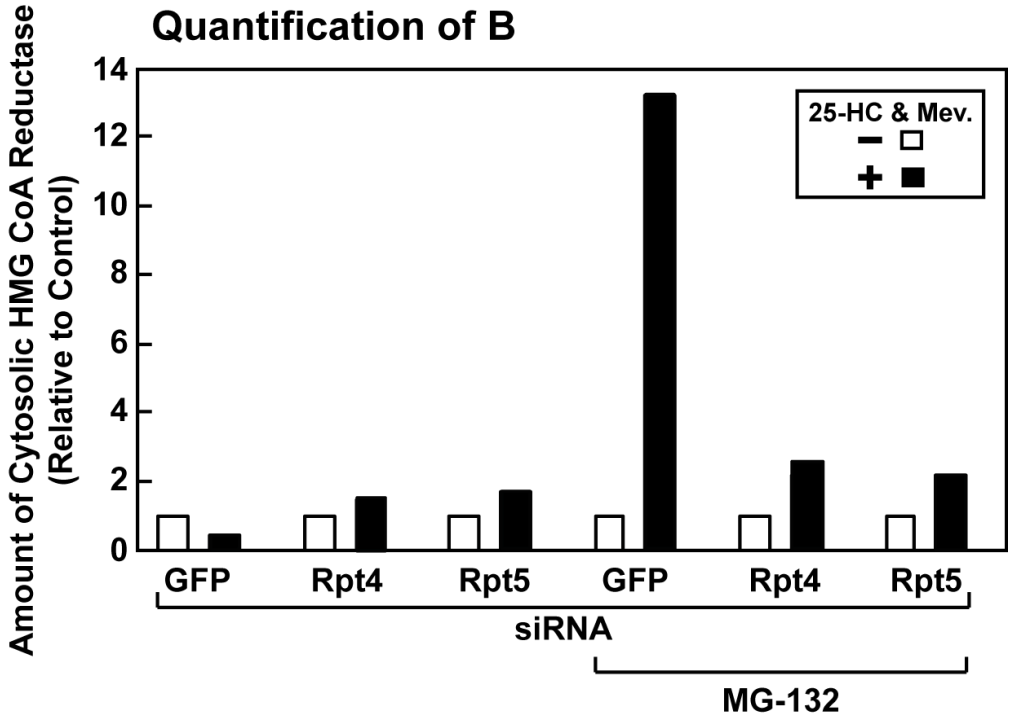

FIGURE 12 CONTINUED:

Figure 12. RNAi-mediated knockdown of AAA-ATPases of the proteasome 19S regulatory particle blunts sterol-accelerated degradation and cytosolic dislocation of HMG CoA reductase. CHO-K1 cells were set up on day 0 at a density of 1.5 X 10^5 cells per 60-mm dish (*A*) or 5 X 10^5 cells per 100-mm dish (*B*) in medium A containing 5% FCS. On day 1, cells were transfected with the indicated duplex of siRNA as described in the legend to Figure 9. Four hours following transfection, cells were depleted of sterols for 16 h by the direct addition of medium A containing 5% LPDS, 10 μM compactin, and 50 μM mevalonate (final concentrations). Sterol-depleted cells were pretreated for 1 h with medium A supplemented with 5% LPDS, 10 μM compactin, and 50 μM mevalonate in the absence or presence of 10 μM MG-132. Cells then received medium A containing 5% LPDS, 10 μM compactin, and 50 μM mevalonate in the absence or presence of 10 μM MG-132 and 1 μg/ml 25-HC plus 10 mM mevalonate (final concentrations). After 4 h, cells were harvested and post-nuclear supernatants were subjected to centrifugation at 1 X 10^6 g for 30 min at 4 °C. Aliquots of resulting membrane pellet (15-20 μg protein/lane) and cytosolic supernatant (10-40 μg protein/lane) fractions were subjected to SDS-PAGE and immunoblot analysis with IgG-A9 (against reductase), IgG-TBP1-19 (against Rpt5), IgG-p42-23 (against Rpt4), and anti-actin IgG. Bands corresponding to cytosolically dislocated reductase were quantified using ImageJ software. The intensities of these bands in the absence of 25-HC plus mevalonate were arbitrarily set as 1 for each of the RNAi-mediated knockdowns.

Figure 13:

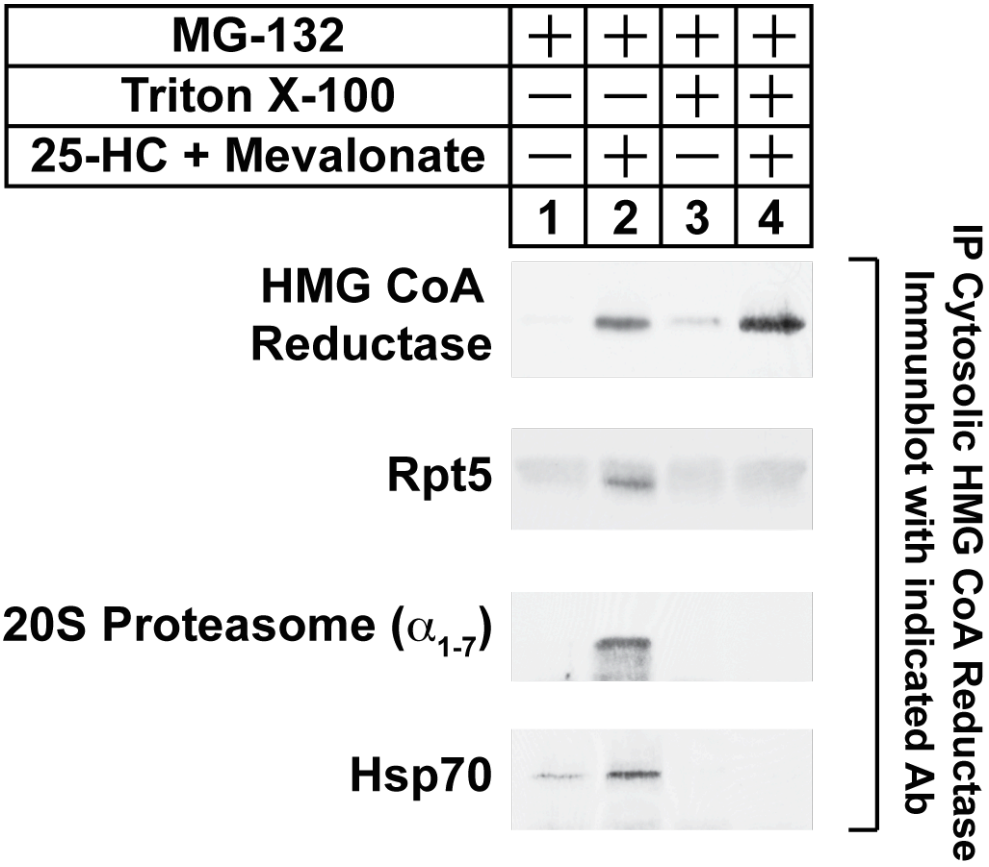
MG-132 + + + +
Triton X-100 − − + +
25-HC + Mevalonate − + − +
1 2 3 4
HMG CoA Reductase
Rpt5
20S Proteasome (α_{1-7})
Hsp70
IP Cytosolic HMG CoA Reductase
Immunblot with indicated Ab

Figure 13 continued:

Figure 13. Association of proteasomes with cytosolic HMG CoA reductase. Experiment performed by Dr. Isamu Hartman. CHO-K1 cells were set up on day 0 at a density of 4 X 10^5 cells per 100-mm dish in medium A containing 5% FCS. The cells were depleted of sterols and incubated for 4 h in medium A containing 5% LPDS, 10 μM compactin, 50 μM mevalonate, and 10 μM MG-132 in the absence or presence of 1 μg/ml 25-HC plus 10 mM mevalonate. Cells were harvested and cytosolic fractions were mixed with buffer in the absence or presence of 0.1% NP-40 and immunoprecipitated with anti-reductase. Precipitated material was analyzed by immunoblotting with IgG-A9 (against reductase), IgG-TBP1-19 (against Rpt5), anti-20S proteasome, and anti-Hsp70 IgG.

Figure 14:

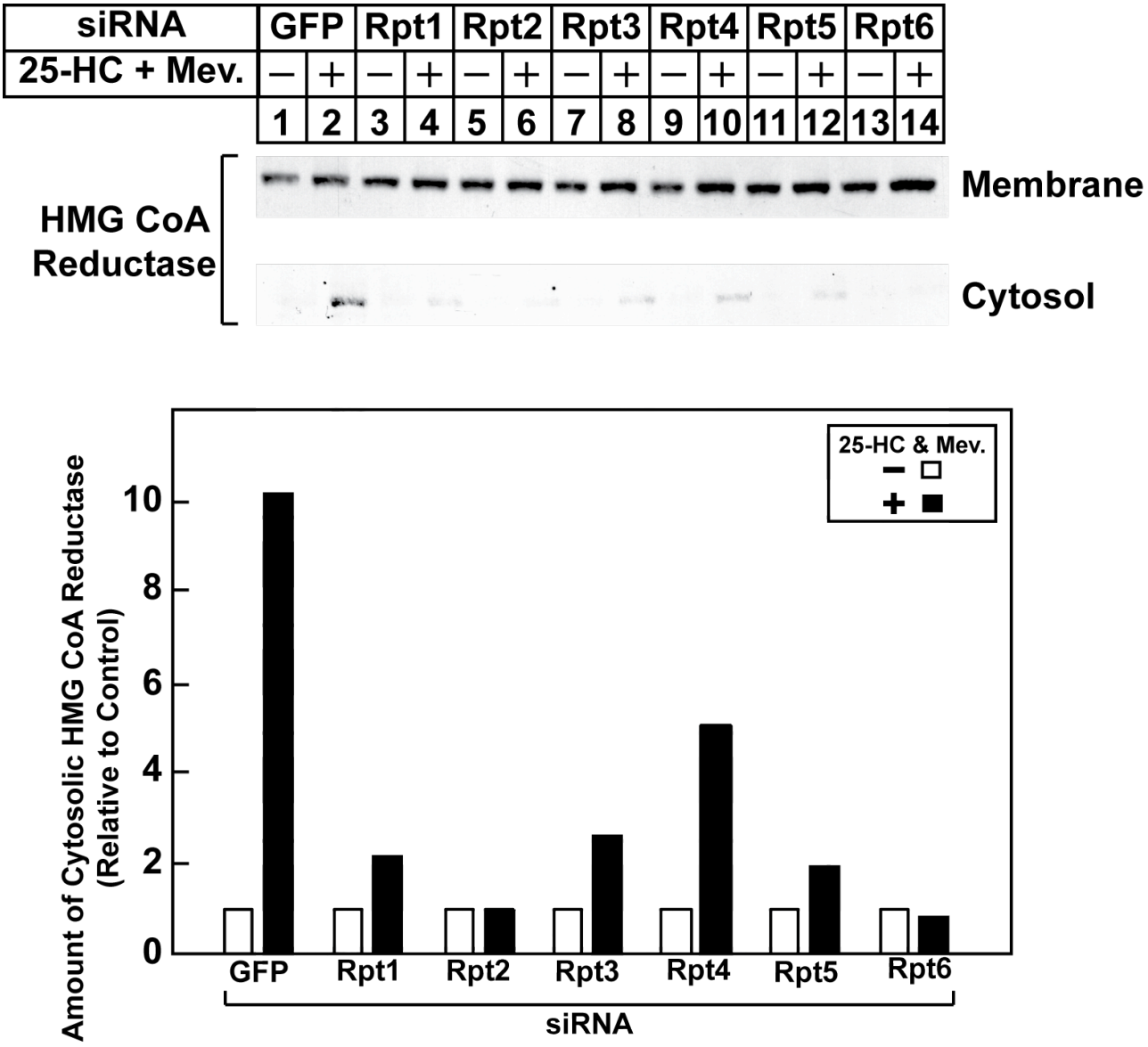
siRNA
GFP
Rpt1
Rpt2
Rpt3
Rpt4
Rpt5
Rpt6
25-HC + Mev.
– + – + – + – + – + – + – +
1 2 3 4 5 6 7 8 9 10 11 12 13 14
HMG CoA Reductase
Membrane
Cytosol
25-HC & Mev.
– □
+ ■
Amount of Cytosolic HMG CoA Reductase (Relative to Control)
0
2
4
6
8
10
GFP
Rpt1
Rpt2
Rpt3
Rpt4
Rpt5
Rpt6
siRNA

Figure 14 continued:

Figure 14. RNAi-mediated knockdown of AAA-ATPases of the proteasome 19S regulatory particle blunts sterol-induced, cytosolic dislocation of HMG CoA reductase. CHO-K1 cells were set up for experiments on day 0 at a density of 2.5 X 10^5 cells per 100-mm dish in medium A containing 5% FCS. On day 1, cells were transfected with the indicated duplex of siRNA as described in the legend to Figure 9. Four hours following transfection, cells were depleted of sterols for 16 h by the direct addition of medium A containing 5% LPDS, 10 μM compactin, and 50 μM mevalonate (final concentrations). Sterol-depleted cells were switched to identical medium containing 10 μM MG-132 in the absence or presence of 1 μg/ml 25-HC plus 10 mM mevalonate as indicated. After 4-5 h, cells were harvested and post nuclear supernatants were subjected to 1 X 10^6 g for 30 min at 4 ºC. Aliquots of resulting membrane pellet and cytosolic supernatant fractions (10-40 μg protein/lane) were subjected to SDS-PAGE and immunoblot analysis with IgG-A9 (against reductase). Bands corresponding to cytosolically dislocated reductase were quantified using ImageJ software. The intensities of these bands in the absence of 25-HC plus mevalonate were arbitrarily set as 1 for each of the RNAi-mediated knockdowns.

Figure 15:

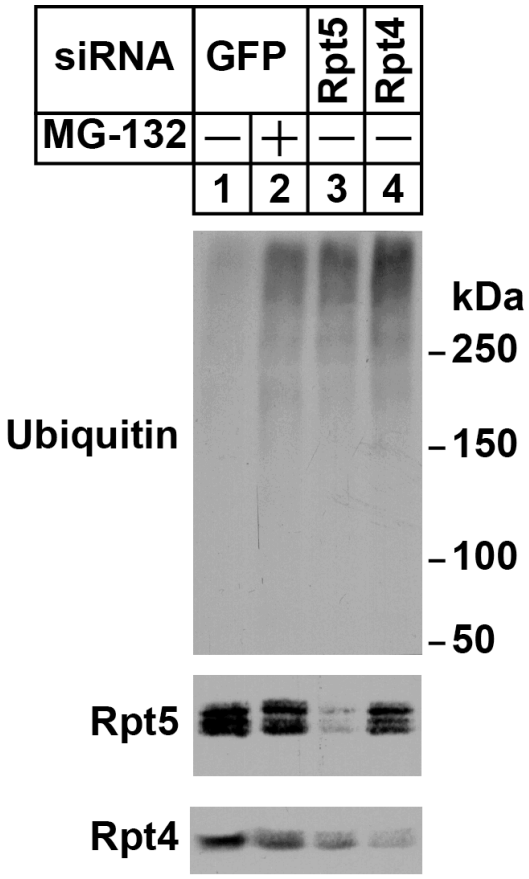
siRNA
GFP
Rpt5
Rpt4
MG-132
—
+
—
—
1
2
3
4
kDa
250
150
100
50
Ubiquitin
Rpt5
Rpt4

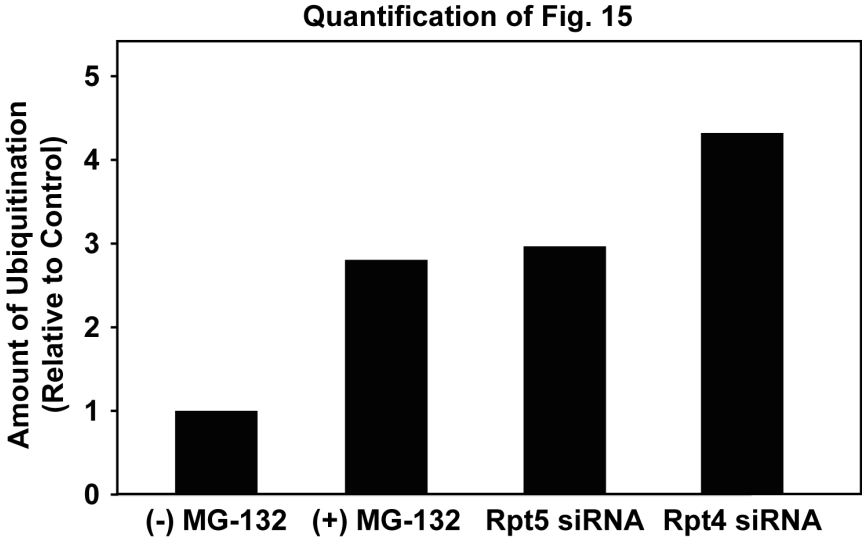
Quantification of Fig. 15
Amount of Ubiquitination
(Relative to Control)
0
1
2
3
4
5
(-) MG-132
(+) MG-132
Rpt5 siRNA
Rpt4 siRNA

Figure 15 continued:

Figure 15. RNAi-mediated knockdown of AAA-ATPases of the proteasome 19S regulatory particle causes accumulation of ubiquitinated proteins. CHO-K1 cells were set up on day 0 at a density of 2.5 X 105 cells per 60-mm dish in medium A containing 5% FCS. On day 1, cells were transfected with the indicated duplex of siRNA as described in the legend to Figure 9. On day 2, the cells were treated for 4 h with medium A supplemented with 5% FCS in the absence or presence of 10 μM MG-132. The cells were harvested and aliquots of the resulting lysates (10-20 μg protein/lane) were subjected to SDS-PAGE and immunoblot analysis with IgG-P4D1 (against ubiquitin), IgG-TBP1-19 (against Rpt5), and IgG-p42-23 (against Rpt4). Bands corresponding to ubiquitinated proteins were quantified using ImageJ software. The intensity of the ubiquitin smear in the absence of MG-132 was arbitrarily set as 1.

FIGURE 16:

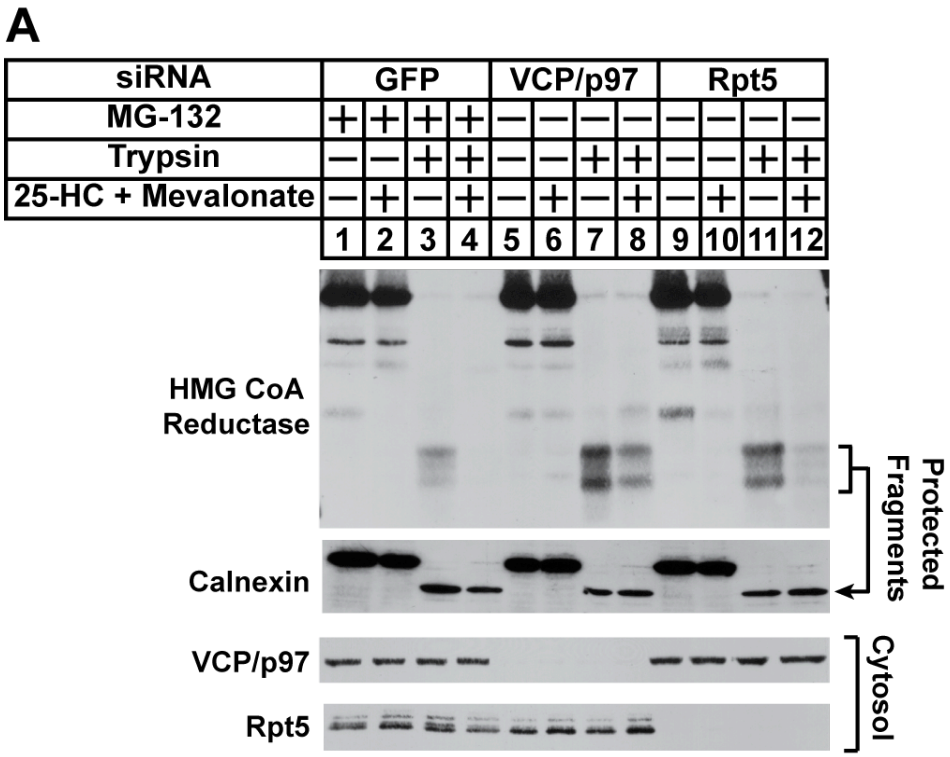
A
siRNA
GFP
VCP/p97
Rpt5
MG-132
Trypsin
25-HC + Mevalonate
1 2 3 4 5 6 7 8 9 10 11 12
HMG CoA Reductase
Calnexin
VCP/p97
Rpt5
Protected Fragments
Cytosol

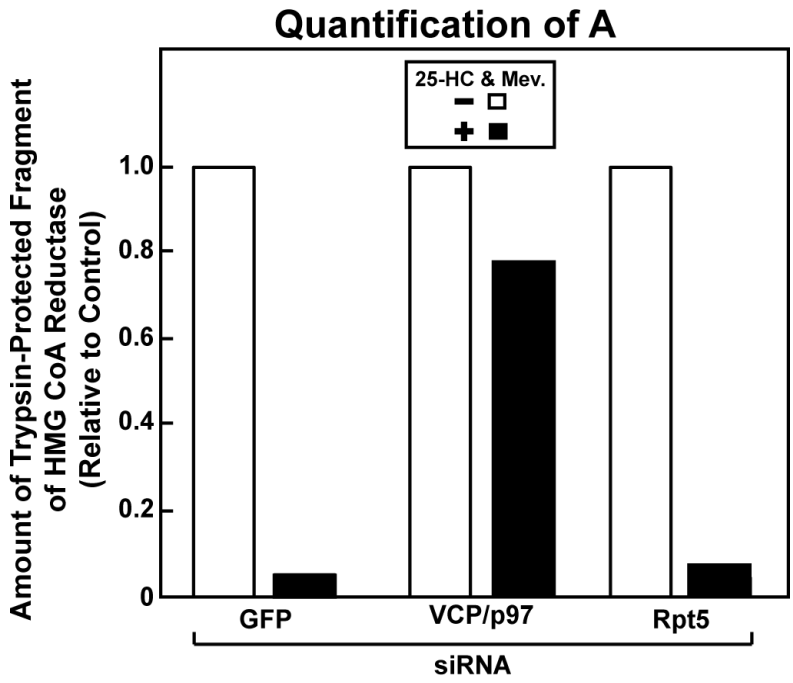
Quantification of A
25-HC & Mev.
Amount of Trypsin-Protected Fragment of HMG CoA Reductase (Relative to Control)
1.0
0.8
0.6
0.4
0.2
0
GFP
VCP/p97
Rpt5
siRNA

FIGURE 16 CONTINUED:

B

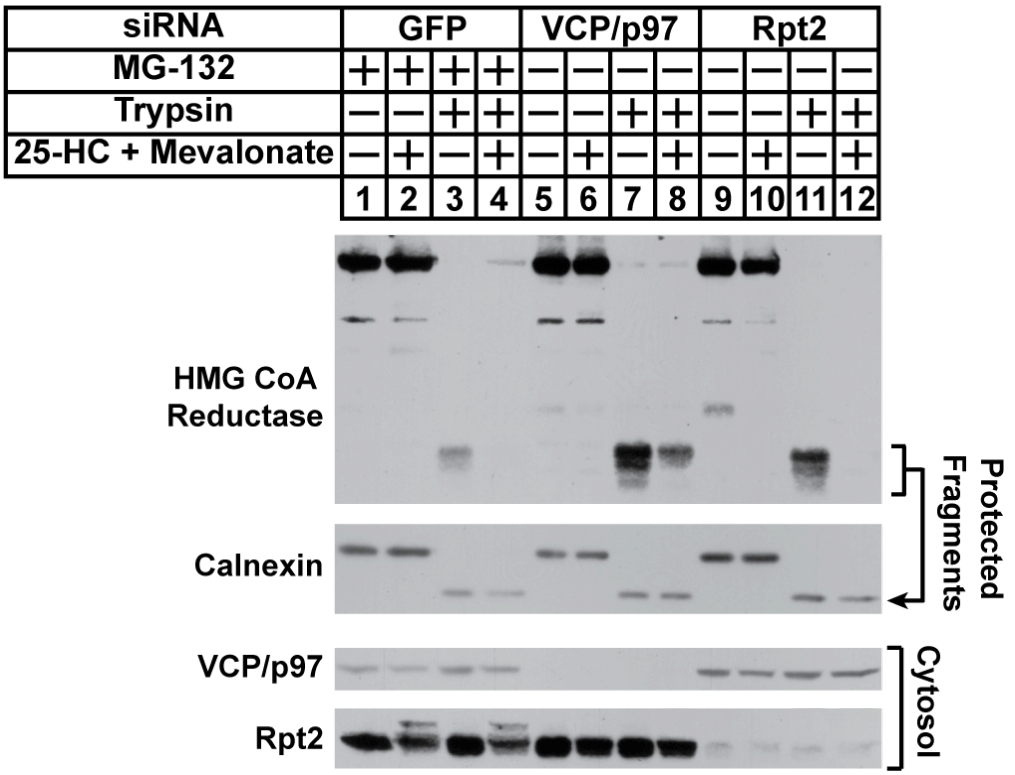

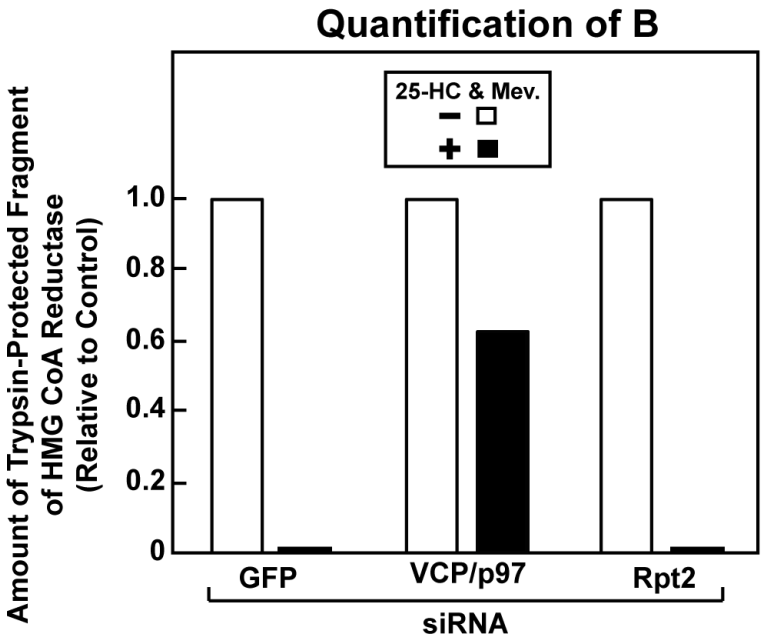

FIGURE 16 CONTINUED:

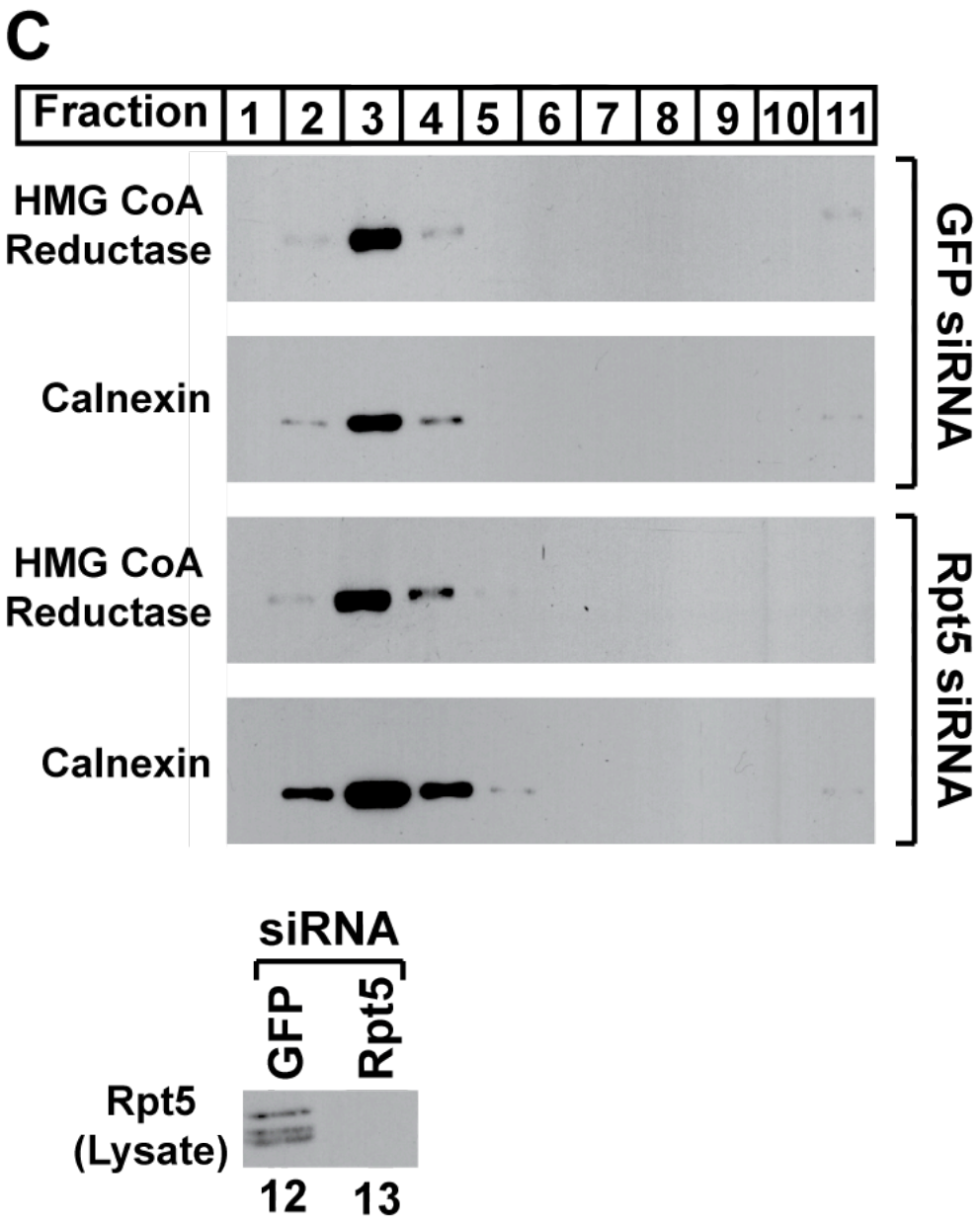

FIGURE 16 CONTINUED:

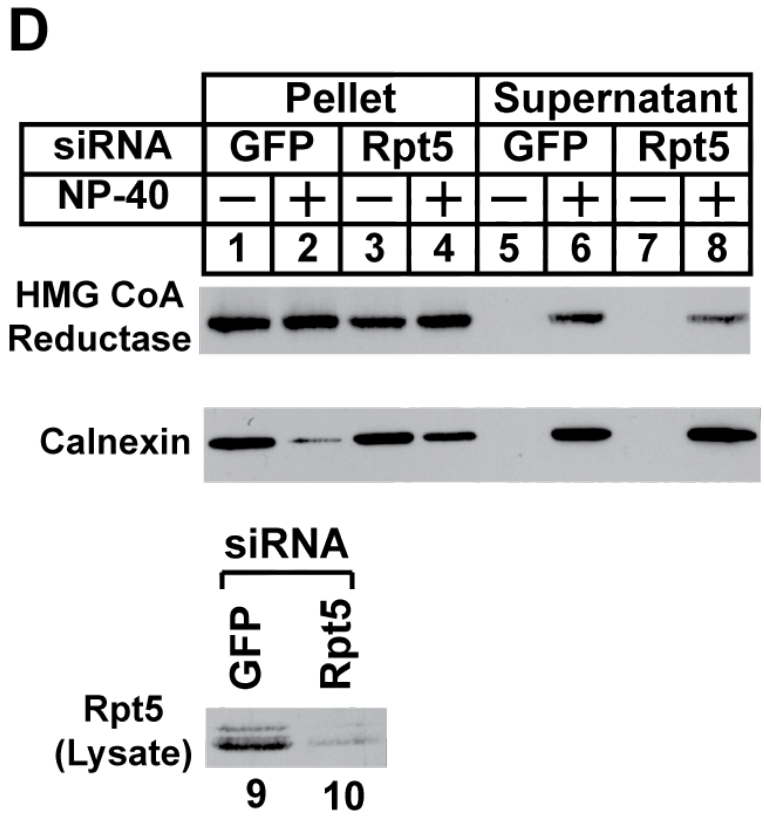

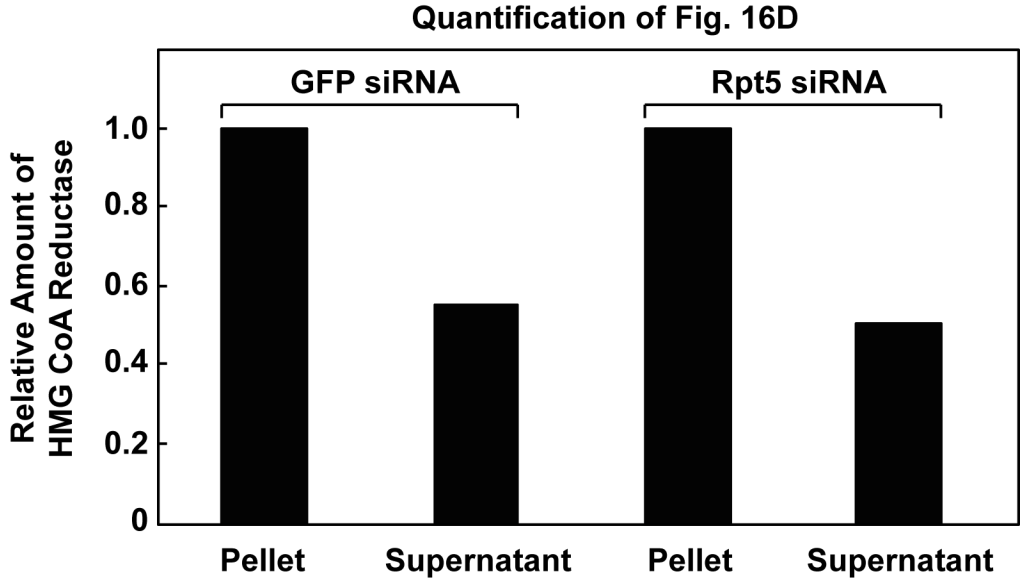

FIGURE 16 CONTINUED:

Figure 16. Sterol and nonsterol isoprenoids trigger membrane extraction of HMG CoA reductase in cells deficient for AAA-ATPases of the proteasome 19S regulatory particle. UT-2/pHMG-Red-T7 cells were set up for experiments, transfected with the indicated siRNA duplex, and treated in the absence or presence of 1 μM MG-132, 1μg/ml 25-HC, and 10 mM mevalonate as described in the legend to Figure 9. (*A* and *B*) Following treatments, cells were harvested for subcellular fractionation using Protocol 1 and aliquots of resulting membranes were subjected to trypsinolysis as described in the legend to 9. Following trypsinolysis, samples together with aliquots of the cytosol, were subjected to SDS-PAGE and immunoblot analysis was carried out with anti-T7 IgG (against reductase), IgG-18 (against VCP/p97), IgG-TBP1-191 (against Rpt5), anti-Rpt2 IgG, and anti-calnexin IgG. Bands corresponding to the protected fragments of reductase in the anti-T7 immunoblots were quantified using ImageJ software. The intensities of the protected fragments of reductase in the absence of 25-HC plus mevalonate were arbitrarily set as 1 for each of the RNAi-mediated knockdowns. (*C*) Membranes from control and Rpt5 knockdown cells treated with 25-HC plus 10 mM mevalonate and 1 μM MG-132 were resuspended in TBS containing 71.5% sucrose; the samples were then overlaid with buffer containing 65% and 10% sucrose. After centrifugation at 100,000 X g for 16 h at 4 ºC, aliquots were removed from the top (lane 1) to the bottom (lane 11) of the gradient. Membranes were seen to float at the interface between the 65% and 10% sucrose layers (lanes 3). Aliquots were analyzed by SDS-PAGE and immunoblot analysis with anti-T7 IgG (against reductase), anti-calnexin IgG, and IgG-TBP1-10 (against Rpt5). (*D*) Membranes from control and Rpt5 knockdown cells treated with 10 μM MG-132, 1 μg/ml 25-HC, and 10 mM mevalonate were resuspended in PBS with or without 0.1% NP-40. Following rotation at 4 ºC for 1 h, the samples were separated into soluble supernatant and insoluble pellet fractions by centrifugation. Aliquots of the fractions were then analyzed by immunoblot analysis as described in (*C*). Bands

corresponding to reductase in the pellet or supernatant fractions were quantified using ImageJ software. The intensities of reductase in pellets were arbitrarily set as 1 for each of the RNAi knockdowns.

Figure 17:

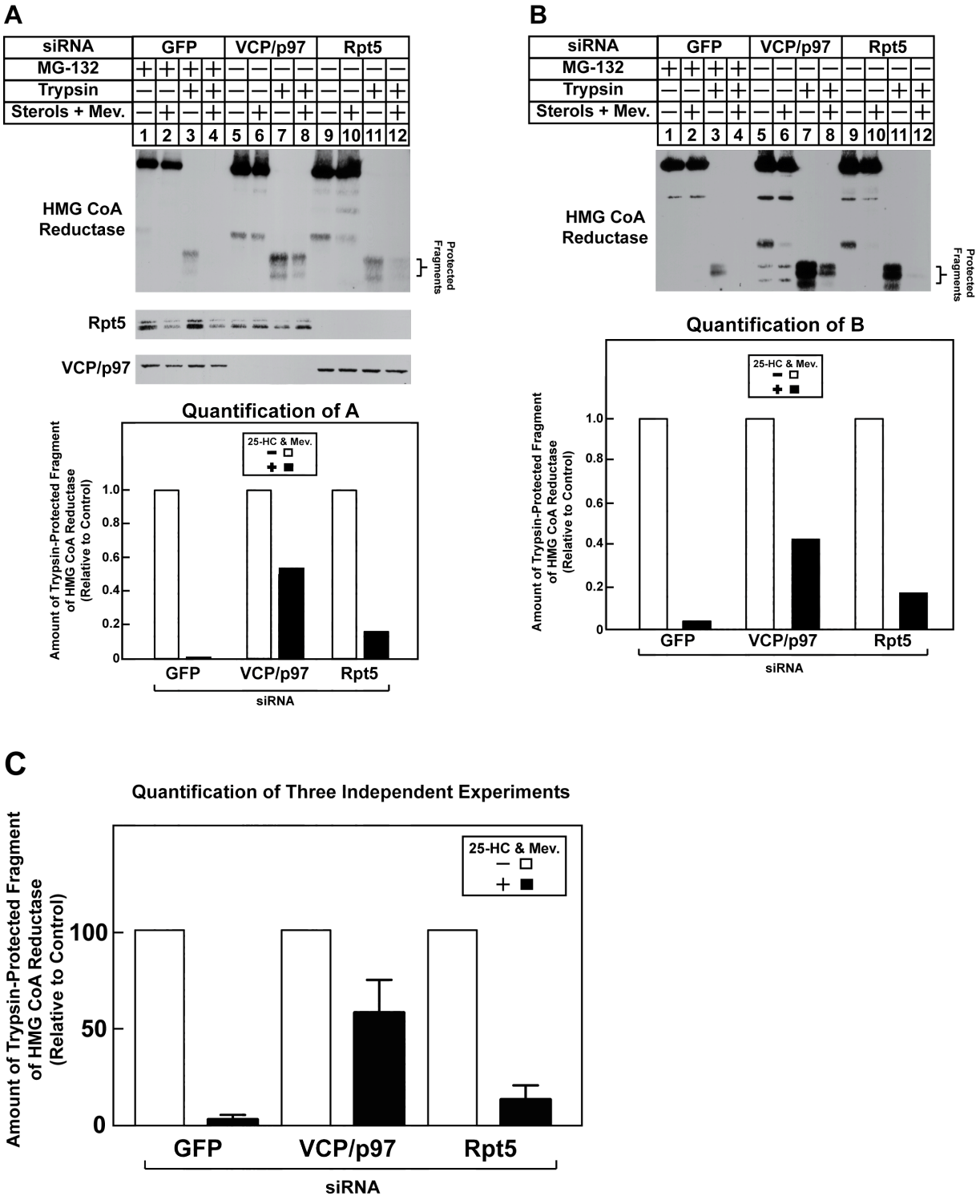
A
siRNA
GFP
VCP/p97
Rpt5
MG-132
Trypsin
Sterols + Mev.
1 2 3 4 5 6 7 8 9 10 11 12
HMG CoA Reductase
Protected Fragments
Rpt5
VCP/p97
Quantification of A
25-HC & Mev.
Amount of Trypsin-Protected Fragment of HMG CoA Reductase (Relative to Control)
1.0
0.8
0.6
0.4
0.2
0
GFP
VCP/p97
Rpt5
siRNA
B
Quantification of B
C
Quantification of Three Independent Experiments
100
50
0

Figure 17 continued:

Figure 17. RNAi-mediated knockdown of AAA-ATPases of the proteasome 19S regulatory particle blunts membrane extraction of HMG CoA reductase. (A and B) UT-2/pHMG-Red-T7 cells were set up for experiments, transfected with the indicated siRNA duplex, and treated with 1 μM MG-132 in the absence or presence of 1 μg/ml 25-HC plus 10 mM mevalonate as described in the legend to Figure 9. Following treatments, the cells were harvested for subcellular fractionation using Protocol 1 and aliquots of resulting membranes were subjected to trypsinolysis as described in the legend to 9. Reactions were terminated and the samples were subjected to SDS-PAGE, followed by immunoblot analysis with anti-T7 IgG (against reductase) and anti-calnexin IgG. Bands corresponding to protected fragments of reductase in the anti-T7 immunoblots were quantified using ImageJ software. The intensities of protected fragments of reductase in the absence of 25-HC plus mevalonate were arbitrarily set as 1 for each of the RNAi knockdowns. (C) Quantification of the combined results from experiments shown in (A), (B), and 6A

FIGURE 18:

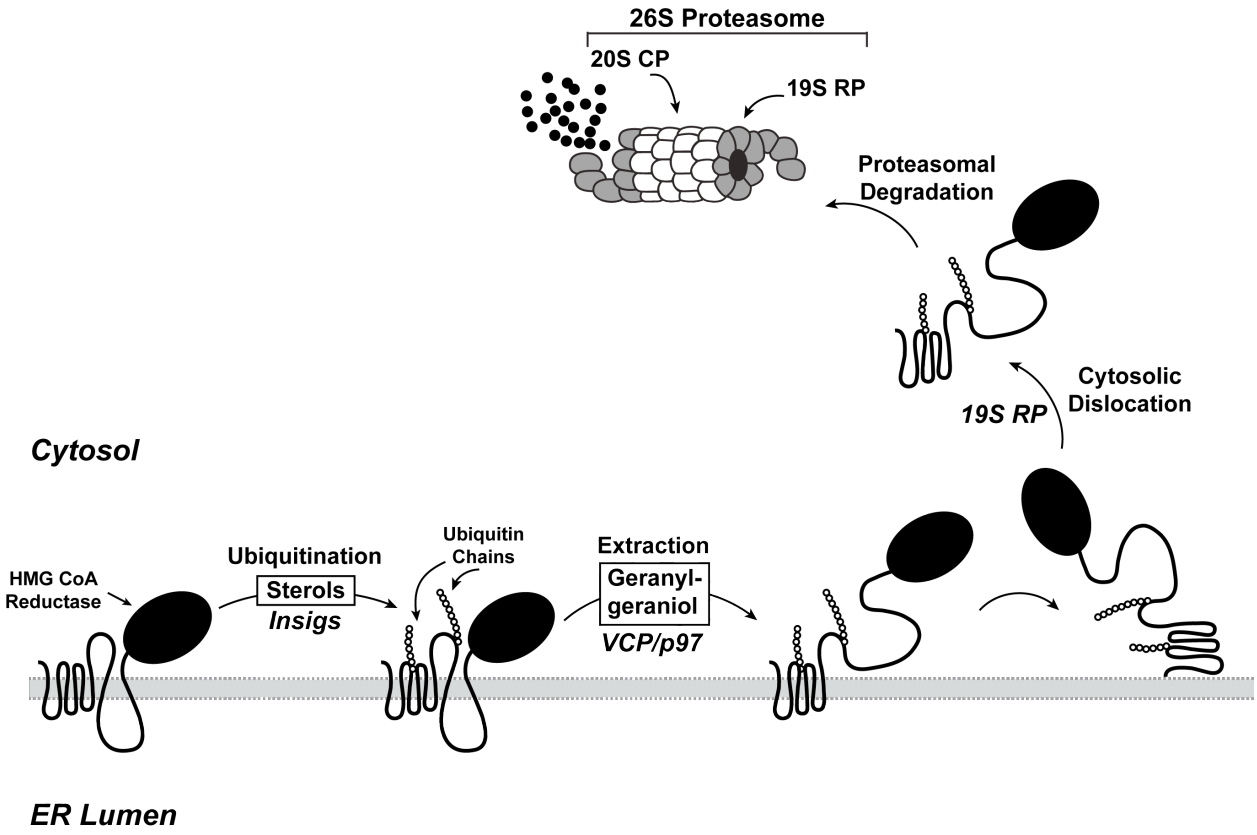
26S Proteasome
20S CP
19S RP
Proteasomal Degradation
Cytosolic Dislocation
19S RP
Cytosol
HMG CoA Reductase
Ubiquitination
Sterols
Insigs
Ubiquitin Chains
Extraction
Geranyl-geraniol
VCP/p97
ER Lumen

FIGURE 18 CONTINUED:

Figure 18. Model for the Insig-mediated, sterol-accelerated ER-associated degradation of HMG CoA reductase. The diagram shows a schematic representation of the sterol-accelerated ERAD of HMG CoA reductase. Sterol-induced binding to Insigs results in ubiquitination of HMG CoA reductase on two cytosolic lysine residues in the membrane domain. Ubiquitination of reductase, which is mediated by two Insig-associated ubiquitin ligases called gp78 and Trc8, marks the enzyme for VCP/p97-mediated extraction across ER membranes through a reaction that is enhanced by geranylgeraniol. Once extracted, reductase is released from membranes into the cytosol through a reaction mediated by the proteasome 19S regulatory particle (19S RP), and finally delivered into the 20S proteasome core particle (20S CP) for degradation.

CHAPTER THREE:

Additional Studies of HMG CoA Reductase Degradation and Membrane Extraction

3.1 Introduction

My goal during my time with the DeBose-Boyd laboratory was to set up an assay to study postubiquitination steps in reductase degradation. Prior to developing the trypsin assay to study membrane extraction of reductase, I attempted to establish three other assays for postubiquitination steps of reductase degradation. These assays were intended for use in studying the degradation or extraction of reductase, but they were either too inefficient to provide a robust assay for further analysis or it was not possible to optimize the experimental conditions in a way that made the assay worthwhile to pursue.

3.2 Materials and Methods

Materials

We obtained MG-132 from Boston Biochem (Cambridge, MA); TEV protease from Eton Biosciences; methotrexate from (Sigma, St. Louis, MO); horseradish peroxidase-conjugated donkey anti-mouse and anti-rabbit, IgGs (affinity-purified) from Jackson ImmunoResearch Laboratories (West Grove, PA); and 25-hydroxycholesterol from Steraloids (Newport, RI). Other reagents, including lipoprotein-deficient serum (LPDS, d > 1.215 g/ml), sodium compactin, and sodium mevalonate was prepared or obtained from previously described sources [75, 76].

Expression Plasmids

Wild type and lysine mutant (K89R/K248R) versions of pCMV-HMG-DHFR-3HA, encodes amino acids 1–346 of hamster HMG-CoA reductase followed by dihydrofolate reductase (DHFR) and three HA epitopes. pCMV-Insig-1-Myc, which encodes amino acids 1–277 of human Insig-1 followed by 6 tandem copies of a c-Myc epitope tag. pCMV-HMG TM, encodes amino acids 1–346 of hamster HMG-CoA reductase followed by 3 tandem copies of the T7

epitope tag. pCMV-HMG TM ($I_{143}T$), pertains to pCMV-HMG TM with the amino acid isoleucine 143 changed to a threonine. pCMV-Insig1-T7-TEV-ProtA, encodes amino acids 1-277 of human Insig-1 followed by a T7 epitope tag, a TEV protease cleavage site and protein A (provided by Dr. Youngah Jo). pCMV-HSV-HMGR-TEV, encodes a HSV epitope tag followed by full length hamster HMG-CoA reductase containing a TEV protease site between transmembrane helices seven and eight.

Cell Culture

Monolayers of CHO-K1 cells were maintained in tissue culture at 37 °C in 8-9% CO_2. Stock cultures were maintained in medium A (1:1 mixture of Ham's F-12 medium and Dulbecco's modified Eagle's medium containing 100 units/ml penicillin and 100 µg/ml streptomycin sulfate) supplemented with 5% FCS.

Transient Transfection

Transfection of CHO-K1 cells was carried out in 60-mm dishes using FuGENE 6 (Roche Applied Science) as described previously with minor modifications [65]. The cells received 2 µg of DNA per dish using a ratio of 3 µl of FuGENE 6 to 2 µg of DNA in medium A (without antibiotics) in a final volume of 200 µl per dish.

Isolation of Cell Membranes

(Protocol 1) **–** Triplicate dishes of cells were harvested into culture medium and washed with PBS. The cell pellets were resuspended in 500 µl of Buffer A (10 mM HEPES-KOH [pH 7.4], 10 mM KCL, 1.5 mM $MgCl_2$, 5 mM sodium EDTA, 5 mM sodium EGTA, 250 mM sucrose, 5 mM dithiothreitol, and 0.1 mM leupeptin), passed through a 22.5-gauge needle 30 times, and centrifuged at 1000 X g for 7 min at 4 °C. The resulting post-nuclear supernatants were then subjected to an additional round of centrifugation at 16,000 X g for 15 min at 4 °C. The resulting

pellets were designated as the membrane fraction. (Protocol 2) – Triplicate dishes of cells were harvested into culture medium, washed with PBS, resuspended in Buffer A, and lysed for preparation of post-nuclear supernatants as described above. The post-nuclear supernatants were then subjected to centrifugation at 100,000 X g for 45 min at 4 °C. The resulting pellet and supernatant fractions were designated membrane and cytosol, respectively.

GST-TEV Protease Isolation

Frozen cultures of *E. Coli* BL21 expressing GST-TEV Protease were provided by an assistant professor, Dr. Tong-jin Zhao. Bacteria were incubated in 10 mL of LB containing ampicillin and placed in a shaker overnight. Bacteria culture was diluted 1:100 in 1 liter of LB with ampicillin and allowed to shake for three hours at 37 ^{o}C. Isopropyl-1-thio-β-D-galactopyranoside (IPTG) was added at a final concentration of 0.25 mM and allowed to shake 5 hours at 30 ^{o}C. Cultures were subjected to centrifugation at 4000 x g for ten minutes and bacteria pellets were stored at -80 ^{o}C overnight. Bacteria were resuspended in 40 mL Buffer E (20 mM Tris [pH 7.5], 150 mM NaCl, 1 mM EDTA, 1 mM DTT, 1 mg/ml lysozyme) containing protease inhibitor cocktail. Suspensions were left at 4 ^{o}C for 30 minutes before being subjected to sonication five times (20 second sonication followed by 59.9 seconds cool down). Samples were allowed to rotate for 15 min at 4 ^{o}C and then centrifuged at 100,000 x g for 30 minutes. Supernatant was loaded two separate times on a gel column containing 3 mL of GST-bead slurry overlaid with 20 mL Buffer E containing protease inhibitors. The column was then washed with 100 mL Buffer E without protease inhibitors. The GST-TEV protease was eluted from the column using 15 ml of elution buffer (25 mM Tris [pH 8.0], 1 mM EDTA, 1 mM DTT, 15 mM GSH, 20 µg/ml PMSF). An Amicon/Millipore centrifugal filter was used to concentrate and dialyze the protein. Final protein concentration was measured by nanodrop (approximately 2 mg/ml).

TEV Protease Cleavage Assay

Cells were harvested and the membrane fractions were prepared using Protocol 1 as indicated in the figure legends. The membrane pellets were resuspended in 50 µl Buffer B (Buffer A without dithiothreitol and leupeptin supplemented with 100 mM NaCl). The resuspended membranes were pooled together when appropriate and divided into 45 µl aliquots for TEV protease treatment. Some of the aliquots of membranes were treated with 1% NP-40 (final concentration) prior to TEV protease digestion as indicated in the figure legends. TEV protease (4 µg) was added to the resuspended membranes and DTT was added at a final concentration of 1 mM. Samples were incubated at 37 °C for one hour and mixed approximately every fifteen minutes. TEV proteolysis was terminated by the addition of Buffer C and 4X SDS loading buffer (1X final concentration). Samples were then heated at 37 °C for 20 min and subjected to SDS-PAGE, followed by immunoblot analysis.

Immunoblot Analysis

The protein concentration of membrane and cytosol fractions was determined using the Coomassie Bradford and the BCA protein assay kits, respectively (Thermo Scientific, Rockford, IL). Aliquots of the fractions were mixed with an equal volume of Buffer C and 4X SDS loading buffer added to a final concentration of 1X. For anti-Scap immunoblots, fractions were directly mixed with 4X SDS loading buffer to a final concentration of 1X. Samples were fractionated on SDS-PAGE gels calibrated with prestained molecular mass markers (Bio-Rad, Hercules, CA), after which the proteins were transferred to nitrocellulose membranes and subjected to immunoblot analysis. Primary antibodies used for immunoblotting were as follows: mouse monoclonal anti-HA tag IgG (Sigma, St. Louis, MO); monoclonal anti-T7 Tag IgG (EMD Biosciences, Darmstadt, Germany); mouse monoclonal anti-HSV IgG (EMD Biosciences,

Darmstadt, Germany); IgG-9E10, a mouse monoclonal antibody against myc; and rabbit polyclonal anti-calnexin IgG (Novus Biologicals, Littleton, CO). Bound antibodies were visualized with peroxidase-conjugated donkey anti-mouse or anti-rabbit IgG using the SuperSignal West Pico Chemiluminescent Substrate (Thermo Scientific, Rockford, IL) according to the manufacturer's instructions. Filters were exposed to film at room temperature.

3.3 Results and Discussions

The following sections describe the goals/aims of each set of experiments, brief discussions on the reasons for abandoning each set of experiments, and representative examples of data collected.

3.3.1 Development of cell-free system for ERAD of HMG CoA reductase-DHFR fusion protein

The goal of this project was to adapt our in vitro ubiquitination assay to study reductase degradation in vitro [63]. A plasmid was made by a postdoctoral fellow in the lab, Dr. Isamu Hartman, expressing the membrane domain of reductase with the catalytic domain replaced by dihydrofolate reductase (DHFR) and three hemagglutinin (HA) tags. The membrane domain was used, as it is necessary and sufficient for reductase degradation [62, 65]. DHFR when in the presence of methotrexate (MTX) is known to assume a very tightly folded confirmation and become resistant to degradation by the proteasome [102]. Thus, a chimeric protein consisting of the membrane domain of reductase fused to DHFR will be ubiquitinated and degraded in the presence of Insigs and sterols. Whenever this chimeric protein is also incubated in the presence of MTX the proteasome will stop degrading upon reaching the proteasome resistant DHFR and will release the DHFR into the cytosol (Fig. 19). This cytosolic release of DHFR can be monitored by immunoblot analysis and used as an indicator of reductase degradation.

In transient transfections, the reductase-DHFR fusion protein was degraded in a sterol and

Insig-1 dependent manner (Fig. 20, lanes 1, 2, 5, and 6). In the presence of MTX, the degradation of reductase was blunted and the cytosolic release of DHFR was enhanced in a sterol and Insig-1 dependent manner (Fig. 20, lanes 4 and 8). In further studies, the cytosolic release of DHFR could be blocked when transfecting an ubiquitination resistant lysine mutant version of reductase-DHFR (Fig. 21, compare lanes 4 and 8 of cytosol).

The cytosolic release of DHFR appeared to be a sensitive indicator of reductase degradation that might serve well for use in an in vitro degradation assay. For this purpose, a stable cell line was produced expressing the reductase-DHFR fusion protein. These cells were permeabilized as described previously and incubated with ATP, rat liver cytosol, ubiquitin, and incubated in the absence or presence of proteasome inhibitors [63]. Samples were incubated at 37 ^{o}C, separated into pellet and supernatants through centrifugation, and then analyzed by immunoblot with anti-HA antibodies. Unfortunately, the degradation of reductase *in vitro* is very inefficient and the cytosolic release of DHFR is likewise inefficient, hindering future efforts to use this *in vitro* assay. In hindsight, this might serve as a viable assay *in vitro* if cells were transfected transiently for each experiment with the reductase chimeric protein and Insig-1 such that expression levels of reductase could be enhanced.

Additionally, during the course of this project we found that the addition of methotrexate and sterols blunted the degradation of the fusion protein (Fig. 20, lanes 4 and 8). A plausible explanation for this is potential directionality to reductase degradation. If the proteasome, for unknown reasons, prefers to begin degrading reductase from the C-terminus then the addition of methotrexate would make the DHFR fused to the C-terminus of reductase and the membrane domain of reductase resistant to degradation. To investigate this possibility fusion proteins of the transmembrane domain of reductase with DHFR on the N-terminus or both N- and C-termini were made. These experiments showed the same results, where the addition of sterols and

methotrexate led to increased cytosolic release of a DHFR fragment and blunted degradation of reductase from the ER membrane.

3.3.2 Development of Double Glycosylated HMG CoA Reductase

One hallmark of cytosolically dislocated ER membrane proteins is the absence of N-linked sugars when the protein reaches the cytosol. During ERAD proteins are ubiquitinated and dislocated to the cytosol where they can then be deglycosylated by cytosolic N-glycanases. Reductase contains a single N-linked sugar and has been shown in prior studies to be deglycosylated in the cytosol as would be expected [70, 103]. In a similar experiment it was noticed that when cells were treated with sterols and membranes were isolated, a noticeable change in the migration of reductase could be observed by SDS-PAGE. Indicating that reductase could be extracted from the ER membrane but still retain a membrane association such that the lumenal loop could be deglycosylated.

Efforts were initiated to use deglycosylation in our *in vitro* assay as an indicator of membrane extraction, but unfortunately, the removal of a single N-linked sugar does not result in a large shift in reductase migration. In an effort to increase the difference in reductase migration upon deglycosylation, Dr. Isamu Hartman produced a construct of the reductase membrane domain containing an additional glycosylation site in the first luminal loop (Fig. 22). In the absence of sterols HMG TM was found to be singly glycosylated and shows a small shift to a lower deglycosylated band in cells treated with sterols (Fig. 23, lanes 1 and 2). HMG TM ($I_{143}T$) was found in two bands by immunoblot analysis of sterol-deprived cells, corresponding to double and single glycosylated reductase (Fig. 23, lanes 3, 5, and 7). When treated with sterols reductase shifts down to another third band that corresponds to fully deglycosylated reductase (Fig. 23, lanes 6 and 8). A stable cell line was produced in collaboration with a postdoctoral fellow, Dr. Rania Elsabrouty, in hopes that all of the stably expressed HMG TM ($I_{143}T$) would be

fully glycosylated as opposed to existing as a population of either double or single glycosylated proteins in the absence of sterols. However, the stable cell line did not resolve this issue. It is possible that the new glycosylation site added into the first luminal loop was not easily accessible to glycosylating enzymes.

3.3.3 TEV Protease Cleavage Assay

The final *in vitro* assay I attempted to develop involved using a reductase construct containing a TEV protease cleavage site in the luminal loop between transmembrane helices seven and eight. As with the glycosylation assay, reductase will remain in the membrane in the absence of sterols but would be extracted out of the membrane in the presence of sterols allowing for exposure of the TEV protease cleavage site to the cytosol. Isolated membrane fractions could then be treated with a TEV protease so that the chimeric protein is clipped at the cleavage site and the C-terminal half of the protein would be released from the membrane. Membrane fractions would be isolated and subjected to SDS-PAGE and immunoblot analysis for reductase. It was expected that cleavage of the protein would result in a change in molecular weight of reductase in the immunoblots, leaving a fragment that is only released from cells treated with sterols.

Early studies demonstrated that sterols and Insigs regulate degradation of the chimeric protein. A postdoctoral fellow in the laboratory, Dr. Youngah Jo, supplied a control protein, Insig1-T7-TEV-proteinA. This protein contains a TEV site on the cytosolic face of the ER and was used to indicate that reaction conditions (time, temperature, and amount of protease) were optimized. A fragment of Insig-1 was seen when membranes were treated with TurboTEV protease (Eton Biosciences) regardless of the absence or presence of detergents (Fig. 24, lanes 3 and 4). A fragment for reductase was observed regardless of the absence or presence of sterols or detergents (Fig. 24, lanes 7-10). A closer examination of the buffer TurboTEV

protease is supplied in revealed the presence of detergents. Any detergent in solution with the TEV protease would allow for solubilization of reductase and cleavage of the TEV site regardless of the absence or presence of sterols. In an effort to circumvent this issue, a GST tagged TEV protease was isolated from BL21 bacteria and stored in buffer lacking detergents. Dr. Tong-jin Zhao, an assistant professor, provided an aliquot of the bacteria for use in subsequent experiments. The GST-TEV protease caused a fragment of Insig-1 to be formed (Fig. 25, lane 2). However, the fragment seen in reductase immunoblots was unaffected by the absence or presence of detergents (Fig. 25, lanes 3-10). This project was not pursued any further.

Figure 19

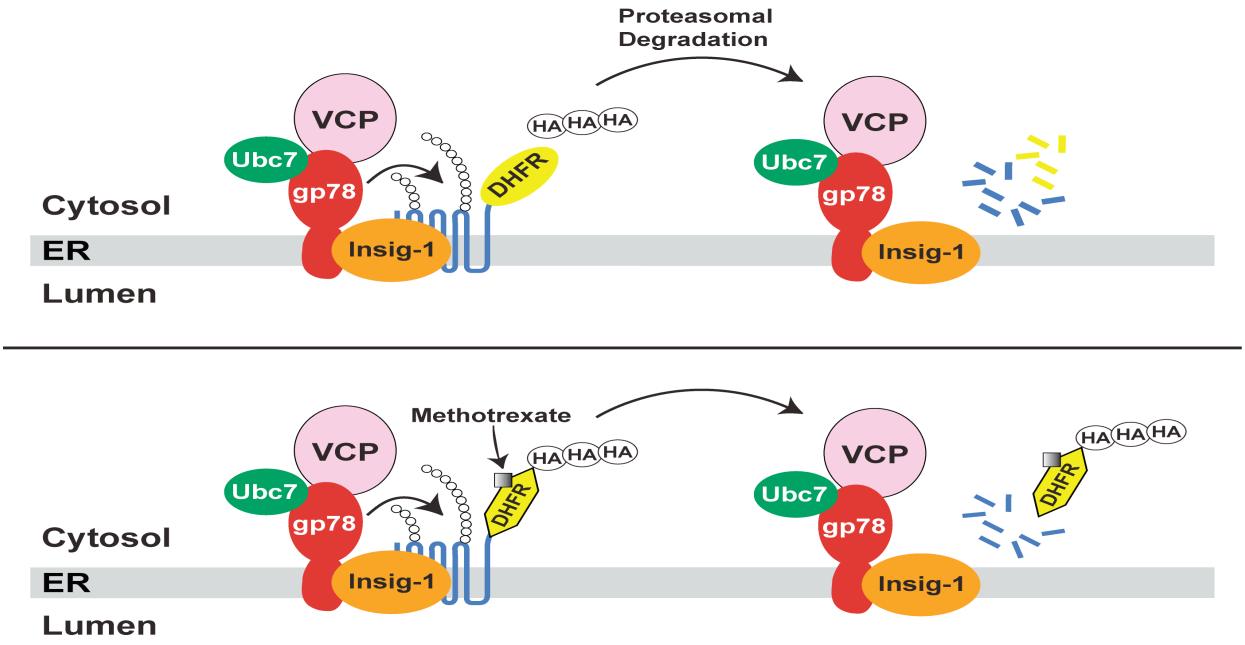

Figure 19. Degradation of HMG CoA Reductase-DHFR Fusion Protein. In the absence of methotrexate, both reductase and DHFR will be degraded by the proteasome. In the presence of methotrexate, the proteasome resistant DHFR will be released into the cytosol as a product of reductase degradation.

Figure 20

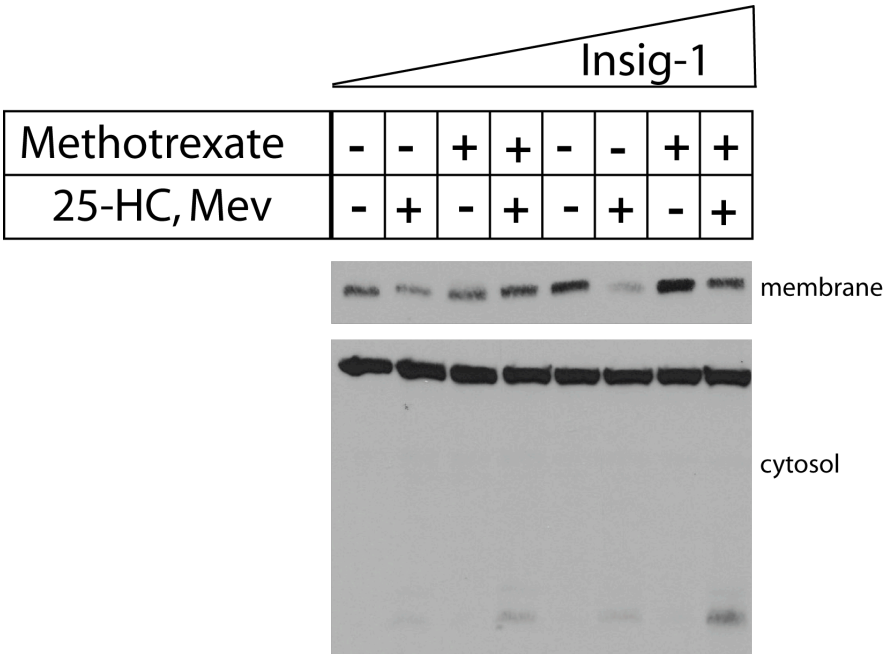

Figure 20. Methotrexate Enhances Sterol-Regulated Release of DHFR-HA in Intact Cells. On day 0, CHO-K1 cells were plated at $4x10^5$ per 60-mm plates in medium A. On day 1, cells were transfected with 0.5 μg HMG-DHFR and 10 ng (lanes 1-4) or 30 ng (lanes 5-8) of Insig-1 in medium A supplemented with 5% LPDS. After 4 hours the cells were treated with direct addition of medium A supplemented with 5% LPDS, 10 μM compactin, and 50 μM mevalonate (final concentrations). On day 2, cells were treated with medium A supplemented with 5% LPDS, 10 μM compactin, and 50 μM mevalonate in the absence or presence of 20 μM methotrexate. Cells were incubated for 30 min at 37 ^oC. Cells then received direct addition of medium A supplemented with 5% LPDS, 10 μM compactin, and 50 μM mevalonate in the absence or presence of 20 μM methotrexate and 1 μg/ml 25-HC plus 10 mM mevalonate (final concentrations). After 4 hours cells were subjected to subcellular fractionation using Protocol 2. Resulting membrane and cytosolic fractions were subjected to SDS-PAGE, followed by immunoblot analysis with anti-HA IgG (against reductase).

Figure 21

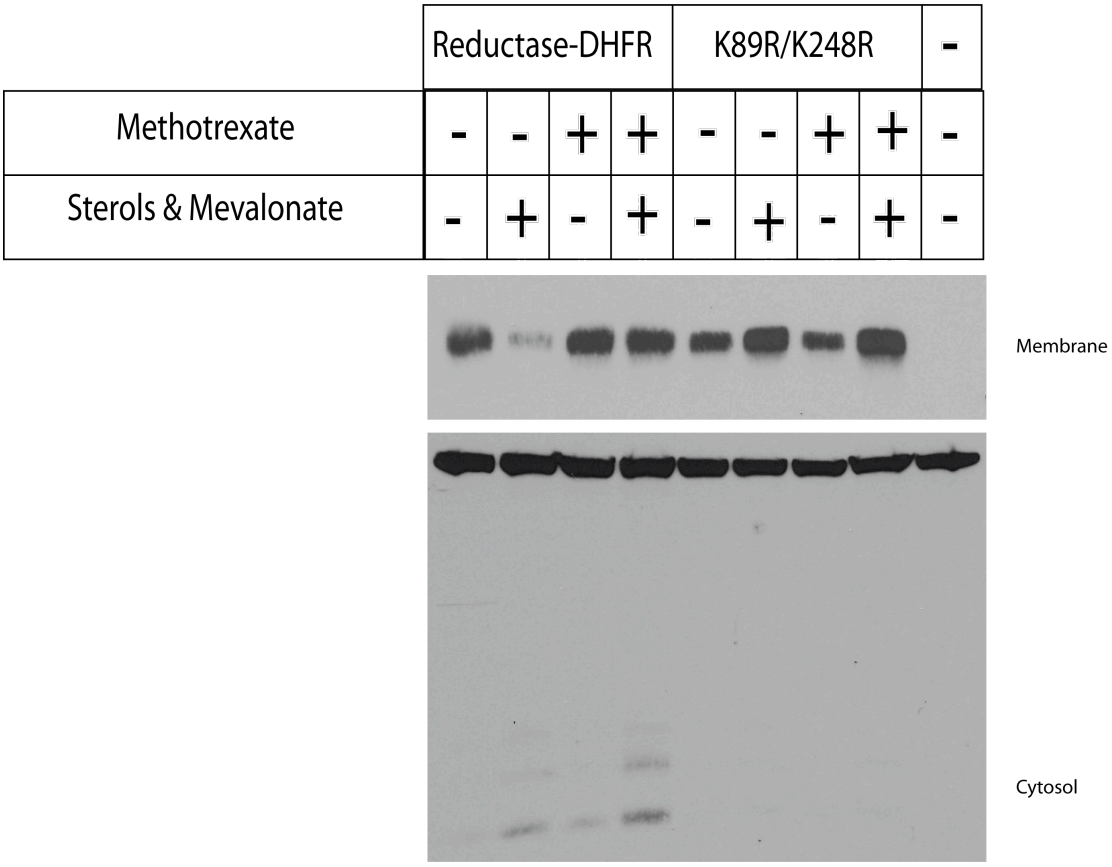

Figure 21. **Ubiquitination Dependent Release of DHFR-HA.** On day 0, cells were plated as described in figure 20. On day 1, cells were transfected with 0.5 μg Reductase-DHFR or Reductase-DHFR (K89R/K248R) and 30 ng of Insig-1 in medium A supplemented with 5% LPDS. After 4 hours the cells were treated with direct addition of medium A supplemented with 5% LPDS, 10 μM compactin, and 50 μM mevalonate (final concentrations). On day 2, cells were subjected to cellular fractionation using Protocol 2 and were subjected to SDS-PAGE, followed by immunoblot analysis with anti-HA IgG (against reductase) as described in figure 20.

Figure 22

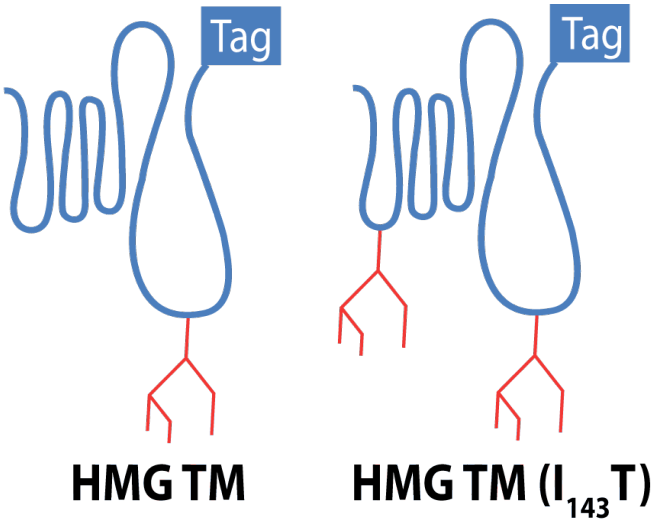

Figure 22. Schematic of HMG TM and HMG TM (I_{143}T). Schematic of HMG TM and HMG TM (I_{143}T) indicating the location of the T7 epitope tag. Sites for N-linked glycosylation are indicated in each protein.

Figure 23

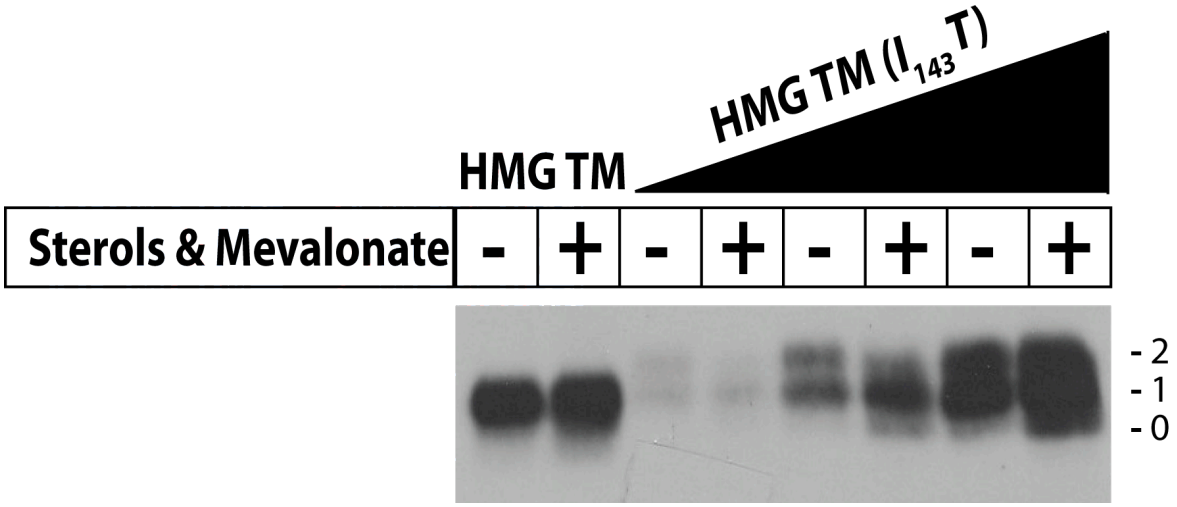

Figure 23. Sterol-Regulated Deglycosylation of HMG TM (I_{143}T). On day 0, CHO-K1 cells were plated at $4x10^5$ per 60-mm plates in medium A. On day 1, cells were transfected with 50 ng Insig1-myc plus 1 μg HMG TM or 0.1 (lanes 3 and 4) to 1 μg (lanes 7 and 8) HMG TM (I_{143}T) in medium A supplemented with 5% LPDS. After 4 hours the cells were treated with direct addition of medium A supplemented with 5% LPDS, 10 μM compactin, and 50 μM mevalonate (final concentrations). On day 2, cells were treated with medium A supplemented with 5% LPDS, 10 μM compactin, 50 μM mevalonate, and 10 μM MG-132. After 1 hour cells received direct addition of medium A supplemented with 5% LPDS, 10 μM compactin, 50 μM mevalonate, and 10 μM MG-132 in the absence or presence and 1 μg/ml 25-HC plus 10 mM mevalonate (final concentrations). After 4 hours cells were subjected to subcellular fractionation using Protocol 1. Resulting membrane fractions were subjected to SDS-PAGE, followed by immunoblot analysis with anti-T7 IgG (against reductase).

Figure 24

Transfected Plasmids	Insig1-T7-TEV				HSV-HMGR-Tev + Insig1-myc					
TEV Protease	-	-	+	+	-	-	+	+	+	+
NP-40	-	+	-	+	-	-	-	-	+	+
25-HC + Mevalonate	-	-	-	-	-	+	-	+	-	+

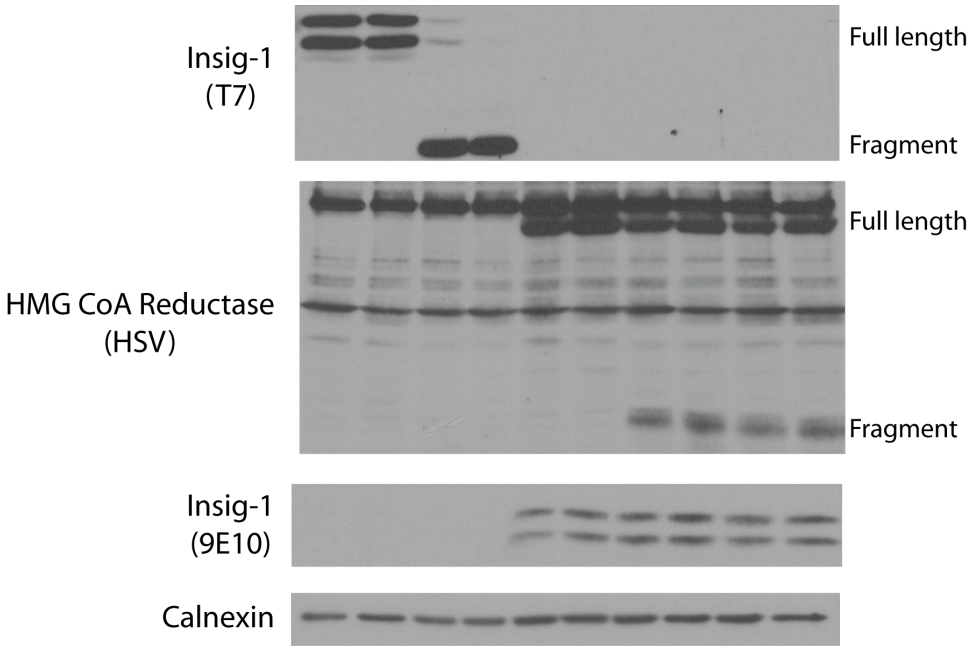

Figure 24. Testing of Eton TEV Protease. On day 0, CHO-K1 cells were plated at $4x10^5$ per 60-mm plates in medium A. On day 1, cells were transfected with 1 μg of Insig1-T7-TEV or 0.5 μg HSV-reductase-TEV plus 100 ng Insig1-myc in medium A supplemented with 5% LPDS. After 4 hours the cells were treated with direct addition of medium A supplemented with 5% LPDS, 10 μM compactin, and 50 μM mevalonate (final concentrations). On day 2, cells were treated with medium A supplemented with 5% LPDS, 10 μM compactin, 50 μM mevalonate, and 10 μM MG-132 in the absence or presence of 1 μg/ml 25-HC plus 10 mM mevalonate (final concentrations). After 3 hours cells were subjected to subcellular fractionation using Protocol 1. Membranes were resuspended in Buffer B and pooled where appropriate. Membranes were aliquoted and treated with or without 1% NP-40 and 4μg TurboTEV protease (Eton Bioscience) plus 1 mM DTT (final concentrations). Samples were incubated at 37 ^oC for one hour. Resulting membrane fractions were subjected to SDS-PAGE, followed by immunoblot analysis with anti-HSV IgG (against reductase), anti-T7 IgG (against Insig-1), anti-9E10 (against Insig1-myc) and anti-Calnexin IgG.

Figure 25

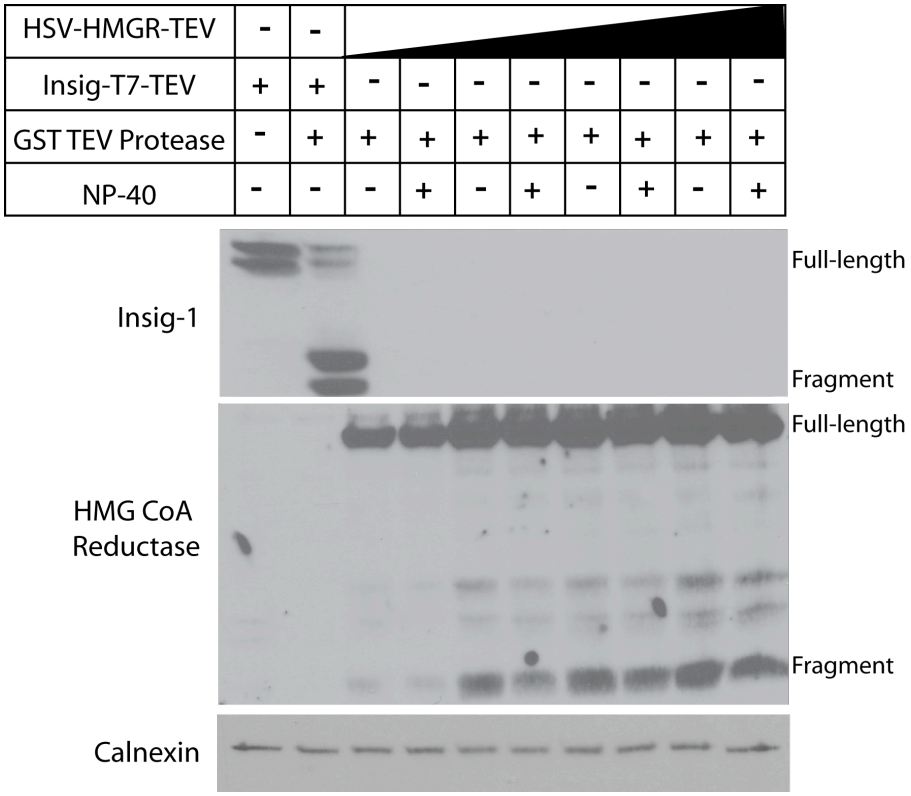

Figure 25. Testing of GST-TEV Protease. On day 0, CHO-K1 cells were plated at $4x10^5$ per 60-mm plates in medium A. On day 1, cells were transfected with 1 μg of Insig1-T7-TEV or HSV-reductase-TEV (lanes 3 and 4: 0.5 μg, lanes 5 and 6: 1 μg, lanes 7 and 8: 3μg, lanes 9 and 10: 5 μg) in medium A supplemented with 5% LPDS. After 4 hours the cells were treated with direct addition of medium A supplemented with 5% LPDS, 10 μM compactin, and 50 μM mevalonate (final concentrations). On day 2, cells were subjected to subcellular fractionation using Protocol 1. Membranes were resuspended, pooled where appropriate, aliquoted and treated as described in Figure 24. Resulting membrane fractions were subjected to SDS-PAGE, followed by immunoblot analysis with anti-HSV IgG (against reductase), anti-T7 IgG (against Insig-1) and anti-Calnexin IgG.

CHAPTER FOUR

Conclusions and Perspectives

4.1 Overall Conclusions

HMG CoA reductase is the target of the statin class of cholesterol-lowering drugs. Statins are utilized to lower plasma LDL-cholesterol and thereby attenuate the occurrence of cardiovascular disease. Because statins reduce sterol and nonsterol regulatory molecules that normally govern feedback regulation of reductase, the enzyme becomes elevated during statin therapy, limiting the effectiveness of this class of drugs [104-106]. Part of this elevation is likely due to slowed degradation of reductase. Thus, a better understanding of reductase degradation will lead to development of new drugs that stimulate the reaction, counteracting the accumulation of the enzyme that accompanies statin therapy.

Studies described here examine sterol-regulated extraction of ubiquitinated HMG CoA reductase from ER membranes and subsequent delivery to proteasomes for ERAD. A novel assay was developed to measure the extraction of reductase across ER membranes. The physiologic relevance of this extraction was revealed by its stimulation by the oxysterol 25-HC and the nonsterol isoprenoid geranylgeraniol (Fig. 6*D*), which also accelerate reductase degradation (Fig. 8*B*). Membrane extraction of reductase required the presence of Insigs (3 independent experiments, Fig. 9*A*, 9*B*, and 10) and VCP/p97 (7 independent experiments, 9*C*, 9*D*, 10, 16*A*, 16*B*, 17*A* and 17*B*). Remarkably, membrane extraction of reductase continued in cells deficient for ATPases of the proteasome 19S RP (4 independent experiments, Fig. 16*A*, 16*B*, 17*A*, and 17*B*). The novel findings of this study include: (1) clarification of the step at which geranylgeraniol augments reductase degradation; (2) demonstration that VCP/p97 mediates membrane extraction of ubiquitinated reductase; and (3) identification of a novel role for the 19S RP ATPases in dislocation of extracted reductase from membranes into cytosol for degradation.

An alternative explanation for the sterol dependent sensitivity of the T7 tagged lumenal loop of reductase is that the addition of sterols alters ER membrane integrity allowing trypsin to leak through the membrane. Sterol dependent loss of ER membrane integrity seems like an unlikely cause. If the membrane integrity were altered by sterols I would expect to see increased trypsin sensitivity of the lumenal domains in SCAP and calnexin in Figure 5. Additionally, apomine (which mimics sterols in stimulating reductase degradation) enhances the trypsin accessibility of the lumenal loop of reductase to a similar degree as seen using 25-HC.

Another potential explanation for my results is a sterol-dependent conformational change that allows the T7 epitopes in reductase to become susceptible to trypsin digestion. However, I feel this is also an unlikely explanation for my results because of two reasons. First, the sensitivity of the protected fragments of reductase to trypsin is restored in the absence of sterols whenever a detergent such as NP-40 is used to solubilize membranes. Secondly, the trypsin accessibility is dependent upon the presence of both Insigs and VCP/p97. These two proteins are involved in very different steps of reductase degradation; the sterol-induced binding of reductase to Insigs is critical for sterol-regulated ubiquitination of the enzyme, whereas VCP/p97 acts after sterol-induced reductase ubiquitination has already taken place. If the sensitivity of the protected fragments of reductase to trypsin digestion results from a sterol-induced conformational change, one would not expect the reaction to be blocked by knockdown of VCP/p97. Taken together, my results are consistent with the conclusion that Insig-mediated, sterol-induced ubiquitination of reductase leads to VCP/p97-mediated extraction of reductase across ER membranes for subsequent cytosolic dislocation through reactions mediated by the 19S RP.

One shortcoming of the experiments described here is the efficiency of RNAi, which can vary somewhat from experiment to experiment. Despite this, knockdown of VCP/p97 and Insigs

always blunts membrane extraction of reductase, whereas knockdown of the 19S RP does not. These experiments rely on the use of RNAi because there are no inhibitors of VCP/p97 that potently inhibit reductase degradation in our hands. In addition, I have not been able to identify any inhibitors that are specific to the ATPases of the 19S RP. To this end, I tried an inhibitor against the 19S RP-associated deubiquitinating enzyme, but it had no effect on reductase degradation. In future experiments we could try using Drosophila S2 cells in which our laboratory and others have demonstrated highly responsive RNAi.

Prior to the current studies, the inefficiency of reductase cytosolic dislocation indicated the possibility that cytosolic reductase may have been an artifact of the cell fractionation process. However, the fact that cytosolic dislocation of reductase can be blunted by knockdown of ATPase subunits of the 19S RP demonstrates that cytosolic dislocation is not an artifact but a meaningful intermediate in reductase degradation. The low levels of peripherally associated or dislocated reductase observed here and in previous experiments could be due to saturation of proteasomes and/or other proteins involved in ERAD. In contrast, the robustness of the trypsin protection assay demonstrates that membrane extraction of reductase would be an ideal intermediate to study in reductase degradation in vitro.

Under physiological conditions, it can be envisioned that membrane extraction, cytosolic dislocation and proteolytic degradation would be fairly fluid and processive events. It would be beneficial to the cell to prevent large amounts of membrane proteins from accumulating in the cytosol when proteasomes are impaired. In fact, recent evidence has indicated that the cell can sense and attempt to relieve proteasome inhibition by upregulating the expression of proteasome subunits through the transcription factor Nrf1 [107]. Proteasome inhibitors are a necessary tool to use in experiments examining the mechanisms involved in reductase degradation and ERAD of other substrates. Without proteasome inhibitors it would be very

difficult to observe and better understand the mechanism of each step of the ERAD pathway for reductase.

An outstanding question in the ERAD field pertains to the way integral membrane substrates are made soluble in the cytosol following dislocation. Again, it seems unlikely that large amounts of integral membrane proteins are allowed to accumulate in the cytosol under physiological conditions. Nevertheless, under physiological conditions one could envision that following membrane extraction, reductase would be released into the cytosol by action of the 19S RP and possibly made soluble through binding to cytosolic chaperones like Hspa8 or Bag6. A postdoctoral fellow in the laboratory, Dr. Dong-Jae Jun, identified Hspa8 to be important for reductase degradation in an RNAi screen performed in *Drosophila* S2 cells. Bag6 is a chaperone that prevents aggregation of at least certain ERAD substrates [88, 108]. Bag6 is known to interact with proteasomes and the ubiquitin ligase gp78 with its functional partner Ubxd8 [88, 109]. An association with gp78 and Ubxd8 allow for Bag6 localization with the ER membrane. This suggests that Bag6 could interact with extracted ERAD substrates providing a means by which ubiquitination, dislocation, and targeting to the proteasome could be accomplished in a very coordinated manner [110]. A key experiment for future studies would be to determine if knockdown of Hspa8 or Bag6 blocks reductase degradation, causing a large fraction of the protein to accumulate in detergent insoluble aggregates. A chaperone, such as Hspa8 or Bag6, could assist in solubilization of reductase during or soon after extraction until the enzyme can be degraded by the proteasome.

4.2 Recommendations for Future Studies

The studies described here open up many opportunities to better understand reductase degradation as well as the ERAD of other integral membrane substrates in future studies. The trypsin protection assay allows for the investigation of factors required for membrane extraction

of reductase. Future studies will focus further on the role of VCP/p97 and geranylgeraniol in membrane extraction as well as look into the potential role lipid droplets may play in reductase membrane extraction. The studies here also describe a novel role of the 19S RP in reductase degradation, opening the possibility of studying the mechanism through which the 19S RP enhances reductase degradation.

4.2.1 Role of Lipid Droplets in Membrane Extraction of Reductase

To further validate that reductase undergoes membrane extraction prior to its cytosolic dislocation and proteasomal degradation, a separate method such as Immunostaining could be used to demonstrate that this event occurs in cells. Confocal immunofluorescent staining would allow for the visualization of sterol-dependent extraction of HMG-Red-T7 from the ER. In initial experiments, a concentration of digitonin will need to be determined that allows for the plasma membrane of cells to become permeabilized while leaving the ER membrane intact. If the ER membrane remains intact during permeabilization with digitonin, the lumenal loop of reductase containing the T7 tag will be inaccessible to any anti-T7 antibody added to the cells. Upon extraction in the presence of sterols, the T7-tagged lumenal loop of HMG-Red-T7 will become accessible to the anti-T7 antibody. If cells are permeabilized with a detergent such as 0.1% Triton X-100 the plasma membrane as well as all organelles will be permeabilized. Thus, the T7-tagged loop of reductase will be bound by its antibody regardless of the absence or presence of sterols in the culture media.

As a control, cells would also be immunostained for an ER lumenal protein such as protein disulfide isomerase (PDI) to control for ER membrane integrity. A signal for PDI should be apparent in cells permeabilized with Triton X-100, but there should be no signal for cells permeabilized with digitonin regardless of the absence or presence of sterols in the culture

medium. Another important control would be to use a monoclonal antibody, designated A9, against the cytosolic catalytic domain of reductase. This antibody will provide a fluorescent signal specific to all reductase in the cells regardless of which detergent is used or whether the cells are treated with or without sterols when MG-132 treatment is used.

A powerful advantage of using confocal fluorescent imaging to examine reductase extraction is the ability to visualize whether reductase accumulates at distinct sites to be extracted from ER membranes. Any such accumulation may be visualized as fluorescent punctae. Previous studies involving immunostaining of reductase degradation in cells have been unable to detect any such punctae given that available endogenous antibodies are unable to distinguish between molecules of reductase that are appropriately integrated into the ER membrane from those that have been extracted from the membrane. The confocal imaging of HMG-Red-T7 in digitonin-permeabilized cells will permit for the focused analysis of reductase molecules engaged in membrane extraction.

Cell imaging will also allow for an opportunity to determine if membrane extracted reductase co-localizes with lipid droplets. Lipid droplets are subdomains of the ER membrane that contain a neutral lipid core composed of triglycerides and cholesteryl esters surrounded by a phospholipid monolayer [111, 112]. Previous studies from other laboratories implicated lipid droplets in degradation through demonstrating induction of lipid droplet formation in the presence of proteasome inhibitors and accumulation of apolipoprotein B-100 (Apo B-100) on lipid droplets when proteasomes are impaired [113]. In addition, a genome-wide screen in *Drosophila* S2 cells indicates that the proteasome pathway plays a role in lipid droplet formation [114]. Previous work in our lab has shown that a subset of reductase co-localizes with lipid droplets [70]. Furthermore, immunoblot analysis of purified lipid droplet fractions were found to contain reductase as well as other proteins required for reductase degradation (VCP/p97 and

gp78), implicating lipid droplets as important factors in reductase degradation. It could be that the subset of reductase previously seen associated with lipid droplets will appear as punctae when imaging extracted HMG-Red-T7.

4.2.1.1 Preliminary Results

Preliminary studies have been conducted on this project, in conjunction with Joachim Seemann, to establish permeabilization conditions and antibodies needed to serve as controls. Attempts were made to use the pore-forming toxin streptolysin O (SLO) to permeabilize cells but all such experiments were unsuccessful. In the first set of images, cells were permeabilized with either methanol or 0.003% digitonin and labeled with an antibody against PDI and calnexin. The proteins are visible and localize to the ER of cells permeabilized with methanol. Digitonin was used to permeabilize cells in a manner that would leave the ER membrane intact while allowing the plasma membrane to be permeabilized and permit entry of antibodies into the cells. As expected, digitonin permeabilization did not affect the labeling of calnexin when using an antibody against the NH_2-terminal cytosolic tail of the protein. However, the lumenal protein PDI is not visible in digitonin-permeabilized cells.

In the second set of images these same conditions were used to look at reductase in UT2/HMG-Red-T7 cells. Sterol dependent degradation of reductase is seen in cells permeabilized with methanol. In the lower two images, cells were treated with MG-132 in the absence or presence of sterols and then permeabilized with digitonin. Consistent with the studies reported here on membrane extraction of reductase, an increased fluorescent signal is detected for reductase in sterol-treated cells suggesting that reductase has been extracted from the ER membrane allowing the T7 epitope to be accessible to its antibody.

An unfortunate artifact consistently seen in these experiments was nonspecific labeling of the nucleus with the T7 antibody in methanol and more so in digitonin permeabilized cells. The UT2/HMG-Red-T7 cell line was isolated for its ability to show reductase degradation by endogenous Insigs without the need to transfect additional Insigs. Typically a stable cell line that is regulated by endogenous Insigs has very low expression levels of reductase. This low abundance of reductase is not a problem in immunoblotting experiments, but in imaging experiments it requires that images be taken at long exposure times to detect reductase. It is only at these long exposure times that nonspecific staining of the nucleus is seen. It seems likely that further progress on this project will require molecular cloning of reductase containing a different epitope tag in the lumenal loop and establishment of a corresponding stable cell line. Alternatively, progress is currently being made to produce a monoclonal antibody against the endogenous lumenal loop between transmembrane helices 7 and 8 in reductase. If an antibody is produced that gives strong and specific labeling of reductase in cells, then conditions used in preliminary experiments might be extended to study membrane extraction of endogenous reductase in CHO-K1 cells.

Immunostaining Protocol

On Day 0 UT2/HMG-Red-T7 cells were plated at $5x10^5$ per 60-mm dish on 12-mm coverslips in medium B. On day 1, the cells were refed medium A supplemented with 5% LPDS, 10 μM compactin, and 50 μM mevalonate, and in the absence or presence of 1 μM MG-132 and 1 μg/ml 25-HC plus 10 mM mevalonate. On day 2, appropriate coverslips were subjected to permeabilization and staining. A subset of coverslips were washed with PBS three times and subsequently incubated on ice for 20 min with 0.003% digitonin. Coverslips were washed three times in PBS and then incubated for 20 min on ice with 20 μl of diluted primary antibody. The coverslips were again washed three times with PBS and then fixed and permeabilized with cold

methanol for 10 minutes. Coverslips were washed again and then treated with Alexa Fluor conjugated secondary antibodies for 30 minutes at room temperature. Coverslips were washed in PBS one more time and then mounted on microscope slides. Cells permeabilized with methanol alone were treated as above, except they were initially put in methanol before incubations with the primary and secondary antibodies were performed.

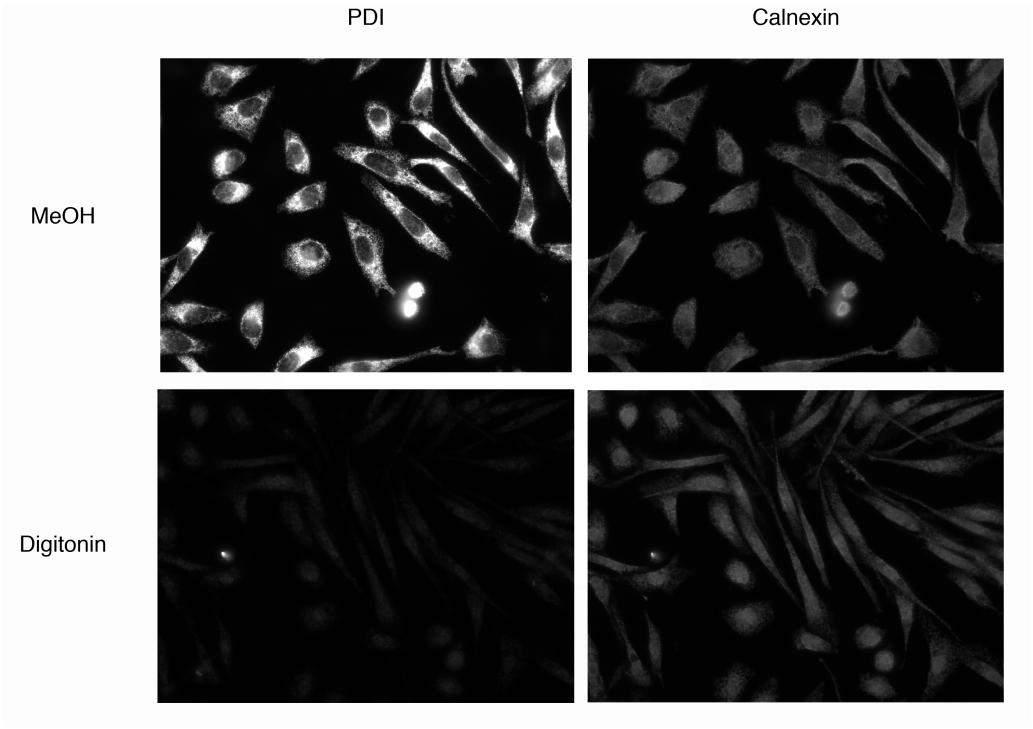

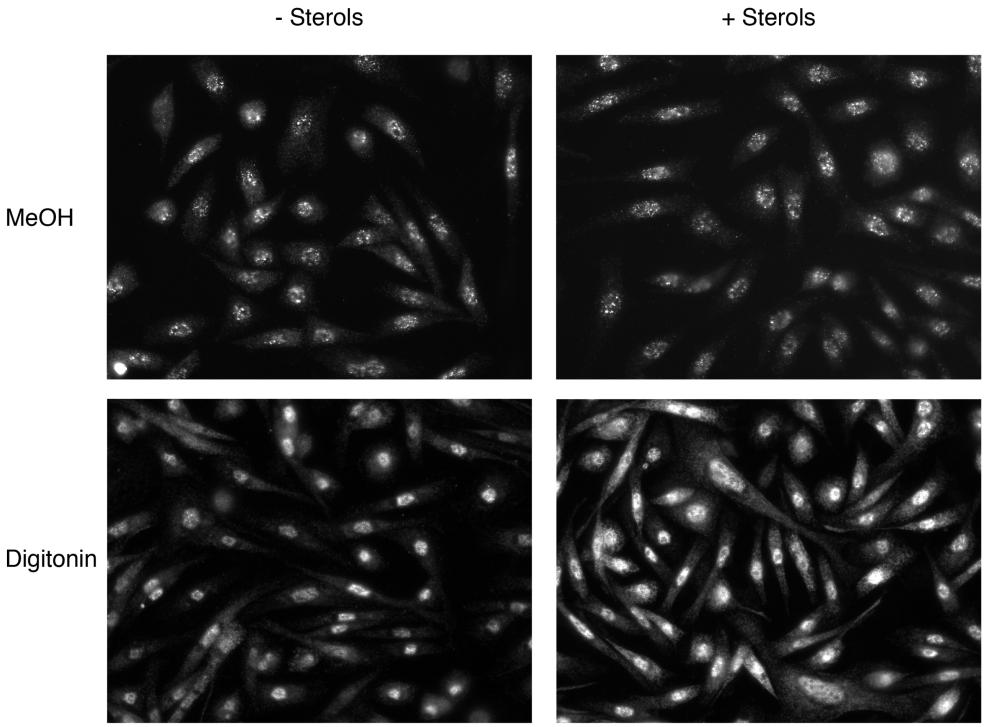

4.2.2 In Vitro Membrane Extraction and Cytosolic Dislocation

Studying biological processes through *in vitro* assays can be a very advantageous tool to delineate the various molecules and proteins required to drive a reaction. Prior studies of reductase degradation have led to the development of an *in vitro* assay used to study reductase ubiquitination in semi-permeabilized cells. In this assay, sterol-depleted cells are permeabilized with a low concentration of the mild detergent digitonin, resulting in release of greater than 90% of cytosolic proteins into the supernatant upon centrifugation, while membrane proteins remain associated with the pellet. The plasma membranes of these cells become permeable to molecules such as proteins and ATP [63]. Pellets of permeabilized cells are resuspended in buffer containing rat liver cytosol, an ATP-regenerating system, ubiquitin, ubiquitin aldehyde and sterols. Following incubation of reactions at 37 ^{o}C for 30 minutes, the cells are then lysed and reductase is immunoprecipitated for immunoblot analysis. Under these conditions, reductase

becomes ubiquitinated in the permeabilized cells, but only when reactions are supplemented with ATP, cytosol, and sterols.

The in vitro assay for reductase ubiquitination has been adapted to study the dislocation of reductase from membranes of permeabilized cells [71]. This dislocation was found to be stimulated by sterols and geranylgeraniol, the reaction was also augmented by inhibitors of deubiquitinating enzymes. We are now poised to use the in vitro dislocation assay to determine the minimal cytosolic components required for reductase dislocation from membranes. Purified forms of VCP/p97, and its co-factors Npl4 and Ufd1 as well as the 19S RP are available. Thus, initial experiments should be designed to determine whether the addition of VCP/p97, Npl4, Ufd1, and the 19S RP to sterol-treated permeabilized cells reconstitutes reductase dislocation. If not, additional cytosolic proteins required for the reaction can be identified using established techniques of protein purification.

Finally, the permeabilized cell system can be used to reconstitute sterol-induced extraction of reductase as determined by the trypsin-protection assay. Briefly, permeabilized cells expressing HMG-Red-T7 will be treated in the absence or presence of sterols and rat liver cytosol. Following incubation at 37 ^{o}C, the cells will be subjected to subcellular fractionation. Resulting membranes will be treated with trypsin and reactions are monitored by immunoblot. I anticipate that sterols will cause a fraction of reductase to become susceptible to trypsinolysis in a similar fashion as observed in intact cells. In subsequent experiments, one could determine whether VCP/p97 replaces cytosol for reductase extraction and whether the target of geranylgeraniol is a membrane-bound or cytosolic protein. Efforts here would begin with a search for and purification of geranylgeranyl-diphosphate or geranylgeraniol-binding proteins from membranes and rat liver cytosol through means of protein purification. Any protein identified would be analyzed for relevance to reductase degradation, ubiquitination, and

membrane extraction through RNAi-mediated knockdown.

4.2.3 Membrane Extraction and Cytosolic Dislocation of SREBP and Insig-1

An intriguing question prompted by the studies described here, is whether a sequential role of VCP/p97 and the 19S RP are required for membrane extraction and cytosolic dislocation of any other integral membrane ERAD substrate. This project would focus first on the regulated degradation and cytosolic dislocation of SREBP or Insig-1. A member of our lab, Rebecca Faulkner, has observed that knockdown of Rpt5 in *Drosophila* S2 cells leads to a noticeable stabilization of SREBP. Experiments here would involve knocking down Rpt5 in SRD-13a cells, a cell line that lacks SCAP, where SREBP is constitutively degraded and determining whether Rpt5 knockdown affects SREBP stability. Follow up experiments would be done to address a role for the 19S RP in cytosolic dislocation of SREBP using RNAi-mediated knockdown of Rpt5 and cellular fractionation. Should these experiments prove to follow the same pattern seen in reductase degradation, a membrane extraction assay would then be formed to look at the role of VCP/p97 in SREBP retrotranslocation. In a similar manner, Insig-1 cytosolic dislocation would be tested for dependency upon the 19S RP and a membrane extraction assay would be formed to examine the role of VCP/p97. Results in which VCP/p97 is involved in retrotranslocation and the 19S RP is involved in cytosolic dislocation of either SREBP or Insig-1 would suggest that the sequential model of degradation seen for reductase could apply to other ERAD substrates as opposed to being a mechanism specific to reductase. I feel that Insig-1 and SREBP would be ideal ERAD substrates in these studies because their degradation can be tightly controlled. For example, Scap is known to be required for the stability of SREBP in both mammalian and Drosophila systems [78, 115]. The physiologic relevance of dislocation and extraction of SREBP can be readily determined by measuring the effect of Scap overexpression on the reaction (Scap should stabilize SREBP and thereby prevent extraction or cytosolic dislocation). The

degradation of Insig-1, like that of reductase, is regulated by lipids [116, 117]. Sterols cause Insig-1 to bind to Scap, which displaces gp78 and prevents Insig-1 ubiquitination [116]. Unsaturated fatty acids block the interaction of ubiquitinated Insig-1 with VCP/p97, thereby stabilizing the protein even in the absence of Scap [117]. Thus, we anticipate that membrane extraction and dislocation of Insig-1 will be blocked by both Scap/sterols and unsaturated fatty acids.

TABLE 1:

siRNA Table

Name	GenBank accession number	Sense Sequence
GFP		CAGCCACAACGUCUAUAUCUU
Insig-1	NM_001244079.1	AAACAUAGGACGACAGUUAUU
Insig-2	NM_001244078.1	UGACAGGCAUCUAGGAGAAUU
VCP/p97	NM_009503.4	GAAUAGAGUUGUUCGGAAUUU
Rpt1 #1 Rpt1 #2	NM_011188.3	GGGAUUUGGCUGCAGAUAAUU GCUCACUGGUAUUAAAGAAUU
Rpt2 #1 Rpt2 #2	NM_008947.3	GCCACAAACCGAAUAGAAAUU AGAAGGAUGACAAGGACAAUU
Rpt3 #1 Rpt3 #2	NM_011874.2	GGCCAAGGACUUCGAGAAAUU AGGUAAUCAUGGCCACAAAUU
Rpt4 #1 Rpt4 #2 Rpt4 #3	NM_025959.3	CAGGAAGAUUAGAUAGAAAUU GCUACAAACAGACCAGAUAUU GAUCAUGGCUACAAACAGAUU
Rpt5 #1 Rpt5 #2 Rpt5 #3	NM_008948.2	GAAUAUGACUCUCGGGUGAUU UCAAGAUCAUGAAGAGUGAUU CGGCAGGAGAAGAUGGCGAUU
Rpt6 #1 Rpt6 #2	NM_008950.1	CUGAACUGGUACAGAAAUUUU CCAAGAACAUCAAGGUUAUUU

BIBLIOGRAPHY

1. Ghaemmaghami, S., et al., *Global analysis of protein expression in yeast.* Nature, 2003. **425**(6959): p. 737-41.
2. Meusser, B., et al., *ERAD: the long road to destruction.* Nat Cell Biol, 2005. **7**(8): p. 766-72.
3. Romisch, K., *Endoplasmic reticulum-associated degradation.* Annu Rev Cell Dev Biol, 2005. **21**: p. 435-56.
4. Cheng, S.H., et al., *Defective intracellular transport and processing of CFTR is the molecular basis of most cystic fibrosis.* Cell, 1990. **63**(4): p. 827-34.
5. Bonifacino, J.S., et al., *Pre-Golgi degradation of newly synthesized T-cell antigen receptor chains: intrinsic sensitivity and the role of subunit assembly.* J Cell Biol, 1989. **109**(1): p. 73-83.
6. Goldberg, A.L., *Protein degradation and protection against misfolded or damaged proteins.* Nature, 2003. **426**(6968): p. 895-9.
7. Aridor, M., *Visiting the ER: the endoplasmic reticulum as a target for therapeutics in traffic related diseases.* Adv Drug Deliv Rev, 2007. **59**(8): p. 759-81.
8. Zhao, L. and S.L. Ackerman, *Endoplasmic reticulum stress in health and disease.* Curr Opin Cell Biol, 2006. **18**(4): p. 444-52.
9. Shamu, C.E. and P. Walter, *Oligomerization and phosphorylation of the Ire1p kinase during intracellular signaling from the endoplasmic reticulum to the nucleus.* EMBO J, 1996. **15**(12): p. 3028-39.
10. Korennykh, A.V., et al., *The unfolded protein response signals through high-order assembly of Ire1.* Nature, 2009. **457**(7230): p. 687-93.
11. Hollien, J. and J.S. Weissman, *Decay of endoplasmic reticulum-localized mRNAs during the unfolded protein response.* Science, 2006. **313**(5783): p. 104-7.
12. Calfon, M., et al., *IRE1 couples endoplasmic reticulum load to secretory capacity by processing the XBP-1 mRNA.* Nature, 2002. **415**(6867): p. 92-6.
13. Lee, A.H., N.N. Iwakoshi, and L.H. Glimcher, *XBP-1 regulates a subset of endoplasmic reticulum resident chaperone genes in the unfolded protein response.* Mol Cell Biol, 2003. **23**(21): p. 7448-59.
14. Shen, J., et al., *ER stress regulation of ATF6 localization by dissociation of BiP/GRP78 binding and unmasking of Golgi localization signals.* Dev Cell, 2002. **3**(1): p. 99-111.
15. Ye, J., et al., *ER stress induces cleavage of membrane-bound ATF6 by the same proteases that process SREBPs.* Mol Cell, 2000. **6**(6): p. 1355-64.
16. Kaufman, R.J., *Regulation of mRNA translation by protein folding in the endoplasmic reticulum.* Trends Biochem Sci, 2004. **29**(3): p. 152-8.
17. Travers, K.J., et al., *Functional and genomic analyses reveal an essential coordination between the unfolded protein response and ER-associated degradation.* Cell, 2000. **101**(3): p. 249-58.
18. Carvalho, P., V. Goder, and T.A. Rapoport, *Distinct ubiquitin-ligase complexes define convergent pathways for the degradation of ER proteins.* Cell, 2006. **126**(2): p. 361-73.
19. Denic, V., E.M. Quan, and J.S. Weissman, *A luminal surveillance complex that selects misfolded glycoproteins for ER-associated degradation.* Cell, 2006. **126**(2): p. 349-59.

20. Kostova, Z., Y.C. Tsai, and A.M. Weissman, *Ubiquitin ligases, critical mediators of endoplasmic reticulum-associated degradation.* Semin Cell Dev Biol, 2007. **18**(6): p. 770-9.
21. Hiller, M.M., et al., *ER degradation of a misfolded luminal protein by the cytosolic ubiquitin-proteasome pathway.* Science, 1996. **273**(5282): p. 1725-8.
22. Caplan, S., et al., *Glycosylation and structure of the yeast MF alpha 1 alpha-factor precursor is important for efficient transport through the secretory pathway.* J Bacteriol, 1991. **173**(2): p. 627-35.
23. Christianson, J.C., et al., *OS-9 and GRP94 deliver mutant alpha1-antitrypsin to the Hrd1-SEL1L ubiquitin ligase complex for ERAD.* Nat Cell Biol, 2008. **10**(3): p. 272-82.
24. Nishikawa, S., J.L. Brodsky, and K. Nakatsukasa, *Roles of molecular chaperones in endoplasmic reticulum (ER) quality control and ER-associated degradation (ERAD).* J Biochem, 2005. **137**(5): p. 551-5.
25. Ye, Y., et al., *A membrane protein complex mediates retro-translocation from the ER lumen into the cytosol.* Nature, 2004. **429**(6994): p. 841-7.
26. Lilley, B.N. and H.L. Ploegh, *A membrane protein required for dislocation of misfolded proteins from the ER.* Nature, 2004. **429**(6994): p. 834-40.
27. Rapoport, T.A., *Protein translocation across the eukaryotic endoplasmic reticulum and bacterial plasma membranes.* Nature, 2007. **450**(7170): p. 663-9.
28. Johnson, A.E. and N.G. Haigh, *The ER translocon and retrotranslocation: is the shift into reverse manual or automatic?* Cell, 2000. **102**(6): p. 709-12.
29. Ye, Y., H.H. Meyer, and T.A. Rapoport, *The AAA ATPase Cdc48/p97 and its partners transport proteins from the ER into the cytosol.* Nature, 2001. **414**(6864): p. 652-6.
30. Jarosch, E., et al., *Protein dislocation from the ER requires polyubiquitination and the AAA-ATPase Cdc48.* Nat Cell Biol, 2002. **4**(2): p. 134-9.
31. Pickart, C.M., *Mechanisms underlying ubiquitination.* Annu Rev Biochem, 2001. **70**: p. 503-33.
32. Swanson, R., M. Locher, and M. Hochstrasser, *A conserved ubiquitin ligase of the nuclear envelope/endoplasmic reticulum that functions in both ER-associated and Matalpha2 repressor degradation.* Genes Dev, 2001. **15**(20): p. 2660-74.
33. Carvalho, P., A.M. Stanley, and T.A. Rapoport, *Retrotranslocation of a misfolded luminal ER protein by the ubiquitin-ligase Hrd1p.* Cell, 2010. **143**(4): p. 579-91.
34. Ernst, R., et al., *The otubain YOD1 is a deubiquitinating enzyme that associates with p97 to facilitate protein dislocation from the ER.* Mol Cell, 2009. **36**(1): p. 28-38.
35. Ernst, R., et al., *Enzymatic blockade of the ubiquitin-proteasome pathway.* PLoS Biol, 2011. **8**(3): p. e1000605.
36. Schuberth, C. and A. Buchberger, *UBX domain proteins: major regulators of the AAA ATPase Cdc48/p97.* Cell Mol Life Sci, 2008. **65**(15): p. 2360-71.
37. Koegl, M., et al., *A novel ubiquitination factor, E4, is involved in multiubiquitin chain assembly.* Cell, 1999. **96**(5): p. 635-44.
38. Raasi, S. and D.H. Wolf, *Ubiquitin receptors and ERAD: a network of pathways to the proteasome.* Semin Cell Dev Biol, 2007. **18**(6): p. 780-91.
39. Wahlman, J., et al., *Real-time fluorescence detection of ERAD substrate retrotranslocation in a mammalian in vitro system.* Cell, 2007. **129**(5): p. 943-55.

40. Wiertz, E.J., et al., *The human cytomegalovirus US11 gene product dislocates MHC class I heavy chains from the endoplasmic reticulum to the cytosol.* Cell, 1996. **84**(5): p. 769-79.
41. Matsumura, Y., L.L. David, and W.R. Skach, *Role of Hsc70 binding cycle in CFTR folding and endoplasmic reticulum-associated degradation.* Mol Biol Cell, 2011. **22**(16): p. 2797-809.
42. VanSlyke, J.K. and L.S. Musil, *Dislocation and degradation from the ER are regulated by cytosolic stress.* J Cell Biol, 2002. **157**(3): p. 381-94.
43. Nakatsukasa, K., et al., *Dissecting the ER-associated degradation of a misfolded polytopic membrane protein.* Cell, 2008. **132**(1): p. 101-12.
44. Bebok, Z., et al., *The mechanism underlying cystic fibrosis transmembrane conductance regulator transport from the endoplasmic reticulum to the proteasome includes Sec61beta and a cytosolic, deglycosylated intermediary.* J Biol Chem, 1998. **273**(45): p. 29873-8.
45. Ikeda, Y., et al., *Regulated endoplasmic reticulum-associated degradation of a polytopic protein: p97 recruits proteasomes to Insig-1 before extraction from membranes.* J Biol Chem, 2009. **284**(50): p. 34889-900.
46. Johnston, J.A., C.L. Ward, and R.R. Kopito, *Aggresomes: a cellular response to misfolded proteins.* J Cell Biol, 1998. **143**(7): p. 1883-98.
47. Ikonen, E., *Mechanisms for cellular cholesterol transport: defects and human disease.* Physiol Rev, 2006. **86**(4): p. 1237-61.
48. Russell, D.W., *Nuclear orphan receptors control cholesterol catabolism.* Cell, 1999. **97**(5): p. 539-42.
49. Libby, P., M. Aikawa, and U. Schonbeck, *Cholesterol and atherosclerosis.* Biochim Biophys Acta, 2000. **1529**(1-3): p. 299-309.
50. Goldstein, J.L. and M.S. Brown, *Regulation of the mevalonate pathway.* Nature, 1990. **343**(6257): p. 425-30.
51. Nakanishi, M., J.L. Goldstein, and M.S. Brown, *Multivalent control of 3-hydroxy-3-methylglutaryl coenzyme A reductase. Mevalonate-derived product inhibits translation of mRNA and accelerates degradation of enzyme.* J Biol Chem, 1988. **263**(18): p. 8929-37.
52. Nohturfft, A., M.S. Brown, and J.L. Goldstein, *Topology of SREBP cleavage-activating protein, a polytopic membrane protein with a sterol-sensing domain.* J Biol Chem, 1998. **273**(27): p. 17243-50.
53. Brown, M.S. and J.L. Goldstein, *A proteolytic pathway that controls the cholesterol content of membranes, cells, and blood.* Proc Natl Acad Sci U S A, 1999. **96**(20): p. 11041-8.
54. Yabe, D., et al., *Three mutations in sterol-sensing domain of SCAP block interaction with insig and render SREBP cleavage insensitive to sterols.* Proc Natl Acad Sci U S A, 2002. **99**(26): p. 16672-7.
55. Yang, T., et al., *Crucial step in cholesterol homeostasis: sterols promote binding of SCAP to INSIG-1, a membrane protein that facilitates retention of SREBPs in ER.* Cell, 2002. **110**(4): p. 489-500.
56. Goldstein, J.L., R.A. DeBose-Boyd, and M.S. Brown, *Protein sensors for membrane sterols.* Cell, 2006. **124**(1): p. 35-46.

57. Yabe, D., M.S. Brown, and J.L. Goldstein, *Insig-2, a second endoplasmic reticulum protein that binds SCAP and blocks export of sterol regulatory element-binding proteins.* Proc Natl Acad Sci U S A, 2002. **99**(20): p. 12753-8.
58. Feramisco, J.D., J.L. Goldstein, and M.S. Brown, *Membrane topology of human insig-1, a protein regulator of lipid synthesis.* J Biol Chem, 2004. **279**(9): p. 8487-96.
59. Friedlander, R., et al., *A regulatory link between ER-associated protein degradation and the unfolded-protein response.* Nat Cell Biol, 2000. **2**(7): p. 379-84.
60. Liscum, L., et al., *Domain structure of 3-hydroxy-3-methylglutaryl coenzyme A reductase, a glycoprotein of the endoplasmic reticulum.* J Biol Chem, 1985. **260**(1): p. 522-30.
61. Roitelman, J., et al., *Immunological evidence for eight spans in the membrane domain of 3-hydroxy-3-methylglutaryl coenzyme A reductase: implications for enzyme degradation in the endoplasmic reticulum.* J Cell Biol, 1992. **117**(5): p. 959-73.
62. Gil, G., et al., *Membrane-bound domain of HMG CoA reductase is required for sterol-enhanced degradation of the enzyme.* Cell, 1985. **41**(1): p. 249-58.
63. Song, B.L. and R.A. DeBose-Boyd, *Ubiquitination of 3-hydroxy-3-methylglutaryl-CoA reductase in permeabilized cells mediated by cytosolic E1 and a putative membrane-bound ubiquitin ligase.* J Biol Chem, 2004. **279**(27): p. 28798-806.
64. Song, B.L., N.B. Javitt, and R.A. DeBose-Boyd, *Insig-mediated degradation of HMG CoA reductase stimulated by lanosterol, an intermediate in the synthesis of cholesterol.* Cell Metab, 2005. **1**(3): p. 179-89.
65. Sever, N., et al., *Accelerated degradation of HMG CoA reductase mediated by binding of insig-1 to its sterol-sensing domain.* Mol Cell, 2003. **11**(1): p. 25-33.
66. Sever, N., et al., *Insig-dependent ubiquitination and degradation of mammalian 3-hydroxy-3-methylglutaryl-CoA reductase stimulated by sterols and geranylgeraniol.* J Biol Chem, 2003. **278**(52): p. 52479-90.
67. Lee, P.C., A.D. Nguyen, and R.A. Debose-Boyd, *Mutations within the membrane domain of HMG-CoA reductase confer resistance to sterol-accelerated degradation.* J Lipid Res, 2007. **48**(2): p. 318-27.
68. Song, B.L., N. Sever, and R.A. DeBose-Boyd, *Gp78, a membrane-anchored ubiquitin ligase, associates with Insig-1 and couples sterol-regulated ubiquitination to degradation of HMG CoA reductase.* Mol Cell, 2005. **19**(6): p. 829-40.
69. Jo, Y., et al., *Sterol-induced degradation of HMG CoA reductase depends on interplay of two Insigs and two ubiquitin ligases, gp78 and Trc8.* Proc Natl Acad Sci U S A, 2011. **108**(51): p. 20503-8.
70. Hartman, I.Z., et al., *Sterol-induced dislocation of 3-hydroxy-3-methylglutaryl coenzyme A reductase from endoplasmic reticulum membranes into the cytosol through a subcellular compartment resembling lipid droplets.* J Biol Chem, 2010. **285**(25): p. 19288-98.
71. Elsabrouty, R., et al., *Sterol-induced dislocation of 3-hydroxy-3-methylglutaryl coenzyme A reductase from membranes of permeabilized cells.* Mol Biol Cell, 2013. **24**(21): p. 3300-8.
72. Nguyen, A.D., S.H. Lee, and R.A. DeBose-Boyd, *Insig-mediated, sterol-accelerated degradation of the membrane domain of hamster 3-hydroxy-3-methylglutaryl-coenzyme A reductase in insect cells.* J Biol Chem, 2009. **284**(39): p. 26778-88.

73. Ehlinger, A. and K.J. Walters, *Structural insights into proteasome activation by the 19S regulatory particle.* Biochemistry, 2013. **52**(21): p. 3618-28.
74. Bar-Nun, S. and M.H. Glickman, *Proteasomal AAA-ATPases: structure and function.* Biochim Biophys Acta, 2012. **1823**(1): p. 67-82.
75. Goldstein, J.L., S.K. Basu, and M.S. Brown, *Receptor-mediated endocytosis of low-density lipoprotein in cultured cells.* Methods Enzymol, 1983. **98**: p. 241-60.
76. DeBose-Boyd, R.A., et al., *Transport-dependent proteolysis of SREBP: relocation of site-1 protease from Golgi to ER obviates the need for SREBP transport to Golgi.* Cell, 1999. **99**(7): p. 703-12.
77. Mosley, S.T., et al., *Mutant clone of Chinese hamster ovary cells lacking 3-hydroxy-3 - methylglutaryl coenzyme A reductase.* J Biol Chem, 1983. **258**(22): p. 13875-81.
78. Rawson, R.B., et al., *Failure to cleave sterol regulatory element-binding proteins (SREBPs) causes cholesterol auxotrophy in Chinese hamster ovary cells with genetic absence of SREBP cleavage-activating protein.* J Biol Chem, 1999. **274**(40): p. 28549-56.
79. Liscum, L., et al., *Regulation of 3-hydroxy-3-methylglutaryl coenzyme A reductase and its mRNA in rat liver as studied with a monoclonal antibody and a cDNA probe.* J Biol Chem, 1983. **258**(13): p. 8450-5.
80. Sakai, J., et al., *Identification of complexes between the COOH-terminal domains of sterol regulatory element-binding proteins (SREBPs) and SREBP cleavage-activating protein.* J Biol Chem, 1997. **272**(32): p. 20213-21.
81. Nakamura, N., et al., *Characterization of a cis-Golgi matrix protein, GM130.* J Cell Biol, 1995. **131**(6 Pt 2): p. 1715-26.
82. Jo, Y., I.Z. Hartman, and R.A. DeBose-Boyd, *Ancient ubiquitous protein-1 mediates sterol-induced ubiquitination of 3-hydroxy-3-methylglutaryl CoA reductase in lipid droplet-associated endoplasmic reticulum membranes.* Mol Biol Cell, 2013. **24**(3): p. 169-83.
83. Ou, W.J., et al., *Conformational changes induced in the endoplasmic reticulum luminal domain of calnexin by Mg-ATP and Ca2+.* J Biol Chem, 1995. **270**(30): p. 18051-9.
84. Brown, M.S. and J.L. Goldstein, *Multivalent feedback regulation of HMG CoA reductase, a control mechanism coordinating isoprenoid synthesis and cell growth.* J Lipid Res, 1980. **21**(5): p. 505-17.
85. Roitelman, J., et al., *Apomine, a novel hypocholesterolemic agent, accelerates degradation of 3-hydroxy-3-methylglutaryl-coenzyme A reductase and stimulates low density lipoprotein receptor activity.* J Biol Chem, 2004. **279**(8): p. 6465-73.
86. Braun, B.C., et al., *The base of the proteasome regulatory particle exhibits chaperone-like activity.* Nat Cell Biol, 1999. **1**(4): p. 221-6.
87. Pietroni, P., et al., *The proteasome cap RPT5/Rpt5p subunit prevents aggregation of unfolded ricin A chain.* Biochem J, 2013. **453**(3): p. 435-45.
88. Wang, Q., et al., *A ubiquitin ligase-associated chaperone holdase maintains polypeptides in soluble states for proteasome degradation.* Mol Cell, 2011. **42**(6): p. 758-70.
89. Tomko, R.J., Jr. and M. Hochstrasser, *Molecular architecture and assembly of the eukaryotic proteasome.* Annu Rev Biochem, 2013. **82**: p. 415-45.
90. Lee, R.J., et al., *Uncoupling retro-translocation and degradation in the ER-associated degradation of a soluble protein.* EMBO J, 2004. **23**(11): p. 2206-15.

91. Lipson, C., et al., *A proteasomal ATPase contributes to dislocation of endoplasmic reticulum-associated degradation (ERAD) substrates.* J Biol Chem, 2008. **283**(11): p. 7166-75.
92. Mayer, T.U., T. Braun, and S. Jentsch, *Role of the proteasome in membrane extraction of a short-lived ER-transmembrane protein.* EMBO J, 1998. **17**(12): p. 3251-7.
93. Walter, J., et al., *Sec61p-independent degradation of the tail-anchored ER membrane protein Ubc6p.* EMBO J, 2001. **20**(12): p. 3124-31.
94. Elkabetz, Y., et al., *Distinct steps in dislocation of luminal endoplasmic reticulum-associated degradation substrates: roles of endoplamic reticulum-bound p97/Cdc48p and proteasome.* J Biol Chem, 2004. **279**(6): p. 3980-9.
95. Bagola, K., et al., *Protein dislocation from the ER.* Biochim Biophys Acta, 2011. **1808**(3): p. 925-36.
96. Huppa, J.B. and H.L. Ploegh, *The alpha chain of the T cell antigen receptor is degraded in the cytosol.* Immunity, 1997. **7**(1): p. 113-22.
97. Wiertz, E.J., et al., *Sec61-mediated transfer of a membrane protein from the endoplasmic reticulum to the proteasome for destruction.* Nature, 1996. **384**(6608): p. 432-8.
98. VanSlyke, J.K., S.M. Deschenes, and L.S. Musil, *Intracellular transport, assembly, and degradation of wild-type and disease-linked mutant gap junction proteins.* Mol Biol Cell, 2000. **11**(6): p. 1933-46.
99. Garza, R.M., B.K. Sato, and R.Y. Hampton, *In vitro analysis of Hrd1p-mediated retrotranslocation of its multispanning membrane substrate 3-hydroxy-3-methylglutaryl (HMG)-CoA reductase.* J Biol Chem, 2009. **284**(22): p. 14710-22.
100. Xiong, X., E. Chong, and W.R. Skach, *Evidence that endoplasmic reticulum (ER)-associated degradation of cystic fibrosis transmembrane conductance regulator is linked to retrograde translocation from the ER membrane.* J Biol Chem, 1999. **274**(5): p. 2616-24.
101. Faulkner, R.A., et al., *Lipid-regulated degradation of HMG-CoA reductase and Insig-1 through distinct mechanisms in insect cells.* J Lipid Res, 2013. **54**(4): p. 1011-22.
102. Eilers, M. and G. Schatz, *Binding of a specific ligand inhibits import of a purified precursor protein into mitochondria.* Nature, 1986. **322**(6076): p. 228-32.
103. Liscum, L., et al., *3-Hydroxy-3-methylglutaryl-CoA reductase: a transmembrane glycoprotein of the endoplasmic reticulum with N-linked "high-mannose" oligosaccharides.* Proc Natl Acad Sci U S A, 1983. **80**(23): p. 7165-9.
104. Ness, G.C., et al., *Regulation of 3-hydroxy-3-methylglutaryl coenzyme A reductase gene expression by sterols and nonsterols in rat liver.* Arch Biochem Biophys, 1994. **308**(2): p. 420-5.
105. Goldberg, I.J., et al., *Lack of effect of lovastatin therapy on the parameters of whole-body cholesterol metabolism.* J Clin Invest, 1990. **86**(3): p. 801-8.
106. Ness, G.C., C.M. Chambers, and D. Lopez, *Atorvastatin action involves diminished recovery of hepatic HMG-CoA reductase activity.* J Lipid Res, 1998. **39**(1): p. 75-84.
107. Radhakrishnan, S.K., et al., *p97-dependent retrotranslocation and proteolytic processing govern formation of active Nrf1 upon proteasome inhibition.* eLife, 2014. **3**.
108. Claessen, J.H. and H.L. Ploegh, *BAT3 guides misfolded glycoproteins out of the endoplasmic reticulum.* PLoS One, 2011. **6**(12): p. e28542.

109. Minami, R., et al., *BAG-6 is essential for selective elimination of defective proteasomal substrates.* J Cell Biol, 2010. **190**(4): p. 637-50.
110. Xu, Y., et al., *A ubiquitin-like domain recruits an oligomeric chaperone to a retrotranslocation complex in endoplasmic reticulum-associated degradation.* J Biol Chem, 2013. **288**(25): p. 18068-76.
111. Thiele, C. and J. Spandl, *Cell biology of lipid droplets.* Curr Opin Cell Biol, 2008. **20**(4): p. 378-85.
112. Tauchi-Sato, K., et al., *The surface of lipid droplets is a phospholipid monolayer with a unique Fatty Acid composition.* J Biol Chem, 2002. **277**(46): p. 44507-12.
113. Ohsaki, Y., et al., *Cytoplasmic lipid droplets are sites of convergence of proteasomal and autophagic degradation of apolipoprotein B.* Mol Biol Cell, 2006. **17**(6): p. 2674-83.
114. Guo, Y., et al., *Functional genomic screen reveals genes involved in lipid-droplet formation and utilization.* Nature, 2008. **453**(7195): p. 657-61.
115. Seegmiller, A.C., et al., *The SREBP pathway in Drosophila: regulation by palmitate, not sterols.* Dev Cell, 2002. **2**(2): p. 229-38.
116. Lee, J.N., et al., *Sterol-regulated degradation of Insig-1 mediated by the membrane-bound ubiquitin ligase gp78.* J Biol Chem, 2006. **281**(51): p. 39308-15.
117. Lee, J.N., et al., *Unsaturated fatty acids inhibit proteasomal degradation of Insig-1 at a postubiquitination step.* J Biol Chem, 2008. **283**(48): p. 33772-83.